

Aus dem Institut für Transfusionsmedizin und Immunologie  
der Medizinischen Fakultät Mannheim  
Direktor: Prof. Dr. med. Harald Klüter

Comparative analysis of the immunomodulatory properties of different  
mesenchymal stromal cells and their extracellular vesicles

Inauguraldissertation  
zur Erlangung des akademischen Grades  
Doctor scientiarum humanarum (Dr. sc. hum.)  
der  
Medizinischen Fakultät Mannheim  
der Ruprecht-Karls-Universität  
zu  
Heidelberg

vorgelegt von  
Adriana Torres Crigna

aus  
Vigo, Spanien  
2020

Dekan: Prof. Dr. med. Sergij Goerd  
Referentin: Prof. Dr. rer. nat. Karen Bieback

Sections/data reported within this dissertation are part of soon to be or already submitted manuscripts.

Introduction chapter comprises material from the published review article: “Torres Crigna, A., et al., *Stem/stromal cells for treatment of kidney injuries with focus on preclinical models*. Front Med. 5:179.”

# TABLE OF CONTENTS

Page

<b>Abbreviations.....</b>	<b>1</b>
<b>1 Introduction .....</b>	<b>4</b>
<b>1.1 Mesenchymal stromal cells .....</b>	<b>4</b>
1.1.1 General overview .....	4
1.1.2 MSC Immunomodulation properties.....	6
1.1.3 Xenogeneic MSC: Preclinical implications .....	9
<b>1.2 MSC-derived extracellular vesicles .....</b>	<b>10</b>
1.2.1 General overview .....	10
1.2.2 MSC-EV mediated immunomodulatory effects .....	14
<b>2 Aims of the study .....</b>	<b>16</b>
<b>3 Material and methods.....</b>	<b>18</b>
<b>3.1 Material.....</b>	<b>18</b>
3.1.1 Cells.....	18
3.1.2 Cell culture products .....	19
3.1.3 Cell culture media .....	20
3.1.4 Flow cytometry.....	21
3.1.5 Extracellular vesicles .....	23
3.1.6 Western blot.....	24
3.1.7 Protein detection .....	26
3.1.8 Solutions .....	26
3.1.9 Consumable laboratory material .....	27
3.1.10 Laboratory equipment.....	28
3.1.11 Software for data analysis .....	29
<b>3.2 Methods .....</b>	<b>30</b>
3.2.1 Evaluation of immunomodulatory potential of different MSC sources ...	30
3.2.2 Evaluation of MSC-derived products modulatory functions.....	42
3.2.3 Evaluation of standardised ultracentrifuge-based EV isolation protocol	51
<b>4 Results .....</b>	<b>55</b>
<b>4.1 Immunomodulatory potential of different human MSC sources .....</b>	<b>55</b>
4.1.1 Inhibition of PBMC proliferation is higher in ASC cocultures, independent of their passage .....	55

4.1.2	Tryptophan addition to cocultures abrogates MSC mediated PBMC inhibition, which is correlated with an increase of IDO and kynurenine secretion	57
4.1.3	Epacadostat abolishes PBMC inhibition and decreases IDO expression and kynurenine secretion .....	58
4.1.4	Human PBMC proliferation is inhibited greater with human than with rat MSC, however, the latter inhibits blood rat PBMC to a higher extent .....	60
4.1.5	Kynurenine secretion is prominently higher in human PBMC immunosuppression assay .....	60
4.1.6	Cultures with rat PBMC exert nitrite production further than SMC .....	61
4.1.7	ASC are more immunosuppressive than ABCB5 in human allo-coculture, whereas ABCB5 are stronger inhibitors in xeno-coculture settings .....	63
<b>4.2</b>	<b>MSC-derived products modulatory functions.....</b>	<b>65</b>
4.2.1	ASC-derived EV flow cytometry measurement favours the use of aldehyde/sulfate latex bead-EV coupling.....	66
4.2.2	ASC-derived EV present typical EV characteristics which are unaffected by IFN $\gamma$ priming .....	69
4.2.3	Direct and transwell coculture inhibit the proliferation of stimulated PBMC via IDO-Kynurenine pathway.....	73
4.2.4	Stimulated PBMC were not inhibited by conditioned media (CM) transferred from a previous coculture .....	75
4.2.5	Nitrite levels were mainly undetectable amongst all conditions, except for MSC-CM.....	75
<b>4.3</b>	<b>Evaluation of standardised ultracentrifuge-based EV isolation protocol</b>	<b>78</b>
4.3.1	Comparative EV isolation - First round .....	78
4.3.2	Comparative EV isolation - Second round .....	80
4.3.3	Calculation of actual centrifugation forces and k-factors.....	83
<b>5</b>	<b>Discussion .....</b>	<b>86</b>
5.1	Human MSC immunomodulation .....	86
5.2	MSC immunomodulation in allogeneic and xenogeneic settings.....	91
5.3	MSC secretome products .....	95
5.4	Inter-laboratory comparative study .....	100
<b>6</b>	<b>Summary .....</b>	<b>103</b>

<b>7</b>	<b>References .....</b>	<b>107</b>
<b>8</b>	<b>Curriculum vitae .....</b>	<b>121</b>
<b>9</b>	<b>Acknowledgements.....</b>	<b>124</b>

## ABBREVIATIONS

<b>A</b>	
ABCB5	ATP-binding cassette member B5 cells
ADA	Adipogenic differentiation
AKI	Acute kidney injury
AMI	Acute myocardial infarction
APCs	Antigen presenting cells
ASC	Adipose-derived mesenchymal stromal cells
<b>B</b>	
BM-MSC	Bone marrow-derived mesenchymal stromal cells
<b>C</b>	
CB	Cord blood-derived mesenchymal stromal cells
CCM	Cell conditioned medium
CD	Cell doubling
CD4	Cluster of differentiation 4
CM	Conditioned medium/media
ConA	Concanavalin
COX	Cyclooxygenase
<b>D</b>	
DCs	Dendritic cells
DGC	Density gradient centrifugation
DIRCs	Dermal immune-regulatory cells
DLS	Dynamic light scattering
DMEM	Dulbecco's modified eagle medium
DMSO	Dimethylsulphoxide
DT	Doubling time
dUC	Differential ultracentrifugation
<b>E</b>	
ECACC	European Collection of Authenticated Cell Cultures
eNOS	Endothelial NOS
Epac	Epacadostat
EV/EVs	Extracellular vesicle/s
<b>F</b>	
FACS	Fluorescence-activated cell sorting
FASL	FAS Ligand
FBS	Fetal bovine serum
FCM	Flow cytometry
FGF	Fibroblast growth factor
FITC	Fluorescein isothiocyanate
FSC	Forward scatter
<b>G</b>	
GMP	Good manufacturing practices
GvHD	Graft versus host disease
<b>H</b>	

HGF	Hepatocyte growth factor
HLA	Human leukocyte antigen
hMSC	Human mesenchymal stromal cells
<b>I</b>	
IDO	Indoleamine 2,3-dioxygenase
IDO-1	Indoleamine 2,3-dioxygenase 1
IFN $\gamma$	Interferon gamma
IL	Interleukin
iNOS	Inducible nitric oxide synthases
IQR	Interquartile range
ISCT	International society for cell therapy
ISEV	International society of extracellular vesicles
<b>J</b>	
<b>K</b>	
KMO	Kynurenine 3-monooxygenase
<b>L</b>	
LPS	Lypopolysaccharides
<b>M</b>	
MC	Mononuclear cells
MHC	Major histocompatibility complex
miRNA	MicroRNA
MISEV	Minimal information for studies of extracellular vesicles
MLR	Mixed lymphocyte reaction
MSC	Mesenchymal stromal cells
MVBs	Multi-vesicular bodies
MVs	Microvesicles
<b>N</b>	
NK	Natural killer cells
nNOS	Neuronal NOS
NO	Nitric oxide
NOS	Nitric oxide synthases
NTA	Nanoparticle Tracking Analysis
<b>O</b>	
OD	Optical density
ODA	Osteogenic differentiaiton
<b>P</b>	
PBMC	Peripheral blood mononuclear cell
PCR	Polymerase chain reaction
PD-1	Programmed cell death 1
PDGF	Platelet-derived growth factor
PDL-1	Programmed death ligand-1
PE	Phycoerythrin
PEG	Polyethylene glycol
PFA	Paraformaldehyd
PGE2	Prostaglandin E2



PHA	Phytohemagglutinin
<b>Q</b>	
QPRT	Quinolinate phosphoribosyltransferase
<b>R</b>	
rMSC	Rat mesenchymal stromal cells
rPBMC	Blood-derived rat PBMC
RPMI	Roswell park memorial institute medium
<b>S</b>	
SD	Sprague-Dawley
SEC	Size-exclusion chromatography
SMC	Spleen-derived rat mononuclear cells
SSC	Side scatter
STAT	Signal transducer and activator of transcription
SVF	Stromal vascular fraction
<b>T</b>	
TEM	Transmission electron microscopy
TFF	Tangential flow filtration
TGF- $\beta$	Transforming growth factor- $\beta$
Th	T helper cells
TNF- $\alpha$	Tumor necrosis factor $\alpha$
Treg	Regulatory T cells
Tryp	Tryptophan
TSG101	Tumor susceptibility gene 101
TSG-6	Tumor necrosis factor-inducible gene 6
<b>U</b>	
UC	Umbilical cord-derived mesenchymal stromal cells
<b>V</b>	
VEGF	Vascular endothelial growth factor
<b>W</b>	
WB	Western blot
WJ	Wharton's jelly-derived mesenchymal stromal cells
<b>X</b>	
<b>Y</b>	
<b>Z</b>	

# 1 INTRODUCTION

## 1.1 Mesenchymal stromal cells

### 1.1.1 General overview

Multipotent mesenchymal stromal cells (MSC) are mesoderm derived fibroblast colony-forming and shuttle-shaped cells under *in vitro* conditions [1]. Friedenstein and colleagues were the first to describe MSC as such. They demonstrated the osteogenic potential of soft connective tissue bone marrow-derived stromal cells to form fibroblastic colonies *in vitro* [2]. Moreover, their potency to differentiate into chondrocytes as well as myoblasts and adipocytes was promptly proven [3, 4]. The hematopoietic stromal activities further increased the interest in MSC research. Subsequently, they were isolated from a variety of adult or fetal sources such as adipose tissue (adipose-derived MSC – ASC), bone marrow (bone marrow-derived MSC – BM), umbilical cord tissue (UC) or cord blood (cord blood-derived MSC – CB), periosteum, synovium, dental pulp, placenta, Wharton’s jelly (WJ)-derived MSC and amniotic fluids, among others [5-7].

Nonetheless, the increasing number of MSC isolation and culture protocols, resulted in a rising number of misconceptions within the field [8]. Some of MSC misconception clarifications are: (1) Although MSC from different sources might be similar in phenotype, they differ in terms of function, immunomodulatory activity and differentiation potential, (2) mismatch in MSC potency *in vitro* and *in vivo*, (3) heterogeneity of MSC amongst diverse species and (4) clinical data is essential to further assess MSC mechanisms of action [8]. Heterogeneity and discordances in terminology and criteria for stromal/stem cells also spread with the increase of research in the field. Therefore, the International Society for Cellular Therapy (ISCT) remarked the appropriate designation as “multipotent mesenchymal stromal cells” [9]. The minimal criteria to define the human derived-MSC (hMSC) are: (a) Plastic-adherence under standard culture conditions, (b) More than 95% of the cell population must be positive for CD105, CD73, and CD90. Moreover, CD45 (leucocytes), CD34 (hematopoietic progenitor), CD14 or CD11b (monocytes and macrophages), CD79a or CD19 (B cells) must be negative, and (c) Differentiation potential to adipocytes, chondrocytes, and osteoblasts [10, 11].

Altogether, these properties have increased MSC interest for their use as a potential cell-based therapy and use in translational research [12]. MSC have been studied in

regards to tissue regeneration, immunomodulation, or graft improvement [6]. Initially, it was widely believed that MSC therapeutic potential were attributed to their differentiation ability. However, nowadays their potentials have been accounted to multiple “modes of action” such as: (1) Differentiation potential, (2) Secretion of trophic factors and (3) Immunomodulatory function, among others (Figure 1).

(1) Differentiation potential is mainly ascribed to their multipotent nature, differentiating into several lineages [13]. MSC skeletal differentiation potential towards chondrogenic and osteogenic lineages, have made them attractive in the context of cartilage defect and bone repair [14]. They have also been reported to differentiate into adipogenic lineages to give rise to connective tissues such as adipose apart from reports suggesting trans-differentiation potential into other lineages as well [14, 15].

(2) The secretion of trophic mediators [16] is particularly essential. MSC ability to affect cells in vicinity and modulate their microenvironment by secreting a broad range of paracrine factors, namely, cytokines and growth factors has been long described [17-19]. Indeed, hepatocyte growth factor (HGF), fibroblast growth factors (FGF), transforming growth factor- $\beta$  (TGF- $\beta$ ), interleukins (IL-1 $\beta$ , IL-6, and IL-8) are some of the factors involved [20, 21]. MSC secreted conditioned medium (CM) also possesses substantial trophic effect, influencing wound acceleration, migration and cell proliferation [22]. Another more recently described possible paracrine mechanism is MSC secreted extracellular vesicles (EV), exosomes or microvesicles (MVs) [23]. EV have strongly arisen as a potential alternative cell-free therapeutic prospect circumventing many of the safety challenges regarded in cell therapy [24].

(3) MSC interact with a wide range of immune cells and have been reported to regulate immune responses in many diseases [25-29]. They present low immunogenicity and express intermediate levels of human leukocyte antigen (HLA) class I antigens and negligibly low levels of HLA class II, aside from lacking expression of costimulatory molecules such as CD40 or CD86 [30-33]. Adult MSC suppression of T-cell proliferation and regulation of Th1/Th2 balance [27, 34, 35], together with MSC action on regulatory T cell (Treg) functions [35] are some of MSC immune modulatory most reported topics.

Indeed, evidences of MSC “modes of action” have been reported in several diseased contexts, as excellently reviewed by Saaedi et al. and Peired et al. [7, 36]. MSC

application mediates and reduces inflammation and fibrosis, decreases apoptosis, promotes angiogenesis and recruits resident progenitor cells.

Altogether, these aspects render them suitable for their application in therapy. Nevertheless, further elucidations on MSC engraftment and specific mechanisms of action involved need to be further assessed. Subsequently, some specific MSC trophic functions and immunomodulatory mechanisms will be reported hereunder.

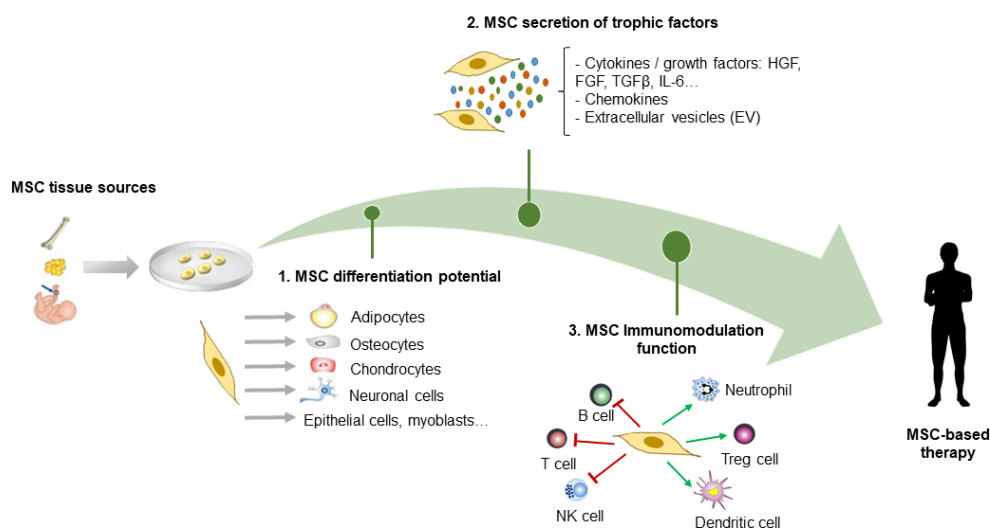


**Figure 1 MSC properties supporting their clinical applications.** MSC are isolated from a wide range of tissue sources (top to bottom- bone marrow, adipose tissue, cord blood...) and can be expanded and characterised. The therapeutic potential of MSC relies on their unique modes of action 1. Differentiation potential, 2. Secretion of trophic factors and 3. Immunomodulatory functions. These characteristics render them suitable for their use in cell-based therapies. HGF: hepatocyte growth factor; FGF: fibroblast growth factor; TGFβ: transforming growth factor beta; IL-6: interleukin 6.

### 1.1.2 MSC Immunomodulation properties

MSC are strong immunomodulators, able to regulate inflammatory progress, skewing microenvironments to an anti-inflammatory state [37], and mediating in numerous immune responses.

It is known that MSC interact with many types of immune cells such as B and T cells, natural killer (NK) cells, dendritic cells (DCs) and macrophages [38]. MSC are efficient at exerting inhibition of activated T cell proliferation through cellular (mixed lymphocyte reaction (MLR)) or mitogenic stimuli, such as anti-CD3/CD28 monoclonal

antibodies or non-specific phytohemagglutinin (PHA) [39-41]. MSC-T cell mechanism of interaction is modulated by direct cell-cell contact, such as programmed death ligand-1 (PDL-1) and vascular cell adhesion molecule-1 [42-44], in cooperation with secreted soluble factors to prompt immunosuppression [32, 45]. Some immune factors involved in exerting modulation are TGF- $\beta$ 1, HGF, prostaglandin E2 (PGE-2), indoleamine 2,3-dioxygenase (IDO), nitric oxide (NO) and interleukin-10 (IL-10) [46-48]. It has been demonstrated that MSC induce immunoregulation involving Fas/Fas-ligand pathway of T cell apoptosis [49], whereas others support arrest of cell cycle at phase G0, promoted by MSC-T cell contact [32]. In direct and indirect MSC and peripheral blood mononuclear cell (PBMC) cocultures, a strong immunosuppression was observed in absence of cell-cell contact [40, 50], while other researchers found a diminished T cell proliferation suppression [42, 51]. This suggests a potential paracrine mechanism [52]. In fact, MSC conditioned media (CM) inhibited CD4 T cell activation via suppression of signal transducer and activator of transcription 3 (STAT3) phosphorylation [53]. Comparably to CM paracrine effect on suppressing T cell proliferation [50], EV isolated from CM exhibited dose-dependent T cell suppression [50].

However, it appears that MSC need to be “licensed” or “activated” to exert their paracrine function optimally, which can be attained by several different external stimuli. This process can be operated through an interferon gamma (IFN $\gamma$ )-independent or –dependent pathway [54]. MSC IFN $\gamma$ -independent priming results in prostaglandin E2 (PGE2) production via cyclooxygenase (COX)-1 and -2, while MSC priming with IFN $\gamma$  induces expression of IDO [19]. The combination of IFN $\gamma$  with tumor necrosis factor  $\alpha$  (TNF $\alpha$ ), IL-1 $\alpha$  or IL-1 $\beta$  can enhance their modulatory effects [55]. In fact, François and colleagues have demonstrated that IFN $\gamma$  priming in cooperation with TNF $\alpha$  increases IDO production in MSC. This, promotes macrophage differentiation into M2 state, which secretes IL-10 and further amplifies MSC immune suppressive function [56].

MSC T cell proliferation inhibition has been closely related to an increased IDO secretion, breaking down the essential amino acid tryptophan (Tryp). Tryptophan depletion, along with an accumulation of metabolites along the kynurenine pathway may lead to a tolerogenic milieu (Figure 2) [19, 56, 57].

### Kynurenine pathway

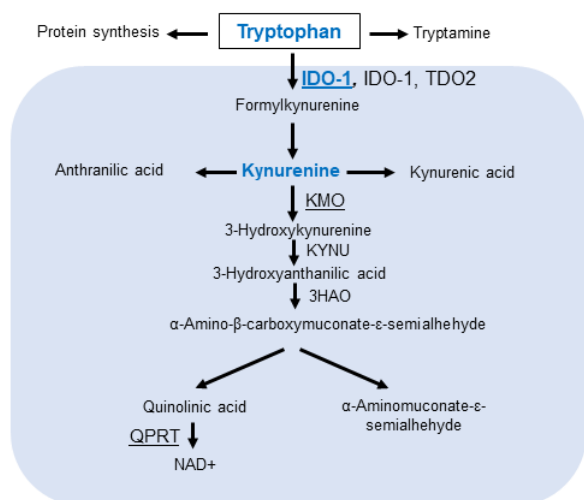


**Figure 2 Simplified diagram of the kynurenine pathway of tryptophan metabolism.** The three main enzymes: indoleamine 2,3-dioxygenase (IDO-1), kynurenine 3-monooxygenase (KMO) and quinolinate phosphoribosyltransferase (QPRT) are shown abbreviated and underlined. The main metabolites measured in this project are depicted in bold (blue). Figure adapted from Jones et al., 2015 [58].

As previously described, MSC from different sources portray subtle differences related not only to their immunomodulatory potencies [59], which might result from the micro environmental niche [60]. In these terms, ASC, BM and CB appear to be modulated by IDO to a large extent [61]. Although some studies describe comparable suppression of T cell proliferation amongst ASC, BM, UC and WJ-MSC [62], others supported ASC as higher suppressors compared to BM irrespective of T-cell activation stimuli [63]. ATP-binding cassette member B5 (ABCB5) cells, novel human dermal immune-regulatory cell (DIRCs) subset presents immune-regulatory functions similar to MSC [64]. They are pure populations enriched by a single molecular marker which have been described to skew M1 pro-inflammatory macrophages, dampening inflammation and ameliorating impaired wound healing *in vivo* [65]. Furthermore, they express tumor necrosis factor-inducible gene 6 protein (TSG-6), which has previously been described in MSC as immunosuppressors promoting tissue repair [66-71]. For instance, it has been confirmed that ABCB5 immunoregulatory function is mediated, at least partially, through co-expressed immunologic receptor, programmed cell death 1 (PD-1) [64, 72]. Studies directly comparing immunomodulatory functions of MSC from different tissue origins are currently limited. Thus, understanding whether their mechanisms of action are directly dependent on their source of origin is of utmost importance. This will be investigated in detail in section 4.1.

Furthermore, the aforementioned studies provide prospect for pre-clinical and clinical studies in diverse research settings such as graft versus host disease (GvHD), autoimmune diseases and transplantation. However, to obtain maximal clinical

benefit, further elucidations of MSC-mediated immunomodulatory functions are particularly required. Furthermore, standardisation of MSC production is relevant for translation into clinical research.

### ***1.1.3 Xenogeneic MSC: Preclinical implications***

As previously described, MSC have been considered for clinical interventions as cell-based therapies. Indications of their use range from acute lung [73] and kidney injury, autoimmune diseases [74], transplantation [75] and diabetes, among others. To elucidate their mode of action, autologous [76], allogeneic [77] and xenogeneic [78] cells have been tested in animal models. The application of hMSC in animal models is not only done to understand their therapeutic effects but also required by regulatory authorities to perform efficacy but also safety studies. However, the use of hMSC in animal models raises several debates and concerns. The possibility of an adverse immune reaction or even the non-functionality of certain modes of actions represents an important aspect that cannot be underestimated. For a long time, due to MSC low expression of HLA class I and lack of costimulatory molecules, they have been considered to be immune privileged. This, along with their host immune system suppression, make them suitable for transplantation across species [79]. The key modulator effector used by MSC-mediated immunosuppression fall into two categories: mainly IDO-mediated (human, monkey, pig) or mainly inducible nitric oxide synthases (iNOS)-mediated (mouse, rat, rabbit) [80]. Nitric oxide (NO) is a prominent candidate involved in MSC-mediated immunosuppression in murine settings. NO production is catalysed by the nitric oxide synthases (NOS): iNOS, endothelial NOS (eNOS) and neuronal NOS (nNOS). In the presence of proinflammatory cytokines MSC induce iNOS expression which has an imperative role in immune regulation [81, 82]. Nitrite, a stable breakdown product of NO, is generally measured as accumulated in supernatants to quantify nitric oxide secretion [51].

NO ameliorates T cell-mediated murine GvHD [83] and other autoimmune diseases such as experimental autoimmune encephalomyelitis [84] or uveitis [85]. However, the specific mechanism by which NO exerts these effects are controversial. Recruitment of immune cells in close proximity to MSC is thought to be crucial for NO to inhibit T cell proliferation, due to the exertion of local action [51]. In fact, chemotaxis has been described as a crucial component of NO immunosuppression

by murine MSC [55]. Many studies have described cross species function, as for instance, hASC implantation into immunocompetent rat hearts in a murine model of myocardial infarction. ASC were able to survive the xenogeneic mismatch for an extended period of time, revealing significant cardiac function amelioration [86]. hASC infusion in a cisplatin-induced nephrotoxicity murine model portrayed increased survival, improved tissue injury and renal dysfunction [87]. Moreover, multiple other xenogeneic experimental models have demonstrated positive immunomodulatory function in a cross-species framework [88-91]. Some of these regard acute renal failure, diabetes mellitus or autoimmune diseases.

After xenogeneic MSC administration, conversely, some studies reported humoral and/or cellular responses [92, 93]. Additionally, in a recent study conducted by Lohan et al., immunomodulation of hMSC were ineffective in a rat model of corneal transplantation due to interspecies incompatibilities. Indeed, the authors claim hMSC are not able to be properly primed in a xenogeneic environment and therefore cannot exert their immune modulatory action [94]. Moreover, *in vitro* experiments performed by the aforementioned group revealed that hMSC did not respond to rat pro-inflammatory cytokines and did not suppress proliferation of rat T-lymphocytes, highlighting a potential preclinical barrier to clinical translation.

Taken together these data clearly indicate pronounced discordances regarding the outcome of xenogeneic MSC infusion. Overall, it is challenging to guarantee hMSC long-term engraftment or functionality in animals. Thus, preclinical data need to be carefully interpreted especially when considering a possible translation to clinical field.

## **1.2 MSC-derived extracellular vesicles**

### **1.2.1 General overview**

MSC secrete a wide variety of soluble factors such as cytokines, chemokines, growth factors and immunomodulatory molecules [95], in addition to vesicles secreted to the extracellular space, which have been described as “MSC secretome”. Their secretome has been investigated in numerous clinical settings, either by utilising MSC conditioned media (CM) or MSC-derived extracellular vesicles (EV) [96]. They are known to modulate responses in a diversity of physiological processes [97, 98]. EV are bilayer membrane structures released by all cell types under normal- or



patho-physiological conditions. EV is a term that comprises a broad variety of released vesicles, namely, exosomes and MV. MV are commonly referred to as released vesicles with sizes ranging from 50 to 1000 nm by direct budding or shedding of the plasma membrane [99]. On the other hand, exosomes, ranging 40 to 200 nm, are originated by invagination of the endosomal membrane of multi-vesicular bodies (MVB) with the subsequent release of exosomes due to fusion of MVB with the plasma membrane [100, 101]. Nevertheless, the term EV is used as a collective description for both small and larger released vesicles. MSC-EV carry a wide range of molecules that directly affect their mode of action. These comprise proteins involved in cell trafficking, membrane receptors, adhesion molecules, cytokines and chemokines [102]. Moreover, they also present nucleic acids such as mRNAs, microRNAs (miRNA) and extra-chromosomal DNA [100, 103].

They bear a vital role in intercellular communication and regulation of recipient cell action through autocrine [104], paracrine [105], endocrine [106] or exocrine cell signalling [100]. EV seem to depict similar biophysical characteristics of parental MSC, possessing anti-apoptotic, angiogenic and immunomodulatory properties [107]. These properties could benefit EV modulation through enhancement of the inflammatory niche. Additionally, MSC-CM is also able to replicate MSC-mediated immunosuppression effects [108, 109]. Despite numerous functions having been strongly attributed to EV, the specific roles and immunological effects are still poorly understood.

EV represent a novel cell-free alternative which may overcome the limitations of MSC based therapy [110]. Thus, they have been utilized for clinical applications as immunosuppressants, enhancing repair and differentiation or as therapeutic drug carriers [111-113]. In spite of EV-mediated therapy being considered safe, a relevant hindrance is the commonly low EV yield [23], together with the lack of robustness in EV isolation methods [114]. Data comparability has become challenging due to the production of dissimilar EV populations, strongly dependent on the method of isolation.

Differential ultracentrifugation (dUC) was considered the “golden standard” of EV isolation. EV are isolated based on their density and size by sequentially increasing centrifugal forces to pellet cells and cell-debris (<1500g), microvesicles (10.000-20.000g) and exosomes (100.000-200.000g) [115, 116]. Although UC is well

established and cost-efficient, this method has major limitations, such as being inconsistent in reproducing isolation data [117]. Consequently, this method is vastly susceptible to multiple parameters, which might be challenging to control, such as rotor type, k-factor or solution viscosity [117]. However, alternative isolation methods such as polyethylene glycol (PEG)-based precipitation, size-exclusion chromatography (SEC) or precipitation [117-120], also present many drawbacks. Table 1 depicts an overview of the commonly used methods of EV isolation, describing their principles, main advantages and disadvantages [115-117, 121].

**Table 1 Overview of commonly used EV isolation methods.** dUC indicates differential ultracentrifugation; DGC, density gradient centrifugation; SEC, size-exclusion chromatography and EV, extracellular vesicles.

Method	Principle	Advantages	Disadvantages
dUC	Sequential separation of EV and other biofluid components based on their density and sedimentation rate	High EV yield, medium to large sample volumes, easily scalable, established protocols	Potential EV damage, vesicle aggregation, low purity, time-consuming
DGC		Prone to combine with other methods, higher purity compared to dUC	Low yield, low throughput, time-consuming
Ultrafiltration	EV isolation is exclusively based on the size differences between EV and other constituents	Parallel sample processing, prone to combine with other methods, small to large sample volumes, portable, fast	Shear stress, EV loss on membrane, potential particle aggregates
SEC		Moderate to high purity, availability of commercial kits, moderate to high purity, preservation of EV integrity	Fractions might be sample-dependent, not suitable for large scale studies, laborious
Precipitation	Solubility of EVs is altered by water-excluding polymers or manipulation of EV surface charge	Small to large sample volumes, high yield, parallel sample processing, prone to combine with other methods, scalable, fast	Highly unspecific, co-precipitation of protein complex, washing of precipitation reagent (for some applications)
Affinity	Interaction between capture antibodies and specific EV surface molecules	High purity, subtyping of EV populations, commercial kits available, parallel sample processing	Limited scalability, small sample volume, expensive, bias for specific populations
Microfluidics	Microscale isolation based on a variety of EV properties including immunoaffinity, size and density	Minimal volume isolation, portable, fast, easy integration	Lack of standardisation and validation, low to moderate throughput, expensive

Furthermore, the Minimal information for studies of extracellular vesicles (MISEV) guidelines [122] specifies a list that defines EV isolation/separation, characterisation and principles of their functional studies. Correctly characterizing EV isolates is

crucial to be able to associate functions uniquely to EV rather than their co-isolated particles [123]. The International Society of Extracellular Vesicles (ISEV) suggests to (1) quantify numbers of EV secreting cells, (2) determine EV particle numbers, (3) define presence of EV associated constituents and (4) define existence of co-isolated components. The principal objective of these guidelines was to raise awareness in the EV field (researchers, journal editors/reviewers) and to create a solid basis for the translation to future therapeutic applications. Thus, NTA, TEM, western blot (WB) and FACS are the most typical characterisation methods used. Table 2 depicts an overview of these and other commonly used methods of EV characterisation, describing their main advantages and disadvantages [115, 116, 124-128].

**Table 2 Overview of commonly used EV characterisation methods.** NTA indicates Nanoparticle Tracking Analysis; TEM, transmission electron microscopy; FCM, flow cytometry; DLS, dynamic light scattering; WB, western blot; PCR, polymerase chain reaction.

Measured analyte	Method	Advantages	Disadvantages
Particle	NTA	Analysis of EV size, concentration and charge	Issues with fluorescence detection, limited specificity, detection of contaminants
	TEM	Visualises EV morphology	Possible loss/damage of samples due to preparation, dedicated equipment
	FCM	Able to measure samples with low yield	Limited sensitivity, prone to "swarm" artefacts, bead-based approach needed for detection, dedicated equipment
	DLS	Physiological condition analysis	Limited specificity, low sample resolution
	Cryo-EM	No fixation or dehydration artefacts, stain-free visualisation	Low signal-to-noise ratio, dedicated equipment, artefacts
Protein	WB	Established protocols, simple readout, low cost	Low throughput, not quantitative method
	ELISA	Availability of commercial kits, already established protocols	Antibody-dependent immunoreactivity, possible cross-reactivity
Nucleic acids	Northern/Southern blot	High specificity	Large amount of sample required, time consuming
	Microarray	Established protocols, multiple gene simultaneous analysis	Low sign-to-noise ratio, hybridisation-dependent

Thus, even when considering MISEV guidelines, the need of combining several methods of characterisation to correctly define EV isolates within your sample might

be an important point of inflexion. Therefore, interpretation of characterisation data must be cautiously evaluated. In short, in order to implement MSC-EV in clinical studies, it has become necessary to perform EV scalable good manufacturing practices (GMP)-manufacturing [129] along with technical standardisation of EV methodology to ensure comparability amongst studies [130].

### **1.2.2 MSC-EV mediated immunomodulatory effects**

MSC secretome has been widely used in many different systems, stimulating vascularisation [131], modulating the immune system [131], operating as response modulators [97, 98], recruiting other cells. Growth factors and cytokines (vascular endothelial growth factor (VEGF), TGF $\beta$ , interleukins) secreted in MSC-CM or enclosed in EV, serve as paracrine MSC effector molecules.

EV inhibitory functions on activation of immune cells has been demonstrated in several studies. For instance, EV have been described to inhibit activity of B cell proliferation [132], as well as increase IL-10 immunosuppressive cytokine secretion and regulatory / effector T cell ratio [133]. Moreover, human ASC-derived EV managed to suppress T cell proliferation and IFN $\gamma$  release [134]. In another study, testing MSC-EV effect on type 1 diabetic patient PBMC's, they suggested a switch of T cells from a pro- to an anti-inflammatory state [135].

Although these studies have reported EV modulatory functions on immune cell proliferation, there are opposing evidences. For instance, Gouveia de Andrade et al. and Conforti et al. have described an absence or reduction in immunomodulatory effects of EV on lymphocyte suppression [132, 136]. These outcome discrepancies might be dependent on changes in the microenvironment, which could potentially influence the release and biological state of EV [99]. In addition, EV potential effectors of immunomodulation might vary with respect to MSC modulatory mechanisms.

In fact, immunomodulation exerted by EV seems not to be mediated by IDO pathway, unlike MSC, but by PD-L1 [137]. Furthermore, galectin-1, endogenous leptin also present on EV surface, has been found to be involved in immunomodulatory action [133]. Priming in an inflammatory environment increased miRNA (miR-155 and -146) EV levels, that intervene in inflammatory reaction regulation [137]. Moreover, CD73 present on MSC-EV actively induces adenosine formation, which thereby suppresses immune responses [138]. Due to the various EV-derived effectors involved in

immunomodulation and the controversial *in vitro* outcomes reported, further studies are suggested to elucidate their emerging role in the immune system.

EV application in *in vivo* studies have portrayed similar results as those seen with MSC. For instance, MSC-EV application in acute kidney injury (AKI) murine models have specifically seen a decrease in apoptosis, fibrosis and oxidative stress [139-142], together with a promotion of angiogenesis [143-145]. A concomitant increase of anti-inflammatory cytokines and decrease of pro-inflammatory ones was also observed [139, 146, 147]. Given the fact that MSC-EV exert similar effects as their parental cells, some researchers consider them as an alternative to cell therapy. EV could probably overcome some of the regulatory challenges that cells face in clinical translation.

Although research on MSC-EV still presents numerous challenges, their *in vivo* stability, low immunogenicity and long half-life provide them with potential advantages in the growing development of cell-free therapy. Further understanding of their specific mechanisms, underlying the identification of the “active substance/component” responsible for the biological activity of novel EV therapeutics, is required.

## 2 AIMS OF THE STUDY

The use of MSC as instruments for cell-based therapy has been the focus of intense research opening new perspectives for treatment of numerous diseases. The diverse sources from which MSC can be isolated might affect their immune modulatory properties. However, even if MSC are known to modulate immune responses and regeneration, the lack of consensus in their specific mechanisms of action and their thorough safety and efficacy evaluation, restrict the translation into clinical research. Some studies have reported that MSC-secretome, including CM and EV may pose further benefit with respect to increased homogeneity and purity. In fact, EV are considered biologicals, with a much less regulatory burden than their cellular counterpart. However, EV are quite a recent field of investigation and not much is currently known regarding their optimal isolation, characterisation and use. Thus far, conflicting evidences have proposed them as alternative tools to ameliorate pathological symptoms of GvHD or autoimmune diseases, for instance. We therefore proposed whether EV could take over MSC immunomodulatory potential as cell-free therapeutic tools. In that instance, we first aimed to define different MSC modulatory properties/mechanisms. Second, we evaluated the impact of MSC-secretome on immunomodulation. Finally, we sought to test reproducibility of standardised and well-defined UC-EV isolation protocol. Thus, hereunder we describe the three main aims around which this dissertation was developed (Figure 3).

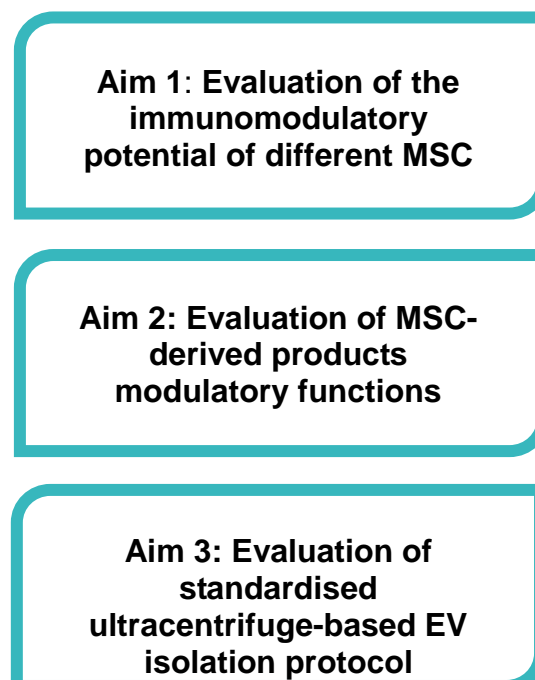


Figure 3 Aims of the study.

**Aim 1: Evaluation of the immunomodulatory potential of different human MSC sources**

We hypothesised that MSC isolated from different human tissue sources would differ in terms of their immunomodulatory functions. Thus, BM-MSC, CB-MSC and ASC modulatory strength was assessed in cocultures with PHA stimulated PBMC or purified CD4 T cells. Similarly, this was tested with ABCB5 cells. Moreover, MSC-IDO expression was evaluated as potential immunosuppressive mechanism. Addition to the cultures of tryptophan, IFN $\gamma$  and IDO inhibitor, Epacadostat (Epac) was further assessed, along with analysis of modulatory factors within the supernatants.

Furthermore, to verify whether MSC modulatory strength is affected by potential interspecies incompatibilities, rat-human allogeneic and xenogeneic cocultures were set. Supernatant analysis was used to investigate factors involved and their specific mechanisms of action.

**Aim 2: Evaluation of MSC-derived products modulatory functions**

Hypothesising that the immunomodulatory potential of MSC-derived products would be similar to their cellular counterpart. First, interactions between MSC and PBMC were assessed through MSC:PBMC direct and indirect (transwell) cocultures.

Second, we established cocultures with human PBMC and CM or isolated MSC-EV derived from +/- IFN $\gamma$  preconditioned MSC. PBMC proliferation and analysis of coculture supernatants were performed. This required the establishment and characterisation of EV. Especially, we established a method for flow cytometric assessment of EV marker expression.

**Aim 3: Evaluation of standardised UC-based EV isolation protocol**

To verify whether a well-defined UC-based EV isolation protocol is reproducible amongst various different laboratory settings we performed a comparative study. This study involving several expert EV groups enriched EV from equal starting material. EV basic characterisation methods (NTA, WB, TEM, FACS) were performed and technical variations induced by equipment and/or operators were assessed.

### 3 MATERIAL AND METHODS

#### 3.1 Material

##### 3.1.1 Cells

Cell type	Source / Manufacturer
Adipose derived human mesenchymal stromal cells (ASC)	Mannheim Ethics Commission II (vote number 2006-192 N-MA);
	Self isolated in laboratory.
Bone marrow derived human mesenchymal stromal cells (BM)	Mannheim Ethics Commission II (vote number 2015-520N-MA);
	Cryopreserved in our laboratory from prior isolations.
Cord blood derived human mesenchymal stromal cells (CB)	Mannheim Ethics Commission II (vote number 49/05);
	Self isolated in laboratory.
Bone marrow derived rat mesenchymal stromal cells (rMSC)	Material kindly provided by Dr. Yuxi Feng from control experiments of licensed animal experimentations;
	Isolated in our laboratory by BTA Susanne Elvers-Hornung.
ABCB5+ cells	Kindly provided by Ticeba-RHEACELL GmbH & Co. (Heidelberg, Germany) as a collaboration.
HCT116 cells	European Collection of Authenticated Cell Cultures (ECACC) (Cat no. 91091005; Salisbury, UK).
Human Peripheral blood mononuclear cells (PBMC)	Provided by the German Red Cross Blood Donor Service in Mannheim, Germany. Leukapheresis samples: Mannheim Ethics Commission II (vote number 2018-594N-MA).
	Self isolated in laboratory from buffy coats or leukapheresis samples.
Rat blood Peripheral blood mononuclear cells (rPBMC)	Kindly provided by Prof. Norbert Gretz from control experiments of licensed animal experimentations;
	Self isolated in laboratory.
Rat spleen mononuclear cells (SMC)	Kindly provided by Prof. Norbert Gretz from control experiments of licensed animal experimentations;
	Self isolated in laboratory.



**3.1.2 Cell culture products**

Product	Company	Catalog No.
DMEM	PAN Biotech	P04-01500
RPMI 1640	Lonza	12-918F
DMEM/F12 (1:1) 1x	Gibco	11320-074
Mesenchymal Stem Cell Adipogenic Differentiation Medium	Promocell	C-28016
Mesenchymal Stem Cell Osteogenic Differentiation Medium	Promocell	C-28013
Supplement mix Adipogenic Differentiation Medium	Promocell	C-39816
Supplement mix Osteogenic Differentiation Medium	Promocell	C-39813
Hoechst 33342	Invitrogen	917368
Adipored assay reagent	Lonza	PT-7009
Collagenase NB 6 GMP Grade	Serva	17458
Human allogeneic serum pooled from healthy AB donors (AB serum)	German Red Cross Blood Donor Service, Institute Mannheim	
Fetal Bovine Serum (FBS serum)	Merck Millipore	50115
Penicillin/Streptomycin	PAN Biotech	P06-07100
L-glutamine		P04-80100
Trypsin/EDTA		P10-024100
EDTA	Applichem	A3145,0500
DPBS (1X)	Gibco	14190-094
Dymethylsulphoxide (DMSO)	Wak-chemie Medical GmbH	WAK-DMSO-10
Ficoll-Paque™ Premium	GE Healthcare Bio-science AB	17-5442-03
Albumin fraction V (bovine serum albumin)	Carl Roth	8076.2
IL-2 human recombinant	PromoCell	C-61240
Phytoemagglutinin-L (PHA)	Merck Millipore	M5030
Concanavalin A (ConA)	Sigma Aldrich	C0412-5MG
Epacadostat (Epac)	Selleckchem	57910

IFN $\gamma$	R&D	285-IF
L -Tryptophan	Santa Cruz	sc-280888
Casy-Ton	OMNI Life Science	5651808

### 3.1.3 Cell culture media

Media	Composition
Full DMEM AB	500 ml DMEM
	10% AB serum
	1% Penicillin/Streptomycin
	2% L-glutamine
Depleted DMEM AB	500 ml DMEM
	10% EV-depleted AB serum
	1% Penicillin/Streptomycin
	2% L-glutamine
DMEM FBS	500 ml DMEM
	10% FBS serum
	1% Penicillin/Streptomycin
	2% L-glutamine
Depleted DMEM FBS	500 ml DMEM
	10% EV-depleted FBS serum
	1% Penicillin/Streptomycin
	2% L-glutamine
DMEM/F12	500 ml DMEM
	10% FBS serum
	1% Penicillin/Streptomycin
Depleted DMEM/F12	500 ml DMEM
	1% EV-depleted FBS serum
	1% Penicillin/Streptomycin
Full RPMI 1640	500 ml RPMI 1640
	10% FBS
	1% Penicillin/Streptomycin
Inactivated RPMI 1640	500 ml RPMI 1640
	10% heat inactivated FBS
	1% Penicillin/Streptomycin
MSCGM (MSC Growth Media)	500 ml MSCGM
	10% FBS serum
	1% Penicillin/Streptomycin

	2% L-glutamine
Ham's F-10	500 ml Ham's F-10
	15% Stem cell media
	1% Penicillin/Streptomycin
	2% L-glutamine

### 3.1.4 Flow cytometry

#### 3.1.4.1 Flow cytometry solutions

Name	Composition
FACS Buffer	1L DPBS
	0.4% BSA
	0.02% NaN <sub>3</sub>
	Adjust to pH 7,4

#### 3.1.4.2 Flow cytometry Antibodies

Antibody	Fluorochrome	Clone	Manufacturer	Catalog No.
Anti-IDO	PE	eyedio	12-9477-42	eBioscience
<b>Human MSC characterisation</b>				
Anti-CD29	Alexa Fluor 488	TS2/16	BioLegend	303016
Anti-CD73	PE	AD2	BD Biosciences	550257
Anti-CD90	APC	5E10	BD Biosciences	559869
Anti-CD44	APC	IM7	BioLegend	103012
Anti-CD31	APC	WM59	eBioscience	17-0319-73
Anti-CD34	PE	8G12	BD Biosciences	345802
Anti-CD146	PE	TEA1/34	Beckman Coulter	A07483
Anti-CD45	FITC	HI30	BD Biosciences	555482
NG-2	Alexa Fluor 488	9.2.27	eBioscience	53-6504
Anti-CD140a	PE	16A1	BioLegend	323506
Anti-CD140b	APC	18A2	BioLegend	323608

Anti-CD105	APC	SN6	eBioscience	17-1057-42
Anti-CD106	FITC	51-10C9	BD Biosciences	551146
Anti-HLA-ABC	PE	REA230	Miltenyi	130-101-460
Anti-HLA-DR	FITC	L243	BioLegend	307618
<b>Rat MSC characterisation</b>				
Anti rat-CD45	FITC	OX-1	Bio-Rad	MCA43GA
Anti rat-CD90	PE	OX-7	BD Biosciences	551401
Anti rat-CD44	APC	12K35	Lifespan Biosciences	LS-C182786
<b>EV characterisation</b>				
<b>Panel 1</b>				
Anti-CD9	PerCP Cy 5.5	M-L13	BD Biosciences	561329
Anti-CD44	APC/Cy7	IM7	BioLegend	103028
Anti-CD73	PE	AD2	BioLegend	344004
Anti-CD81	APC	REA513	Miltenyi	130-107-921
<b>Panel 2</b>				
Anti-CD9	PerCP Cy 5.5	M-L13	BD Biosciences	561329
Anti-CD63	BV421	H5C6	BioLegend	353029
Anti-CD81	PE/Cy7	5A6	BioLegend	349511
Anti-Alix	PE	1A12	Santa Cruz	sc-53540
Anti-TSG101	Alexa Fluor 647	C-2	Santa Cruz	sc-7964
Anti-Calnexin	Alexa Fluor 647	E10	Santa Cruz	sc-46669

### 3.1.4.3 Other buffers and reagents

Product	Company	Catalog No.
Cell wash	BD Biosciences	349524
IC Fixation Buffer	eBioscience	00-8222-49
Permeabilisation Buffer 10x	Invitrogen	00-8333-56
Cytotell Green	ATT Bioquest	22253
Sytox Blue	Invitrogen	S34857
Sytox Red	Invitrogen	S34859
FcR blocking reagent (human)	Miltenyi	130-059-901
Fixable Viability dye eFluor450 (eF450)	Invitrogen	65-0863-14
Precision Count beads	BioLegend	424902

### 3.1.5 Extracellular vesicles

#### 3.1.5.1 Extracellular vesicle solutions/buffers

Name	Composition
Bovine serum albumin 0.1% buffer	50ml DPBS
	0.1% BSA
Bovine serum albumin 1% buffer	50ml DPBS
	1% BSA
Bovine serum albumin 2% buffer	50ml DPBS
	2% BSA
Bovine serum albumin 10% buffer	50ml DPBS
	10% BSA
Glycine 1M	50ml distilled water 3.75g Glycine

#### 3.1.5.2 Extracellular vesicle reagents

Product	Company	Catalog No.
CD9 Exosome-human beads	Invitrogen	10620D
Aldehyde/Sulfate latex beads, 4%, 4µm	Invitrogen	A37304

NaCl 0,9%	Braun	19154450
Glycine	Serva	23390
Albumin Fraction V (bovine serum albumin)	Carl Roth	8076.2

### 3.1.6 Western blot

#### 3.1.6.1 Western blot solutions

Name	Composition
Tris buffer saline (TBS) 10x	1L DPBS
	6.05g Tris
	8.76g NaCl
	Adjust to pH 7,6
Tris buffer saline 1x + Tween (TBS-T)	TBS + 0.1% Tween 20
Towbin buffer	70% deionized water
	20% methanol
	10% 10X TGS
Blocking buffer	5% BSA in TBS-T

#### 3.1.6.2 Primary Antibodies

Antibody	Dilution	Clone	Species	Manufacturer	Catalog No.
Anti human-CD9	1:300	C-4	Mouse	Santa Cruz	sc-13118
Anti human-CD63	1:300	MX-49.129.5	Mouse	Santa Cruz	sc-5274
Anti human-CD81	1:300	5A6	Mouse	BioLegend	349501_02
Anti human-Alix	1:500	3A9	Mouse	BioLegend	634501_02
Anti human-TSG101	1:500	4A10	Mouse	Thermo Fisher	MA1-23296
Anti human-Calnexin	1:500	AF18	Mouse	Santa Cruz	sc-23954

### 3.1.6.3 Secondary Antibodies

Antibody	Dilution	Clone	Species	Manufacturer	Catalog No.
Anti-mouse IgG HRP Linked whole Ab	1:2000	Polyclonal	Sheep	GE Healthcare Bio-science AB	NA931

### 3.1.6.4 Western blot solutions and material

Product	Company	Catalog No.
Run buffer, Tris/Glycine/SDS (TGS)	Bio-Rad	1610772
4x Laemmli sample buffer	Bio-Rad	161-0747
$\beta$ -mercaptoethanol	Sigma Aldrich	M7522-100ml
Page Ruler Plus	Thermo Fisher	26619
Precision plus protein, Dual color standards	Bio-Rad	1610374
Pierce RIPA Buffer	Thermo Fisher	89900
Halt protease inhibitor single-use cocktail (100x)	Thermo Fisher	78430
Tween 20	Serva	37470.01
10X TGS	Bio-Rad	161-0772
Methanol	Carl Roth	8388.5
10X TGS	Bio-Rad	1610732
Nitrocellulose blotting membrane	GE Healthcare Bio-science AB	1060000
Filter paper (Whatman)	Sigma Aldrich	WHA10537138
Mini Trans-blot filter paper	Bio-Rad	1703932
Page blue	Thermo Fisher	24620
Mini-PROTEAN TGX Precast gels, 4-15%	Bio-Rad	456-1083DC
Criterion XT Precast gels; 4-12%	Bio-Rad	345-0124

### 3.1.7 Protein detection

#### 3.1.7.1 Reagents

Product	Company	Catalog No.
L-Kynurenine	Santa Cruz	sc-202688
Trichloroacetic acid	Fluka Riedel-de Haen	33209
4-(Dimethylamino)benzaldehyde	Santa Cruz	sc-202888
Sodium nitrite	AppliChem	A7014,0500
Sulfanilamide	AppliChem	A3971,0100
N-(1-Naphyl)-ethylendiamine dihydrochloride (Naphtylamine)	Carl Roth	4342.1
Double distilled water	Carl Roth	3478.1

#### 3.1.7.2 Kits

Product	Company	Catalog No.
Pierce BCA Protein Kit	Thermo Fisher	23227

### 3.1.8 Solutions

Name	Composition
PBS/EDTA	500 ml DPBS
	2mM EDTA
Stopping Medium	50 ml DPBS
	10% FBS
Freezing Medium	FBS
	10% DMSO
10x Erythrocyte lysis Buffer (ammoniumchlorid)	Distilled water
	1.55 mM NH <sub>4</sub> Cl
	0.1 M NH <sub>4</sub> HCO <sub>3</sub>
	1 mM EDTA



**3.1.9 Consumable laboratory material**

Product	Company	Catalog No.
25 cm <sup>2</sup> cell culture flasks	Thermo Fisher	156367
75 cm <sup>2</sup> cell culture flasks	Thermo Fisher	156499
175 cm <sup>2</sup> cell culture flasks	Thermo Fisher	159910
6-well cell culture plate	Thermo Fisher	140675
12-well cell culture plate	Thermo Fisher	150628
24-well cell culture plate	Thermo Fisher	142475
96-well cell culture plate	Eppendorf	0030 790.119
Round bottom 96-well cell culture plate	Greiner Bio-one	650180
Cell culture inserts (pore size 0.4 µm PET track-etched membrane)	BD Biosciences	35-3095
Petri dish	BD Biosciences	351008
15 ml Cell star tubes	Greiner Bio-one	188271
50 ml Cell star tubes	Greiner Bio-one	227261
10-20 µl sterile filter tips	Star Lab	S1120-3710
200 µl sterile filter tips	SurPhob	VT0243X
1000 µl sterile filter tips	SurPhob	VT0263X
1.25 ml Precision Dispenser (PD) sterile tips	Brand	702386
2.5 ml PD sterile tips	Brand	702388
5 ml PD sterile tips	Brand	702390
10 ml PD sterile tips	Brand	631060
5 ml serological sterile pipettes	Star Lab	180806-069
10 ml serological sterile pipettes	Star Lab	180720-070
25 ml serological sterile pipettes	Star Lab	190105-071
Cell strainer, 70µm	Sarstedt	83.3945.070
Cell strainer, 100µm	Sarstedt	83.3945.100
50 ml syringe	Dispomed	21050
10 ml syringe	Dispomed	20010
5 ml syringe	Braun	4606051
1 ml syringe	BD Biosciences	300013
Rotilabo syringe filters 0.22 µm	Carl Roth	SE2M035I07
Syringe filters 0.45µm	NeoLab	3-1904

ReliaPrep syringe filter 1.2µm	NeoLab	8-7050
0.2 ml thin-walled tubes with flat caps	Thermo Fisher	AB0622
Cryopreservation tubes	Greiner Bio-one	122278
1.5 ml tubes	Eppendorf	0030 125.150
1.6 ml tubes (Low binding, DNA-DNase, RNase free)	Biozym Scientific	710176
5 ml Polystyrene round bottom FACS tubes	Corning	352052
Polycarbonate ultracentrifuge tubes (OAKRIDGE)	BeraneK Laborgeräte	314348
Ultrasealing lid, plug and O-ring	BeraneK Laborgeräte	314347
CASY cup	OMNI Life Science	5651794
Gloves	Hartmann	3538071
Pursept A Xpress	Schülke	SMH 230131
Scalpels	Braun	10567364

### 3.1.10 Laboratory equipment

Device	Model	Manufacturer
Centrifuge	ROTINA 420	Hettich Zentrifugen
Centrifuge	ROTINA 420R	Hettich Zentrifugen
Centrifuge	5415R	Eppendorf
Small Centrifuge	Minispin	Eppendorf
Cell counter	CASY	OMNI Life Science
Cell counter	Nucleo Counter	Chemometec
Microscope	Axiovert 100	ZEISS
Microscope	Axiovert 40C	ZEISS
Microscope Camera	AxioCam M Rc	ZEISS
Live imaging microscope	IncuCyte Zoom live imaging device	Essen BioScience, Ltd.
Sterile laminar flow hood	Hera safe	Thermo Fisher Electron Cooperation
Chemical flow hood	Airflow-Control EN14175	Caspar and Co. Labora
Cell culture incubator	CB210	Binder
Cell culture pump	Vacusaft Comfort	Integra Biosciences
Cell culture shaker	Lab Dancer	IKA
Water bath	Aqualine AL 12	Lauda
Water bath	WNE 7	Memmert

Magnet stirrer	MR Hei-Standard	Heidolph Instruments
pH-Meter	pH 211	Hanna Instruments
Microplate reader	TECAN infinite M200PRO	TECAN
Thermal cycler	DNA Engine Cycler	BioRad
Flow cytometer	BD FACS Canto II	BD Biosciences
Flow cytometer	FACS Aria IIIu	BD Biosciences
Chemiluminescent detector	FusionCapt Advanced Solo 4	Vilbert Lourmat
Horizontal shaker	Thermo Mixer C	Eppendorf
Rotator	SB2	Stuart
Chamber shaker	UniHood 650	Edmund Bühler
Precision scale	EW 2200-2NM	Kern & Sohn
Precision scale	ABJ 22-4M	Kern & Sohn
Electrophoresis power supply	EV331	Peqlab
Ultracentrifuge Sorvall WX Ultra series	Sorvall WX Ultra 100	Thermo Fisher
Ultracentrifuge Fixed angle rotor	Sorvall T-865	Thermo Fisher
Ultracentrifuge Swing out rotor	Sorvall SureSpin 630	Thermo Fisher
Nitrogen tanks	Biosafe UN 1977	Cryotherm
Autoclave	V-150	Systec
Zetaview	PMX 220 ZetaView TWIN Laser	Particle Metrix

### 3.1.11 Software for data analysis

Software	Version	Company
FlowJo	10	FlowJo, LLC, Ashland, OR, USA
	7.6.5	
GraphPad Prism	7	GraphPad Software Inc. San Diego, USA
	6	
Word	Microsoft 10	Redmond, WA, USA
Excel		
Powerpoint		
i-Control	1.10	TECAN

## **3.2 Methods**

### **3.2.1 *Evaluation of immunomodulatory potential of different MSC sources***

#### **3.2.1.1 *MSC Isolation***

##### **3.2.1.1.1 Adipose derived mesenchymal stromal cells (ASC)**

After obtaining informed consent (Mannheim Ethics Commission II; vote numbers 2010-262 N-MA, 2009-210 N-MA, 49/05 and 48/05), adipose derived mesenchymal stromal cells (ASC) were isolated from healthy donors. Raw lipoaspirate samples were extensively washed with sterile PBS to remove cellular debris and red blood cells in a 1:1 ratio and then centrifuged at 420g during 10 minutes (no brake). Samples were treated with 0.15% w/v Collagenase type I for 45-60 min at 37°C with gentle agitation adding the same amount of collagenase as lipoaspirate volume (1:1 dilution). Inactivation of the collagenase was achieved by adding an equal volume of DMEM/10% fetal bovine serum (FBS), then centrifuging at 1200g during 10 minutes to obtain a high density stromal vascular fraction (SVF) pellet. Supernatants were aspirated and pellets incubated during 10 minutes with erythrocyte lysis buffer to remove red blood cells. Following a centrifugation step, SVF pellets were then resuspended in DMEM 10% FBS and filtered through a 100µm nylon mesh filter (Falcon® 100 µm cell strainer) prior to centrifuging the filtrate at 1200g during 10 minutes to obtain the enriched SVF pellet. The pellet was resuspended in DMEM AB and plated in a T25 or T175 (dependent of pellet size) and was incubated overnight at 37°C, 5% CO<sub>2</sub>. On the following day, we performed extensive washings of the plates to remove non-adherent and red blood cells, prior to media change. Cell morphology was constantly monitored by microscope observation. The resulting population of adipose derived mesenchymal stromal cell colonies were splitted and seeded in a new flask at a density of 200 cells/cm<sup>2</sup>.

##### **3.2.1.1.2 Cord blood derived mesenchymal stromal cells (CB)**

Cord blood samples were isolated from healthy donors after having obtained the correct informed consent (Mannheim Ethics Commission II). Cord blood samples were diluted 1:2 with PBS/EDTA and blood was carefully laid on a Ficoll layer avoiding any phase mixing. Samples were centrifuged at 420g for 30 minutes (no brake) at RT. Plasma was removed prior to interphase collection with a glass pipette.

Interphases were pooled, and PBS/EDTA was added to allow washing steps at 420g for 10 minutes at RT. Supernatants were aspirated and incubated during 10 minutes with erythrocyte lysis buffer to eliminate the undesired red blood cells. Pellets were washed and at this point, 10µl of cell suspension was taken at this point to count the cells with the CASY, prior to centrifuging at 420g during 10 minutes at RT. All the pellets were combined and resuspended in MSCGM-Medium + 10% FBS and 2 ml/well cell suspension were seeded in a 6 well plate. On the following day, fresh media was added to the culture. Media was changed once per week until colonies appeared, and then was done twice weekly. Colonies were splitted and seeded in a new flask at a density of 700 cells/cm<sup>2</sup>.

### 3.2.1.2 MSC culture

Following isolation, ASC were continuously cultured at a density of 200 cells/cm<sup>2</sup> and CB at 700 cells/cm<sup>2</sup> in DMEM supplemented with 10% pooled human allogeneic AB serum from healthy donors (German Red Cross Blood Donor Service, Mannheim) and FBS accordingly, 1% Penicillin/Streptomycin (100,000 U/ml Penicillin and 10 mg/ml Streptomycin) and 2% L-glutamine (200mM). Cryopreserved BM cells were thawed and continuously cultured at a density of 200 cells/cm<sup>2</sup> in 10% AB serum, supplemented with 1% Penicillin/Streptomycin and 2% L-glutamine (200mM). Cells were cultured in incubators with a controlled temperature and atmosphere (37°C, 5% CO<sub>2</sub>).

Upon reaching confluency, MSC were trypsinised with 1X Trypsin/EDTA, counted and seeded according to the experiment. All cells were then cryopreserved in fetal bovine serum (FBS) with 10% Dimethylsulphoxide (DMSO) and were always thawed and cultured for at least one passage prior to their use in experiments. Cell growth and morphology was monitored by microscope observation and cell numbers at different passages were tracked. Growth rate values were calculated following the equations of Cell Duplication number (CD) and Doubling Time (DT), where Fcn stands for final cell number and Icn for Initial cell number.

$$\text{Cell Duplication number (CD)} = \frac{\text{Log10 (Fcn)} - \text{Log10 (Icn)}}{\text{Log10 (2)}}$$

$$\text{Doubling Time (DT)} = \frac{\text{Culture duration}}{CD}$$

### 3.2.1.3 MSC characterisation

#### 3.2.1.3.1 Adipogenic differentiation

MSC were tested for their differentiation capacity, and cultured in adipogenic differentiation media (Mesenchymal Stem Cell Adipogenic Differentiation Medium) for 14 to 21 days. Full DMEM AB or FBS media condition was used as control. On the last differentiation day, MSC were fixed with 10% Paraformaldehyde (PFA) for 30 minutes, washed and incubated with Hoechst-33342 (1:100 final concentration, 10 mg/ml stock) for another 30 minutes. Hoechst fluorescence (excitation: 354 nm / emission: 442nm) was measured on a plate reader and taken as baseline normalisation. To test for adipogenic differentiation, AdipoRed Assay was performed following the manufacturer's instructions. After washing with DPBS, Adipored (5 µl/well in a 96 well plate) diluted in DPBS was added and incubated in the dark for 15 minutes. Following incubation, AdipoRed fluorescence was measured on a plate reader at 485/572 nm. Adipored optical density (OD) were normalised on Hoechst OD and presented as a Normalised Ratio.

#### 3.2.1.3.2 Osteogenic differentiation

MSC were tested for their differentiation capacity, and cultured in osteogenic differentiation media (Mesenchymal Stem Cell Osteogenic Differentiation Medium) for 14 to 21 days. Full DMEM AB or FBS media condition was used as control. On the last differentiation day, MSC were fixed with 10% PFA for 30 minutes, washed and incubated with Hoechst-33342 (1:100 final concentration, 10 mg/ml stock) for another 30 minutes. Hoechst fluorescence (excitation: 354 nm / emission: 442nm) was measured on a plate reader and taken as baseline normalisation. To test for osteogenic differentiation, Osteoimage Mineralisation Assay was performed following the manufacturer's instructions. After washing with Wash buffer, Osteoimage staining reagent (1:100 final dilution in Staining Reagent Dilution Buffer) was added to the cells and left in incubation for 30 minutes at RT. Following incubation, staining reagent was removed and three consecutive washing steps were performed with Wash buffer. Osteoimage fluorescence was measured on a plate reader at 492/520

nm. Osteoimage OD were normalised on Hoechst OD and presented as a Normalised Ratio.

### **3.2.1.3.3 Immunophenotyping**

BM, CB and ASC were characterised by fluorescence-activated cell sorting to define their immunophenotype. When MSC (passage 2) cell confluence was reached,  $1 \times 10^5$  cells were collected in FACS tubes, resuspended in FACS buffer and let incubate at 4°C for 5 minutes with 10µl of FcR blocking reagent. Then MSC from multiple donors were analysed with the following anti-human antibodies, at optimal concentrations and following proper titration: Anti-CD73-PE, Anti-CD44-APC, Anti-CD45-PE-Cy7, Anti-CD140a-PE, Anti-CD140b-APC, Anti-HLA-DR-APC Cy7, Anti-CD29-Alexa Fluor 488, Anti-CD90-APC, Anti-CD31-FITC, Anti-CD34-APC, Anti-CD106-FITC, Anti-CD146-PE, Anti-NG-2-AlexaFluor 488, Anti-CD105-PE Cy7, Anti-HLA-ABC-PE Vio770. Staining was performed during 20 minutes in the dark at 4°C after which cells were washed twice with Cell wash and resuspended in Sytox blue dead cell stain (final dilution in FACS buffer, 1:2000) prior to being analysed. A minimum of 10,000 events were acquired with BD FACS Canto and .fcs files were exported and analysed with FlowJo v10 software. The gating strategy applied to calculate positivity of cell surface marker expression is reported in Figure 4. Only MSC where CD29, CD73, CD44, CD90, CD105 and HLA ABC markers were positive, but CD31, CD34, CD14, CD19, CD45 and HLA-DR were negative were used to perform experiments.

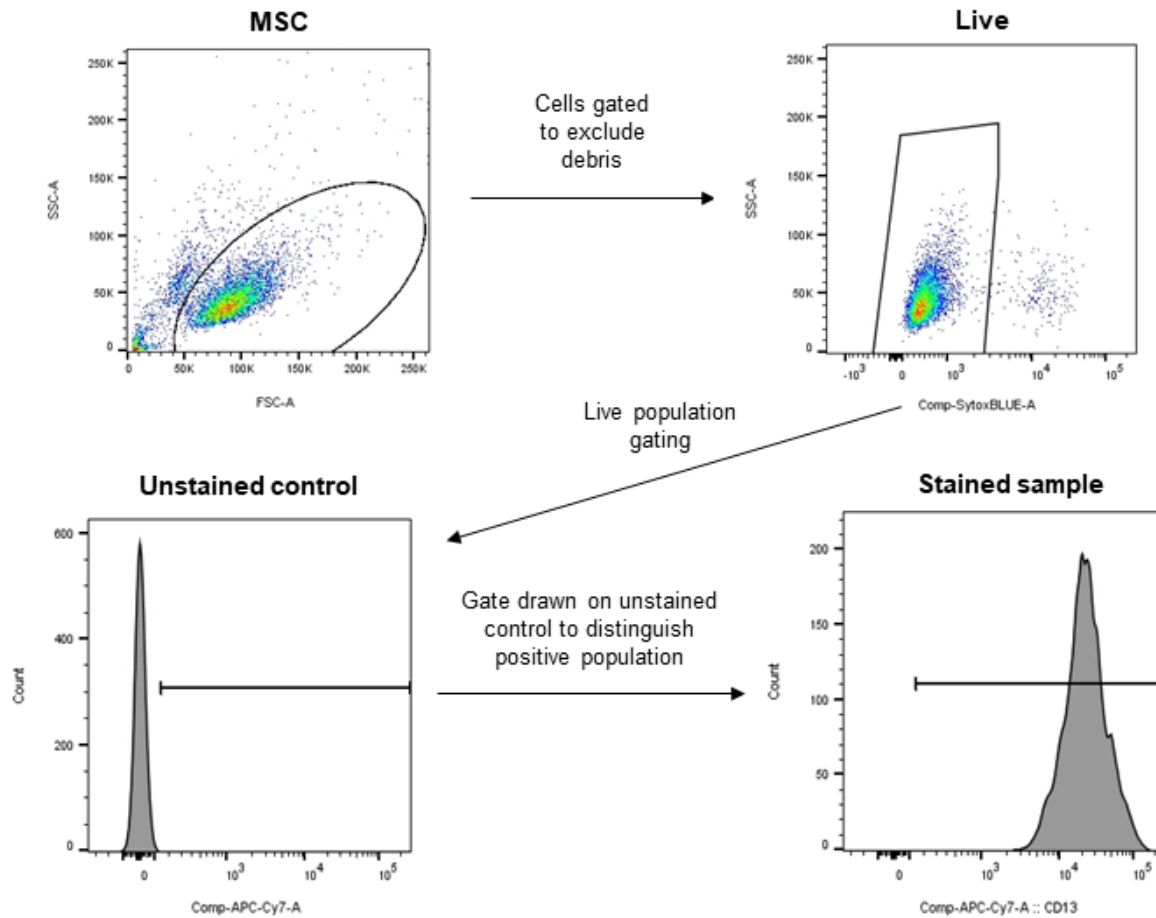


**Figure 4 Representative gating strategy for cell surface marker expression analysis.** To determine specific cell surface marker expression on cells, debris are first gated out by gating on side scatter (SSC) vs forward scatter (FSC), followed by a live/dead gating with Sytox RED/BLUE to define the Live population. Fluorescent unstained controls are used to determine specific position of gate in order to determine % of cell staining positivity for a specific marker.

### 3.2.1.4 Rat mesenchymal stromal cells (rMSC)

#### 3.2.1.4.1 Rat MSC isolation and culture

Rat bone marrow derived MSC (rMSC) were isolated from femurs from male Sprague-Dawley (SD) rats euthanized from control experiments in the frame of other licensed animal experiments. Animals were euthanized by intraperitoneal (i.p.) administration of ketamine and xylazine. Femurs were first washed with PBS + 2mM EDTA + 1% Penicillin/Streptomycin (100,000 U/ml Penicillin and 10 mg/ml Streptomycin). Prior to isolation, bone ends were cut off using a clamp and scissors



prior to flushing the bone marrow and collecting it with a cannula and syringe. Bone marrow suspension was centrifuged at 420g for 10 minutes and pellets were resuspended in media and seeded in a T25 flask. After overnight adherence, extensive washings of the plates were performed to remove non-adherent and red blood cells. New medium was replenished and cells were cultured until reaching a subconfluent stage, at which point they were passaged and vials were cryopreserved. Cell morphology and growth was constantly monitored by microscope observation.

After rMSC isolation, cells were cultured in DMEM supplemented with 10% FBS, 1% Penicillin/Streptomycin, 2% L-glutamine (200 mM).

Upon reaching confluency, rMSC were trypsinised with 1X Trypsin/EDTA, counted and seeded according to the experiment. Cells were then cryopreserved in fetal bovine serum (FBS) with 10% DMSO and were always thawed and cultured for at least one passage prior to their use in experiments. Cell growth and morphology was monitored by microscope observation (AxioVert100 Zeiss).

#### **3.2.1.4.2 Rat MSC characterisation**

rMSC were characterised by fluorescence-activated cell sorting (FACS) to define their immunophenotype as described above using the following anti-rat antibodies: Anti-CD45-FITC (Clone OX-1) to exclude hematopoietic cells, Anti-CD90-PE (Clone OX-7) and Anti-CD44-APC (Clone 12K35) as typical MSC markers.

#### **3.2.1.5 ABCB5+ cells**

Within the TASCOT graduate school, Prof. Gretz's group were working with the ABCB5 cells and based on our *in vitro* results we were also interested in investigating their immune potential. Thus, as this group was also interested in potentially testing ASC in their cisplatin-induced nephrotoxicity murine model we initiated a collaboration. My task contributing to that was to compare the immunosuppressive strengths of both cell types in an *in vitro* xeno-model prior to moving to *in vivo* experiments with the best performers.

Human ABCB5+ cells were provided to us by Ticeba-RHEACELL GmbH & Co. and were cultured in Ham's F-10 media supplemented with 15% stem cell media, 1%

Penicillin/Streptomycin (100,000 U/ml Penicillin and 10 mg/ml Streptomycin) and 2% L-glutamine (200mM). In order to maintain the ABCB5+ MSC phenotype, cells were put in culture only overnight to allow their acclimatisation, and were immediately seeded the next day according to the experiments. Cell growth and morphology was monitored by microscope observation (AxioVert100 Zeiss).

#### *3.2.1.6 Peripheral blood mononuclear cell (PBMC) isolation*

##### **3.2.1.6.1 Human peripheral blood mononuclear cell (PBMC) isolation**

Human peripheral blood mononuclear cells (PBMC) were isolated from either buffy coats or leukapheresis samples from healthy donors, provided by the German Red Cross Blood Donor Service in Mannheim (DRK-Blutspendedienst). Buffy coats were diluted 1:1 with PBS/EDTA. 25ml of diluted blood were gently settled on top of 10 ml of Ficoll-Paque™ in a 50ml tube and centrifuged at 420g for 30 minutes with the lowest deceleration. After centrifugation, plasma (supernatant) were mostly aspirated and the interphases were collected with a glass Pasteur pipette. Interphases from same samples or donors were pooled together and washed with PBS/EDTA (2mM). Tubes were centrifuged at 420g for 10 minutes. After aspirating the supernatants, pellets were resuspended in 1x erythrocyte lysis buffer left incubate 10 minutes at RT. After centrifuging, pellets were resuspended in PBS/EDTA and cell numbers were determined.

According to the experiment, CD4+ T cells were enriched from the PBMC population by using CD4+ T cell isolation kit (human) using CD4+ Biotin antibody cocktail (bead to cell ratio 1:40) following the manufacturer's instructions. Then, a minimum of  $4 \times 10^7$  PBMC or CD4+ T cells were resuspended in PBS and stained with proliferation dye Cytotell Green (final concentration 1:500 dilution from stock). After 15-minute incubation at 37°C, cells were washed, centrifuged and resuspended in full RPMI 1640 and seeded appropriately.

##### **3.2.1.6.2 Rat mononuclear cell isolation**

Rat mononuclear cells (PBMC) were isolated from either blood (rPBMC) or spleen-derived rat MC (SMC) from male SD rats immediately upon arrival.

### **Blood**

Rat blood-derived PBMC were isolated from freshly collected blood of SD rats as described for human PBMC.

### **Spleen**

SMC were isolated from spleen from SD rats immediately after dissection. Spleens were minced finely into small sections and put onto a 100µm and 70µm cell strainer in a PBS-antibiotic/antimycotic solution and then centrifuged and processed as described above.

#### *3.2.1.7 Immunosuppression assays*

##### **3.2.1.7.1 Human Immunosuppression assays**

$2 \times 10^4$ ,  $1 \times 10^4$  or  $5 \times 10^3$  MSC (1:5, 1:10 and 1:20 ratio, respectively) were seeded in full RPMI 1640 supplemented with IL-2 (500 µg/ml stock) on the bottom of a 24 or 96-well plate. Directly after thawing, fresh cryopreserved PBMC were then stained with the proliferation dye Cytotell Green (ATT Bioquest) at a final concentration of 1:500 dilution from stock.  $1 \times 10^5$  PBMC were added either a) directly on top of the MSC (direct coculture system) or b) in a transwell insert pore size 0.4µm. PBMC stimulated and not stimulated with PHA were seeded as controls. Both direct and indirect cocultures were set in parallel for comparison purposes. According to the experiments, MSC were treated with IFN $\gamma$  (final concentration 10ng/ml), tryptophan (Tryp) (final concentration 100µg/ml) or IDO inhibitor Epacadostat (Epac; final concentration 1µM). After 5 days, cocultures were harvested and conditioned media (CM) collected and stored at -80°C for further analysis.

##### **3.2.1.7.2 Rat Immunosuppression assays**

Rat MSC:PBMC cocultures consisted of a series of xeno- and allo-cocultures where their immunomodulatory potencies were investigated. These were: a) human MSC + rat (blood or spleen) PBMC, b) rat MSC + human PBMC (xeno-cocultures); and c) human MSC + human PBMC and d) rat MSC + rat (blood or spleen) PBMC (allo-cocultures). These combinations of MSC:PBMC (1:5, 1:10 and 1:20 ratio) were seeded as described above. Directly after isolation, either rat blood or spleen derived

MC, were stained with the proliferation dye Cytotell Green at a final concentration of 1:500 dilution from stock.  $1 \times 10^5$  PBMC were added directly on top of the MSC (direct coculture system). Rat MC (blood or spleen) stimulated and not stimulated with Concanavalin A (ConA; 4 µg/ml final concentration) were seeded as controls in 10% heat inactivated FBS in RPMI 1640 (inactivated RPMI 1640), supplemented with 1% Penicillin/Streptomycin, IL-2 (1:500 final dilution) and  $\beta$ -mercaptoethanol for rat conditions (50 µM final concentration). When possible, both rat blood or spleen derived MC were set in parallel for comparison purposes. After 3 days, cocultures were harvested and CM was collected and stored at -80°C for further analysis.

#### *3.2.1.8 Flow cytometry based assays*

##### **3.2.1.8.1 CD4+ T cell and PBMC staining and detection**

After day 5, Cytotell green stained stimulated/not stimulated PBMC or CD4+ T cells were harvested from coculture and control conditions. After harvesting and pooling technical replicates, PBMC were collected in FACS tubes, washed and resuspended in FACS Buffer. According to the experiment, to stain for CD4+ T cells, cells were first incubated during 5 minutes with 10 µl of FcR blocking reagent, and stained with extracellular marker Anti-CD4-PE during 20 minutes protected from light at 4°C. After washing step, cells were resuspended in FACS buffer with Sytox Red (1:4000 final concentration) or Sytox Blue (1:2000 final concentration). Cells were analysed immediately after addition of 25 µl of Precision count beads™ at BD FACS Canto II. The .fcs files were exported and analysed with FlowJo v10 software. The gating strategy applied to calculate percentages of CD4+ T cells and PBMC in Live population is reported in Figure 5.

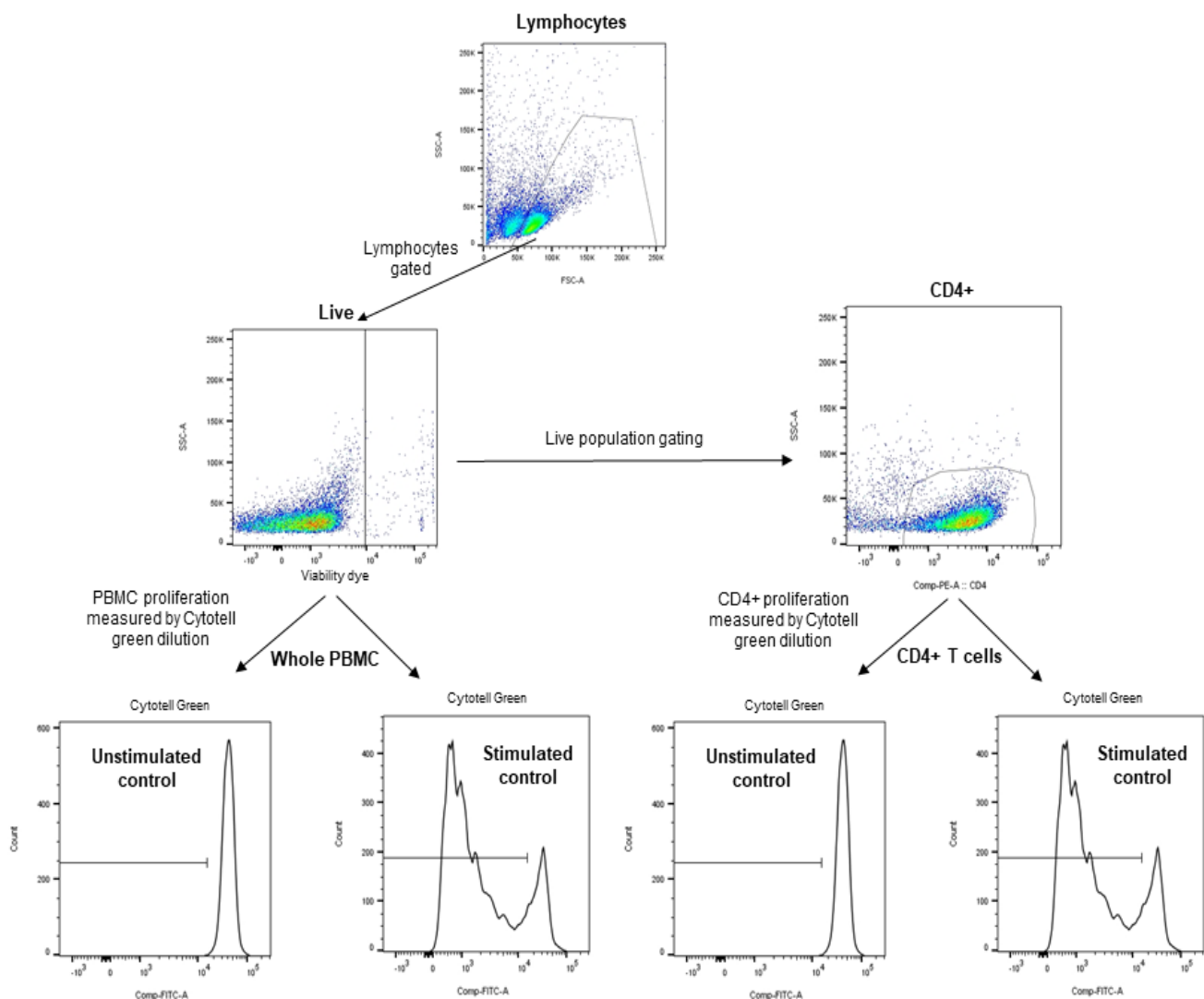


**Figure 5 Representative gating strategy on Live population for either human or rat whole PBMC or human CD4+ T cell proliferation analysis.** Lymphocytes are gated on SSC vs FSC, followed by a live/dead gating with the specific viability dye (Sytox Red or Blue), to define the Live population. Accordingly, either the whole PBMC population (left side graphs), or the specifically selected CD4+ T cells (right side graphs) were assessed for their proliferation capacities. Cytotell green viability dye dilution was investigated for this purpose, where all the dye is present in the unstimulated control but subsequent dye dilution is observed in the stimulated control condition in either PBMC or CD4+ cells.

PBMC proliferation was also analysed with the Proliferation Tool of FlowJo 7 software. It applies mathematical models to the proliferation data and develops statistics to describe it. We focused particularly on the “division index” which is the average number of divisions for all of the cells in the original starting population (FlowJo 7 manual tutorial). A representative picture of how the Proliferation tool works is reported in Figure 6.

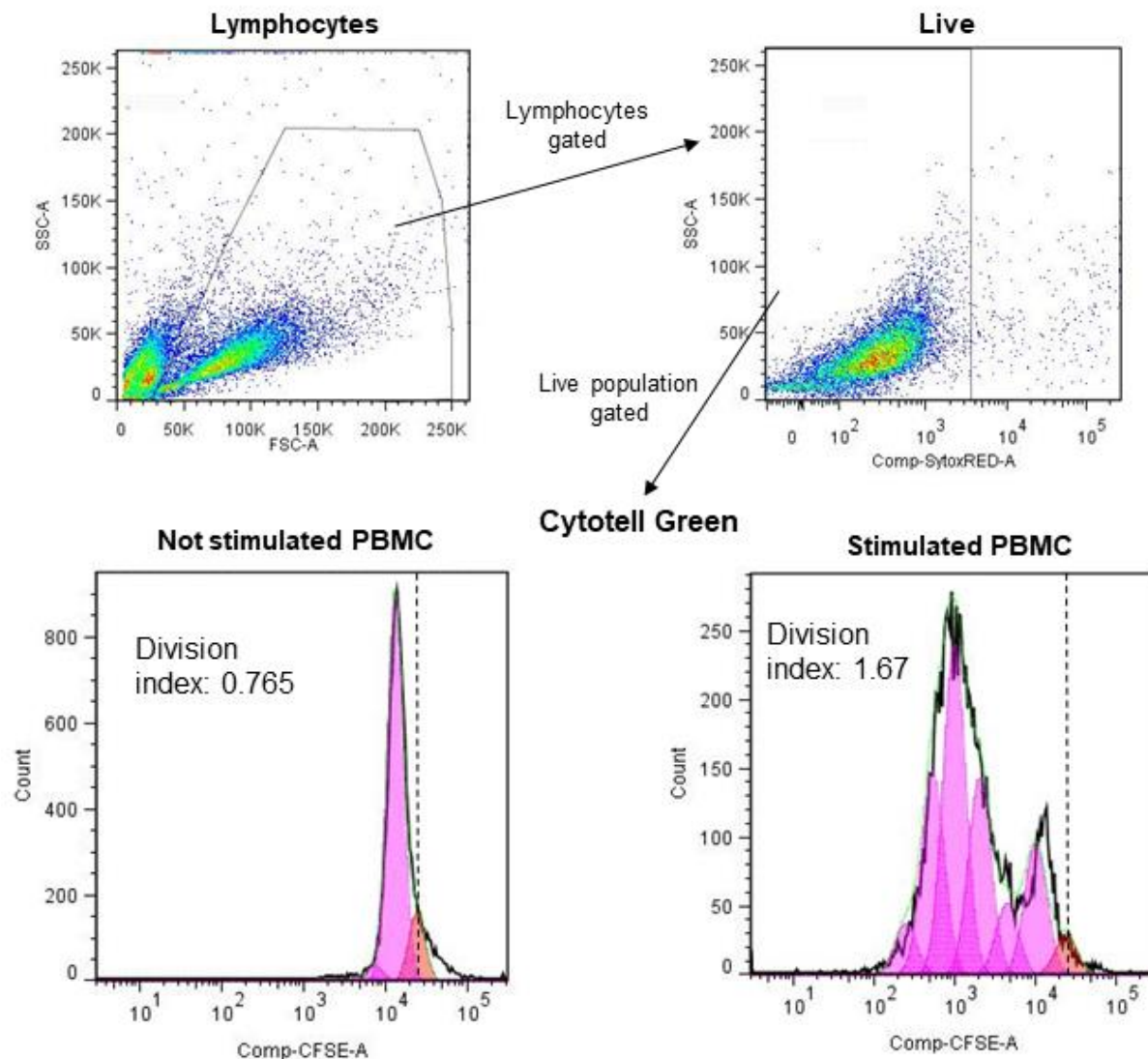


**Figure 6 Representative gating strategy on proliferation tool in FlowJo v.7.6.5 software.** To determine PBMC or CD4<sup>+</sup> T cell proliferation potential, lymphocytes are gated on SSC vs FSC, followed by a live/dead gating to define the live population. Afterwards, cells are evaluated on the Cytotell green proliferation dye staining. FlowJo proliferation tool allows to custom the fluorescence units of Peak zero in the undivided sample. In this manner, Peak 0 (light pink peak, dotted line) depicts where the original population is found and the value is consequently applied to the rest of the samples. The proliferation tool then applies specific mathematical models on the population and issues the proliferation peaks (depicted in dark pink), calculating the division index amongst other proliferation data.

### 3.2.1.8.2 Indoleamine 2,3-dioxygenase (IDO) detection

Indoleamine 2,3-dioxygenase (IDO) detection was measured as follows. MSC were seeded in a 6-well plate at a density of 5000 cells/cm<sup>2</sup> in full RPMI 1640. Once seeded, cells were allowed to attach and then were treated either with IFN $\gamma$  (final

concentration 10ng/ml), Tryp (final concentration 100µg/ml) or Epac (final concentration 1µM), to assess specific IDO secretion. After trypsinisation, MSC were collected in FACS tubes and washed with PBS. After washing, MSC were resuspended in PBS, stained with Fixable Viability dye eF450 (1:4000 final dilution) and incubated for 30 minutes at 4°C. Cell suspension was then incubated with IC Fixation Buffer during 30 minutes at room temperature (RT). After washing/centrifuging samples twice with 1X Permeabilisation Buffer, cells were stained with IDO-PE in 1X Permeabilisation Buffer during 30 minutes. Following this step, cells were washed and analysed immediately at BD FACS Canto II. MSC without IFN $\gamma$  stimulation were also seeded in parallel as controls. Data are represented as Median Fluorescence Intensity (MFI) after subtraction of MFI's respective control.

#### *3.2.1.9 Protein detection*

##### **3.2.1.9.1 Kynurenine assay**

Kynurenine was detected in CM from IDO assay or 5 day coculture CM (human and rat) and control of stimulated and not stimulated conditions. 100µl of standard (serial dilutions of L-Kynurenine 50mM) or probe was added to 50µl of 30% Trichloroacetic acid (TCA) in a 96 well PCR plate (non-skirted, low-profile). The plate was incubated during 30 minutes at 50°C in a thermal cycler (DNAEngine). After incubation, the plate was centrifuged at 4004g for 10 minutes and 75µl of supernatants from each condition were carefully transferred into a 96-well clear plate. 75µl of 22% 4-(Dimethylamino)benzaldehyde (sc-202888) were added and left incubating for 15 minutes in the dark at RT. Then the OD of each well was determined using a microplate reader TECAN infinite M200PRO set to 492nm emission wavelength. Standard curves were elaborated with GraphPad Prism software v6 or 7.

##### **3.2.1.9.2 Nitrite assay**

Nitrite (NO $_2^-$ ) was detected in CM from IDO assay or 5 day coculture CM (human and rat) and control of stimulated and not stimulated conditions. 150µl of probes and standards (Sodium nitrite dissolved in full RPMI 1640 media) were mixed with 50µl of Sulfanilamide (10mg/ml) in a 96-well clear plate. The plate was incubated during two

minutes before the addition of 50µl of N-(1-Naphthyl)-ethylendiamine dihydrochloride (Naphthylamine) (2mg/ml), then was left incubating for a minimum of 30 minutes in the dark at RT. The OD of each well was determined using a microplate reader TECAN infinite M200PRO using 542 nm as measured emission wavelength and 620 nm as reference wavelength. Standard curves were elaborated with GraphPad Prism software v6 or 7 and limit of detection was calculated and applied to measured values.

### **3.2.1.10 Statistical analysis**

Data were shown represented as box-and-whisker plots. The box corresponds to the interquartile range (IQR) and the whiskers depict the minimum a maximum values. In addition, the median is represented as a line within the boxes. Dotted lines at 1 represent the normalisation referred to the respective assay positive control. Two-way ANOVA and Tukey's or Sidak's post-hoc multiple comparisons test were performed. For all statistical tests, p value differences <0.05 were considered as statistically significant. The number of replicates performed for every experiment is indicated in the corresponding Figure legend as n=# (# replicates). Statistical analysis and visualisation of results were performed using GraphPad Prism software v6 or 7.

## **3.2.2 Evaluation of MSC-derived products modulatory functions**

### **3.2.2.1 Conditioned media (CM)**

MSC derived conditioned media was prepared by seeding  $1.5 \times 10^6$  cells in a T175 flask, in full DMEM AB media supplemented with IL-2 (1:500 final dilution, 500 µg/ml stock), cells were allowed to attach overnight (ON). The next day, media was changed to full RPMI 1640 and according to the experiments, MSC were treated with IFN $\gamma$  (final concentration 10ng/ml, which corresponds to 200U/ml), tryptophan (final concentration 100µg/ml) or IDO inhibitor Epacadostat (Epac; final concentration 1µM). This media was left conditioning for 72 hours, after which conditioned media is collected in 50 ml tubes and is either stored at -30°C for its use in near future experiments or continued directly with the extracellular vesicle (EV) isolation procedure. The cells in the flask were washed thoroughly with PBS and trypsinised



with 1X Trypsin/EDTA and cell number was determined to allow us to know the producer cells present at the moment of harvesting.

As a CM control for isolation, characterisation and proliferation assays we defined an EV media control. It was constituted in the same manner as ASC-derived CM aside from being generated in absence of MSC.

#### *3.2.2.2 Extracellular vesicles (EV)*

##### **3.2.2.2.1 Preparation of EV-depleted FBS or AB serum**

EV-depleted serum was obtained by ultracentrifuging regular FBS or AB serum at 4°C, at 100,000g for 18 hours in the WX Ultra Series 100 ultracentrifuge using a fixed angle rotor Sorvall T-865 (k-factor 100,000g: 150.6). Prior to ultracentrifugation, all polycarbonate ultracentrifuge tubes were accurately weighed with a precision scale. Consequently, ultracentrifuge extracellular vesicle depleted serum (UC-dserum) was aliquoted and cryopreserved at -30°C for use in future experiments.

##### **3.2.2.2.2 EV isolation**

1,5x10<sup>6</sup> ASC were seeded in a T175 flask, in full DMEM FBS or AB medium, and cells were allowed to attach overnight (ON). The next day, media was changed to DMEM supplemented with 10% EV depleted FBS or AB serum supplemented with 1% Penicillin/Streptomycin and 2% L-glutamine (200 mM) and according to the experiments, IFN $\gamma$  was also added to the culture (final concentration 10ng/ml). 72 hours later, media was collected in 50 ml tubes and proceeded with the EV isolation procedure. The flask was thoroughly washed with PBS, trypsinised and cell number was determined to monitor the exact producer cell number present.

EV isolation and purification was performed by consecutive steps of differential ultracentrifugation (dUC). Cell culture media was centrifuged at RT during 5 minutes at 525g. Supernatants were retrieved and filtered through a 0.22 $\mu$ m syringe filter in order to eliminate larger cell rests, apoptotic bodies and debris. After filtration, ultracentrifuge tubes were filled with conditioned media and weighed accordingly with a precision scale. Tubes were loaded in WX Ultra Series 100 ultracentrifuge using a fixed angle rotor Sorvall T-865 with a first UC of 10,000g (k-factor 10,000g: 1569.6; 11,800 rpm) at 10°C during 45 minutes. Following the first ultracentrifugation step, supernatants were collected from the original tube and transferred to new sterilised

UC tubes for the next UC step. The microvesicle pellets obtained were resuspended at a ratio of  $2 \times 10^7$  producer cells/200  $\mu$ l sterile filtered PBS and stored in 1,5ml tubes at  $-30^\circ\text{C}$  for no longer than 6 months. UC tubes were weighed and placed in the ultracentrifuge accordingly, to perform the second UC step of 105,000g (k-factor 105,000g: 150.6; 38,100 rpm) at  $10^\circ\text{C}$  during 45 minutes. The EV pellets were resuspended at the same ratio of  $2 \times 10^7$  producer cells/200  $\mu$ l sterile filtered PBS and stored in 1,5ml tubes at  $-30^\circ\text{C}$  for a maximum of 6 months. A small aliquot of supernatant from the second ultracentrifugation step was stored to use as a control in WB analysis or transmission electron microscopy (TEM), the rest was discarded.

### **3.2.2.2.3 EV characterisation**

#### *3.2.2.2.3.1 Nanoparticle tracking analysis (NTA)*

Particle number and size distribution were measured with light scattering technology, NTA. One microliter of concentrated EV were diluted in 0.22  $\mu$ m sterile-filtered PBS in a 1:1000 dilution, EVs were visualized using the ZetaView (Particle Metrix). The device specific configuration was as follows: 80% sensitivity, shutter 100, 11 positions were measured and 2 measurement cycles were performed. Amongst all measurements, 1 to 3 positions from a total of 11, were removed for analysis due to some values being out of range. Data were exported as a PDF report and txt files and further analysed with GraphPad Prism software v6 or 7.

#### *3.2.2.2.3.2 Transmission electron microscopy (TEM)*

Five  $\mu$ l of EV suspensions were left to settle on 100 mesh formvar-coated nickel grids (Plano), contrasted with 4 % uranyl acetate (Serva) as a negative staining, air-dried and visualized using a EM10A transmission microscope (Zeiss) equipped with a CCD Olympus mega view G2 digital camera (Olympus Soft Imaging Solutions GmbH) at 60 KV. TEM image acquisition was performed with the kind help of Hiltraud Hosser.

#### *3.2.2.2.3.3 Western blot*

##### Whole cell lysate preparation

In parallel to the EV isolation, the whole cell lysate of the original EV producer cells was prepared. After retrieving the conditioned media for EV purification, cells were

washed three times with PBS, trypsinised and counted. Cells were centrifuged at 4°C for 5 minutes at 300g, supernatant was discarded and pellets were resuspended in 1 ml of PBS. Two consecutive washing steps were performed before addition of 200µl per  $1 \times 10^7$  cells of radioimmunoprecipitation assay (RIPA) buffer supplemented with protease inhibitor and incubating during 20 minutes on ice. Cells were vortexed thoroughly before and after lysing. A last centrifugation step at 4°C for 20 minutes at 20,000g was performed. Supernatants were aliquoted and stored at -30°C for further use in experiments, as Western blot control.

#### Protein extraction and Western blot

Protein concentration was determined using the BCA assay process with Pierce BCA Protein Assay Kit, following manufacturer's instructions. EV pellets were resuspended in radioimmunoprecipitation assay (RIPA) buffer (50 mM Tris-HCl, pH7.4, 150 mM NaCl, 1 % Triton X-100, 1 % Na-deoxycholate, 0.1 % SDS, 0.1 mM  $\text{CaCl}_2$ , 0.01 mM  $\text{MgCl}_2$ ) supplemented with protease inhibitor cocktail. Proteins extracted from HeLa and HCT116 cells were used as cellular controls. Equal amounts of protein (20 µg) were loaded and separated on 4-15 % Mini-PROTEAN TGX Precast Gels. Protein and cell lysates were treated with protein loading dye (Laemmli sample buffer) with freshly added  $\beta$ -mercaptoethanol (10 %; v/v; final concentration 0.05mM) and boiled for 5 min at 95°C (except for one antibody, see below) before SDS-PAGE. Proteins were subsequently transferred to nitrocellulose blotting membrane (0.2m µm; #1060000). Membranes were blocked in 5 % BSA (Carl Roth) in 0.1% Tween in TBS (TBS-T). After blocking, blots were probed with the following primary antibodies: Anti-TSG-101 (1:500 dilution) (Clone 4A10; MA1-23296), Anti-Alix (1:500 dilution) (Clone 3A9; 634501\_02), Anti-CD81 (1:300 dilution) (Clone 5A6; 349501\_02), and Anti-CD63 (without boiling treatment) (1:300 dilution), Anti-CD9 (1:300 dilution), Calnexin (1:500 dilution) (Clone MX-49.129.5 (sc-5274); Clone C-4 (sc-13118) and Clone AF18 (sc-23954) respectively) overnight at 4°C. After incubation, membranes were washed three times with TBS-T and subsequently incubated with the secondary antibody dilution: ECL Anti-mouse IgG HRP Linked whole Ab (1:2000 dilution; NA931V) for 1 hour at room temperature followed by washing. Blots were then developed using WesternBright ECL (#541004) and protein bands were detected using the FusionCapt Advanced Solo 4.

#### 3.2.2.2.3.4 *Flow cytometry (FACS)*

As a method to assess presence of proteins in EV preparations and quantify them in or on their surface, bead-based flow cytometry was performed. To establish a robust FACS-EV characterisation protocol, several bead-EV combinations were tested. We used two different bead types: Aldehyde/sulfate latex beads and CD9 magnetic human beads. Aldehyde/sulfate latex beads have been reported by several groups as successfully coupling allowing detection of EV isolates in conventional cytometers [148-150]. The rationale to use CD9 magnetic human beads came from published studies that use CD9 antibody for counterstaining already bead-captured EV for detection in flow cytometry [151].

##### Aldehyde/sulfate latex bead coupling

Following isolation and purification, EVs were coupled to Aldehyde/sulfate latex beads to allow their better detection in the FACS due to their small size range. Five µl of beads were mixed with 100µl of PBS to pre-wash the beads, then incubated at room temperature for 15-30 minutes at 800rpm in a horizontal shaker. EVs were added at this point and 400µl of PBS were added prior to incubation at room temperature for 60 minutes at 800rpm in a horizontal shaker. 400µl of 1M glycine (previously filtered through 0.22µm sterile syringe filter) were added and incubated for 60 minutes at 800rpm. Samples were centrifuged for 2 minutes at 9700g and supernatant was discarded leaving no more than 20µl of volume in the tube. Pellets were resuspended in 100µl of 10% BSA solution and incubated at room temperature for 45 minutes at 800rpm in a horizontal rotor. Samples were centrifuged and resuspended in 40µl of 2% BSA solution (0,22µm filtered). To assess antigen expression, samples were incubated overnight at 4°C at 800rpm in a horizontal shaker with the appropriate combination of monoclonal antibodies. To evaluate and assess the strategy for bead-based mediated EV characterisation and to evaluate the specific markers present on ASC and HCT116-derived EVs and cells two different antibody panels were used. **Panel 1:** CD73 PE (Biolegend), CD44 APC-Cy7 (Biolegend), CD9 PerCP-Cy 5.5 (BD Biosciences) and CD81 APC (Miltenyi) and **Panel 2:** CD9 PerCP-Cy 5.5 (BD Biosciences), CD63 Brilliant violet 421 (Biolegend), CD81 PE/Cy7 (Biolegend), Tumor susceptibility gene 101 (TSG101) and Calnexin Alexa fluor 647 and Alix PE (Santa Cruz). Following incubation time, three consecutive washing steps were performed with 200µl of 2% BSA solution. Prior to

measurement, 300µl of PBS were added and beads measured immediately at BD FACSCanto II (BD Biosciences). Unstained beads were used as a negative control, together with beads that were stained in the same manner as the EV samples. EV that were not stained with any antibody were used to discriminate positive and negative population signals. Therefore, starting from bead-EV complex, it was possible to define EV singlets and subsequently identify positively stained EV for specific markers. A representative picture of this gating strategy is reported in Figure 7.

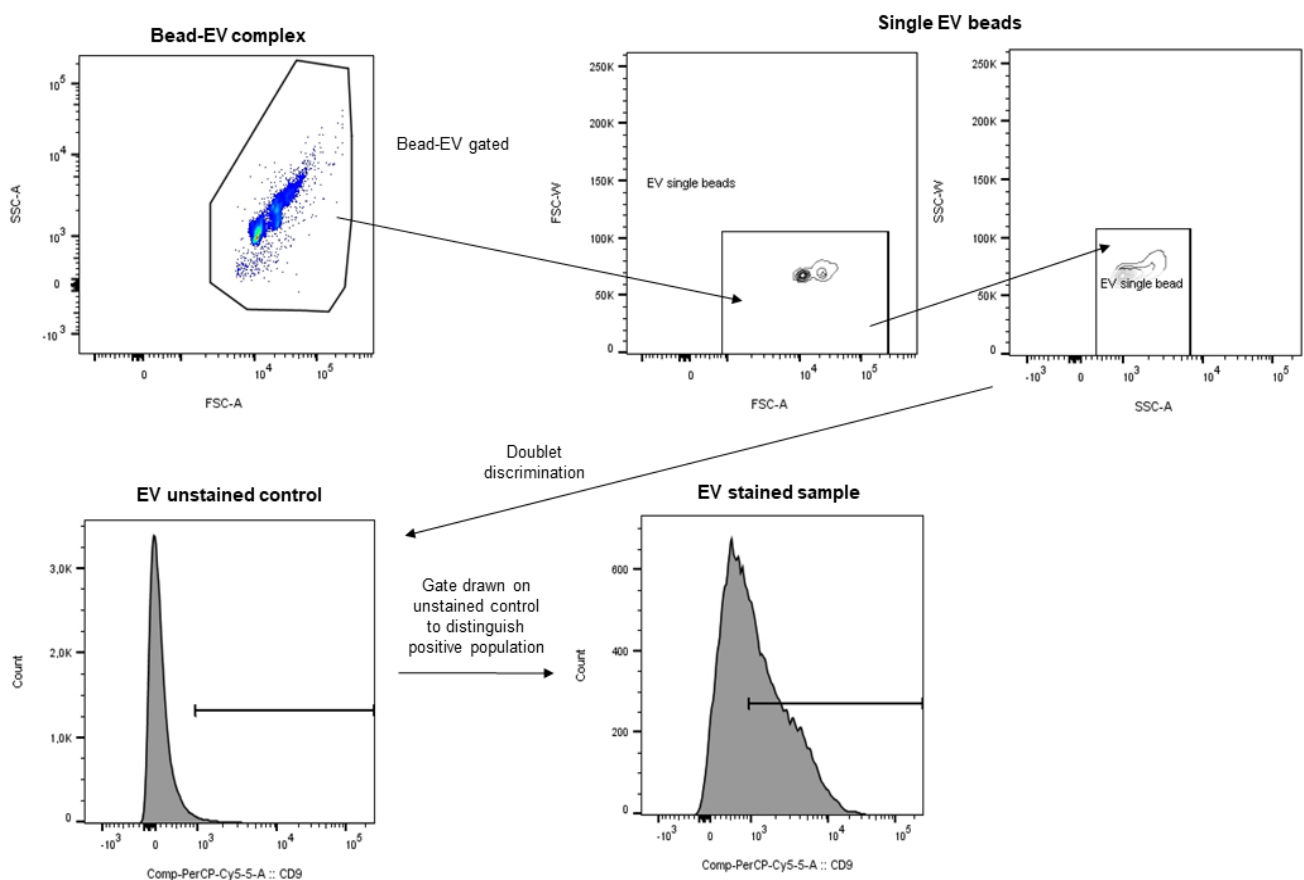


**Figure 7 Representative gating strategy on EVs with Aldehyde/Sulfate latex beads, 4% w/v (4µm).** Bead-EV complex is gated first on SSC vs FSC followed by doublet discrimination with FSC-A vs FSC-W followed by SSC-A and SSC-W, to collect single bead events. Subsequently, EV specific gate was performed on EV unstained control to determine positive population of the specific markers.

### CD9 magnetic bead coupling

Purified EVs were coupled to anti-human CD9 beads for flow detection (Exosome-Human CD9 beads). 20µl of CD9 beads were washed with 1 ml assay buffer (PBS +

0.1% BSA sterile filtered 0,22µm) (BSA), then placed in a magnetic separator. EV were added 1:10 to Assay buffer and incubated overnight at 4°C, end-over-end mixing. On day 2, bead-bound exosomes were isolated with a magnetic separator and washed several times prior to the EV staining. To assess antigen expression, samples were incubated in the dark with the appropriate combination of monoclonal antibodies during 45 min at 1000rpm. To evaluate and assess the strategy for bead-based mediated EV characterisation and to evaluate the specific markers present on ASC and HCT116-derived EVs and cells, the same antibody panels (Panel 1 and Panel 2, correspondingly) as the ones used with the aldehyde/latex beads, were tested. After incubation the excess antibodies were washed with assay buffer and retrieved through magnetic separation. Then samples were diluted in PBS and proceeded with downstream analysis measuring at BD FACSCanto II. EV-bead samples were consecutively loaded and measured. A minimum of 50,000 events were acquired and recorded at low speed. To test for antibody auto-fluorescence or any aggregate formation, we used sterile 0.22 µm filtered PBS as a negative control. PBS control sample was stained in the same manner as the EV samples. EV that were not labelled with any antibody were used to discriminate positive and negative population signals.

Therefore, it was possible to define bead-EV complex and subsequent positively stained EV for specific markers. A representative picture of this gating strategy is reported in Figure 8.

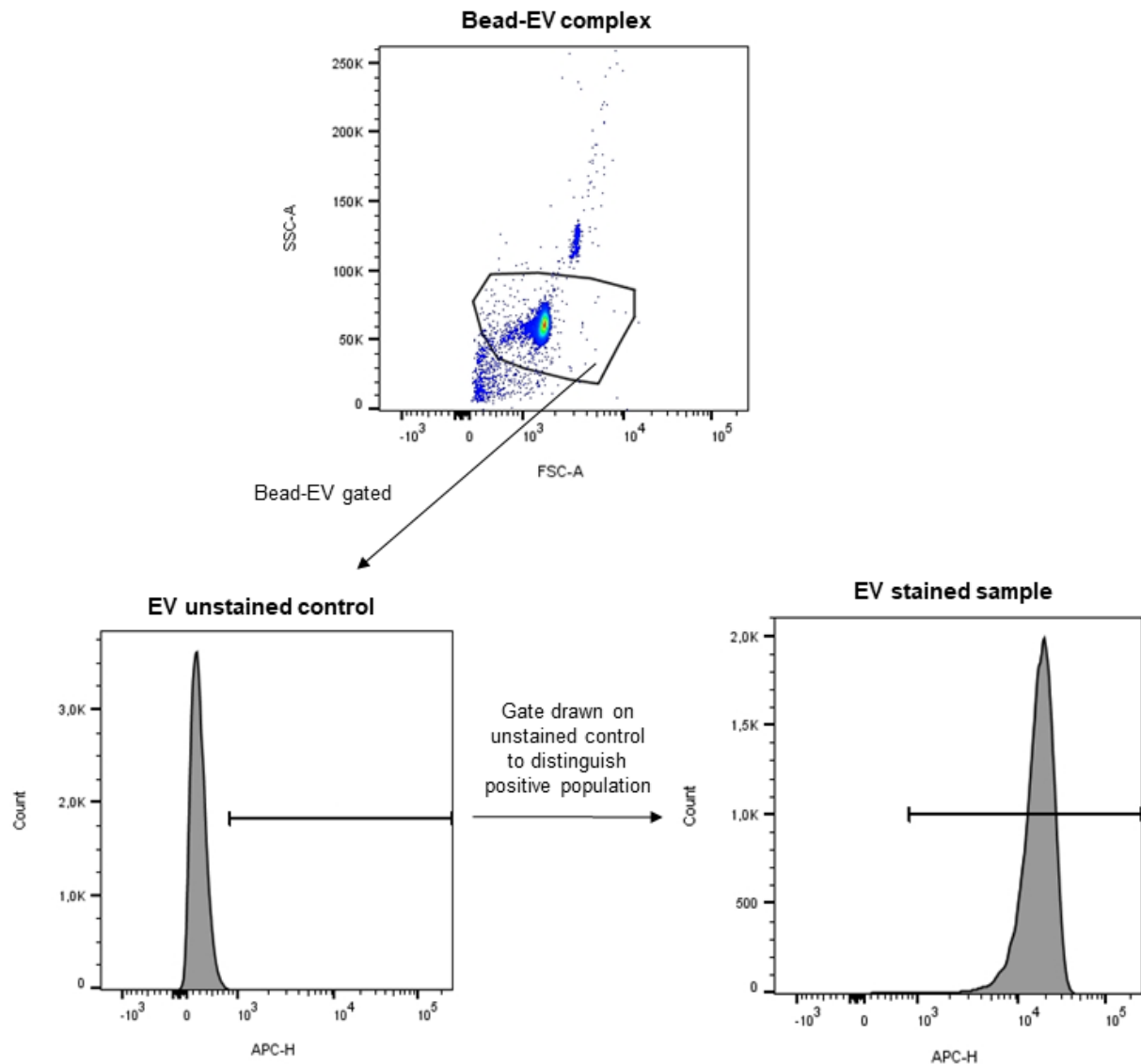


**Figure 8 Representative gating strategy on EVs with CD9 magnetic beads.** Bead-EV complex is gated first on SSC vs FSC. Subsequently, EV specific gate was drawn on EV unstained control to determine positive population of the specific markers.

### 3.2.2.2.4 Modulatory assays of MSC-derived products

#### 3.2.2.2.4.1 Conditioned media assay

These assays were performed with conditioned media (CM) from ASC in culture during 72 hours. Following PBMC thawing and staining with the proliferation dye Cytotell Green (ATT Bioquest), they were resuspended in ASC CM and seeded directly in a 96-well plate to assess CM potential immunomodulatory properties as described in section 3.2.1.7. After 5 days, assays were harvested and PBMC

proliferation activity was assessed in the FACS. Conditioned media (CM) was retrieved and stored at -80°C for further analysis.

Another set of assays were performed with CM from previous cocultures (5 days) that was diluted 1:2 in new full RPMI 1640- Hence, newly thawed PBMC were resuspended and seeded to investigate the potential inhibitory effect of this CM on PBMC proliferation inhibition.

#### **3.2.2.2.4.2 EV assay**

Cytotell-green-stained and PHA stimulated PBMC were seeded as described before directly in a 96-well plate. After thawing, extracellular vesicles (EV) originated by  $2 \times 10^6$  producer cells were added to the specific wells of the plate to assess their immune strength as for the previously described conditioned media assay.

#### **3.2.2.3 Statistical analysis**

Data were shown represented as box-and-whisker plots. The box corresponds to the IQR and the whiskers depict the minimum a maximum values. Regarding the NTA analysis data, results are depicted as box-whisker plots and show IQR, whiskers in this case correspond to 10th and 90th percentile. In addition, the median is represented as a line within the boxes in all representations.

Dotted lines at 1 represent the normalisation referred to the respective assay positive control. Two-way ANOVA and Tukey's or Sidak's post-hoc multiple comparisons test were performed. For all statistical tests, p value differences <0.05 were considered as statistically significant. The number of replicates performed for every experiment is indicated in the corresponding Figure legend as n=# (# replicates). Statistical analysis and visualisation of results were performed using GraphPad Prism software v6 or 7.



### **3.2.3 Evaluation of standardised ultracentrifuge-based EV isolation protocol**

#### *3.2.3.1 HCT116 cell culture and detection*

The colorectal cancer cell line HCT116 was obtained from European Collection of Authenticated Cell Cultures (ECACC) and cultured in incubators with 5 % CO<sub>2</sub> atmosphere at 37 °C. Cell morphology was constantly monitored by microscopic observation (AxioVert100 Zeiss). For marker expression characterisation, HCT116 cells were stained with the same monoclonal antibody panel than HCT116-derived EV as described in section 3.2.3.3 EV characterisation – FACS. The gating strategy applied to calculate positivity of cell surface marker expression is reported in Figure 9.

#### *3.2.3.2 EV isolation*

In the first round cells were cultured by Fabia Fricke, in the second round cells were cultured in our laboratory and then CM was accordingly transferred to the collaborative partners to perform all the ultracentrifugation runs in parallel.

17x10<sup>4</sup> (first round) and 18x10<sup>4</sup> (second round) cells/cm<sup>2</sup> were seeded in T175 flasks (13xT175, first round; 45x T175, second round). After overnight culture, the cells were washed twice with phosphate-buffered saline (PBS) and cultured for 24 h in 20 ml/ T175 flask DMEM-F12 medium containing 1 % EV-depleted FBS (depleted from 20 % FBS via overnight centrifugation at 100,000 x g at 4 °C). Cell conditioned medium (CCM) was collected, pooled, split into 50 ml Falcon tubes and distributed to the participating laboratories. In the first isolation round, the medium was stored at 4 °C and processed within 12 h in each laboratory. In the second isolation, the medium was frozen at -80 °C, and thawed prior to EV isolation. EV isolation was performed by differential centrifugation steps: first, at 300g for 10 min at 4 °C, second at 2,000g for 10 min at 4 °C, third 10,000g for 40 min at 4 °C and fourth 100,000g for 2 h at 4 °C to pellet the EVs. Before the fourth centrifugation step, CCM was filtered using a 0.22 µm pore size filter. This ultracentrifugation step was performed twice in the first isolation and once in the second isolation run. For each centrifugation, fresh tubes were used. In the first isolation, EV pellets each obtained from 12 ml CCM (one tube) were resuspended in 30 and 50 µl PBS for TEM and NTA, respectively. EV pellets

obtained from 24 ml CCM (two tubes) were resuspended in a total volume of 50 µl radioimmunoprecipitation assay (RIPA) buffer supplemented with protease inhibitor. In the second isolation, EV pellets from 34 ml CCM (two tubes) were resuspended in 100 µl PBS, where 45 µl were subjected to Nanoparticle Tracking Analysis (NTA), 25 µl for transmission electron microscopy (TEM) and 30 µl for fluorescence-activated cell sorting (FACS). For Western blot analysis, EV pellets from the 170 ml CCM (ten tubes), were resuspended in 100 µl RIPA buffer supplemented with protease inhibitor.

### *3.2.3.3 EV characterisation*

For EV sample characterisation, certain methods were performed in specific laboratories. NTA measurements were performed by Dr. Thomas Worst (first round) and Lena Hoffmann (second round) from the Urology department Universitätsklinikum Mannheim. TEM characterisation was performed by Fabia Fricke from the German Cancer Research Centre (DKFZ) Im Neuenheimer Feld with assistance for image acquisition from Ulrike Ganserer. WB and FACS characterisation was performed in our laboratory.

#### **3.2.3.3.1 Nanoparticle tracking analysis (NTA)**

In the first round, two microliters of concentrated EV suspensions were diluted in sterile-filtered PBS 1:100 and visualized using the NanoSight LM10 NTA device (Malvern Instruments). Each sample was measured 5 times for 45 s (Screen Gain 1.0, camera level 12) with at least 200 valid tracks per video to obtain particle concentration and size distribution. In the second round, one microliter of concentrated EVs was diluted in sterile-filtered PBS in a dilution range between 1:2000 and 1:4000 and visualized using the ZetaView (sensitivity 80 %, shutter 100, 11 positions, 2 cycles).

#### **3.2.3.3.2 Transmission electron microscopy (TEM)**

Five microliters of EV suspensions were left to settle on 100 mesh formvar-coated copper grids (Plano), contrasted with 2 % aqueous uranyl acetate (negative stain; Serva), air-dried and visualized using a JEM-1400 transmission microscope (JEOL) equipped with a Tietz 2 K digital camera (TVIPS, Gauting) at 80 kV.

### **3.2.3.3.3 Protein extraction and western blotting**

Western blot characterisation was performed as described in section 3.2.2, within the EV characterisation chapter. Proteins extracted from HeLa and HCT116 cells were used as cellular controls. Blots were probed with the following primary antibodies: Anti-TSG-101 (1:500 dilution) (Clone 4A10; MA1-23296), Anti-Alix (1:500 dilution) (Clone 3A9; 634501\_02), Anti-CD81 (1:300 dilution) (Clone 5A6; 349501\_02), and Anti-CD63 (without boiling treatment) (1:300 dilution), Anti-CD9 (1:300 dilution), Calnexin (1:500 dilution) (Clone MX-49.129.5 (sc-5274), Clone C-4 (sc-13118) and Clone AF18 (sc-23954) respectively) overnight at 4°C. After incubation, membranes were washed three times with TBS-T and subsequently incubated with the secondary antibody dilution: ECL Anti-mouse IgG HRP Linked whole Ab (1:2000 dilution) for 1 hour at room temperature followed by washing. Blots were then developed using WesternBright ECL and protein bands were detected using the FusionCapt Advanced Solo 4.

### **3.2.3.3.4 Flow cytometry (FACS)**

FACS measurement of HCT116-derived EVs and cells was performed with BD FACS Canto II, using BD FACSDiva software. HCT116-EVs were captured on anti-human CD9 beads for flow detection as described in section 3.2.2 where FACS characterisation is described. Antibodies CD9 PerCP-Cy 5.5 (BD Biosciences), CD63 Brilliant violet 421 (Biolegend), CD81 PE/Cy7 (Biolegend), TSG101 and Calnexin, both Alexa Fluor 647 and Alix PE (Santa Cruz) were used. After washing, beads were retrieved through magnetic separation. EV-bead samples diluted in PBS were measured acquiring minimum of 50,000 events at low speed. Sterile 0.22 µm filtered PBS and EVs not labelled with any antibody served as controls. An extracellular staining of cells incubated for 20min with CD9, CD63 and CD81 and an intracellular staining (30min fixation in IC fixation buffer, wash with 1x permeabilisation buffer and stain for 30min in 1x permeabilisation buffer) for TSG101, Alix and Calnexin was performed on cells. A representative picture of this gating strategy is reported in Figure 9.

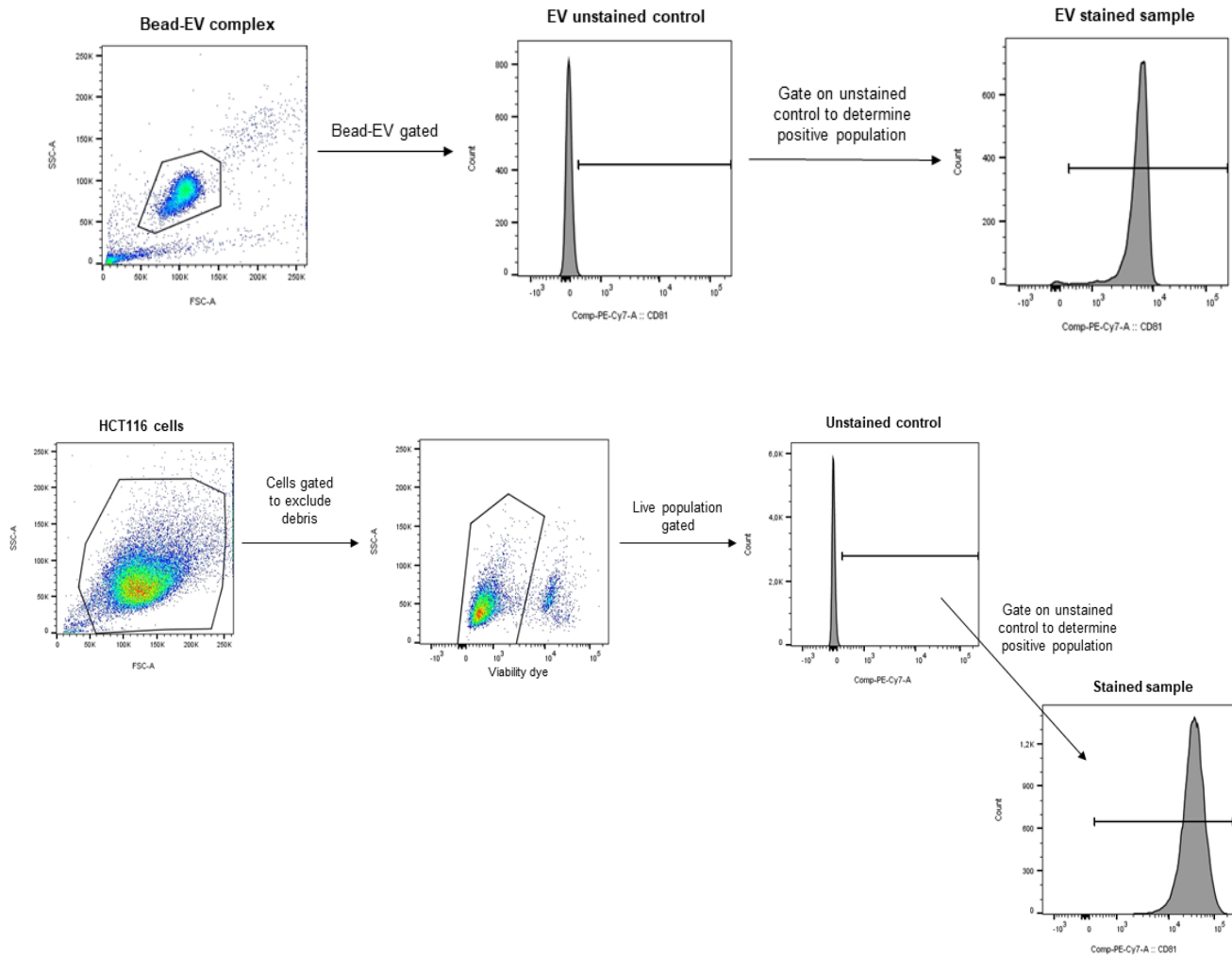


**Figure 9 Representative gating strategy for comparative study EV measurement on HCT116 EV or cells.**

To assess positivity on HCT116 derived EV, first bead-EV complex is gated on SSC vs FSC. Subsequently, EV specific gate was drawn on EV unstained control to determine positive population of the specific markers. To check for positivity on HCT116 cells, cells are gated on SSC vs FSC to exclude debris, followed by a live/dead gating with the specific viability dye, to define the Live population. Then gate was performed on unstained control to determine positive population for the tested markers.

### 3.2.3.4 Statistical analysis

Results of the NTA analysis were analysed using one-way ANOVA and Tukey's post-hoc test with  $p < 0.05$  considered as statistically significant. Results depicted as box-whisker plots show interquartile range; whiskers: 10th and 90th percentile; line: median. GraphPad Prism software v6 or 7 was used for statistical analysis and visualisation of results.

## 4 RESULTS

### 4.1 Immunomodulatory potential of different human MSC sources

#### ***4.1.1 Inhibition of PBMC proliferation is higher in ASC cocultures, independent of their passage***

In order to verify MSC immunomodulatory capacities, direct cocultures with stimulated PBMC were established. MSC from three different sources: bone marrow (BM), cord blood (CB) and adipose-derived (ASC), from passage 3 (P3) and passage 5 (P5) at different ratios (1:5, 1:10, 1:20), were seeded and compared. Stimulated and not stimulated PBMC or CD4 T cells were seeded as controls in monocultures in 96-well plate. Proliferation (or inhibition thereof) was measured by the rate of dye dilution (Cytotell green and calculated division index). After 5 days, PHA stimulated (+PHA positive control) PBMC or CD4 cells had greatly proliferated as denoted by the elevated division index values (dotted line at 1: normalisation of values to positive control).

However, when comparing the three MSC sources, ASC appeared to be more immunosuppressive than CB (ratio 1:5 ASC vs CB,  $p < 0.001$ , 1:10 ASC vs CB,  $p < 0.0001$  and 1:20: ASC vs CB,  $p < 0.01$ , 2-way ANOVA) (Figure 10 A). The tendency was kept amongst all ratios, nevertheless, ASC and BM inhibitory potential was only significant in 1:10 ratio ( $p < 0.01$ ). In all conditions PBMC division index is significantly reduced with respect to the +PHA control ( $p < 0.001$ ), except CB 1:20 ratio ( $p < 0.01$ ) (Figure 10 A). MSC inhibitory strength was passage independent, as differences amongst P3 and P5 cocultures were not significant (n.s.) (Figure 10 B). Division index from all conditions was significantly reduced ( $p < 0.0001$ ) (ASC vs CB,  $p < 0.001$ ), although no differences were observed when comparing enriched CD4 T cells and whole PBMC cocultures (n.s.) (Figure 10 C). As shown, in coculture conditions, PBMC or CD4 cell division index was significantly reduced in all conditions when compared to the maximum proliferation ( $p < 0.0001$ ), demonstrating that MSC presence in the culture were strong effectors of PBMC or CD4 cell proliferation inhibition, independent of MSC source or passage.

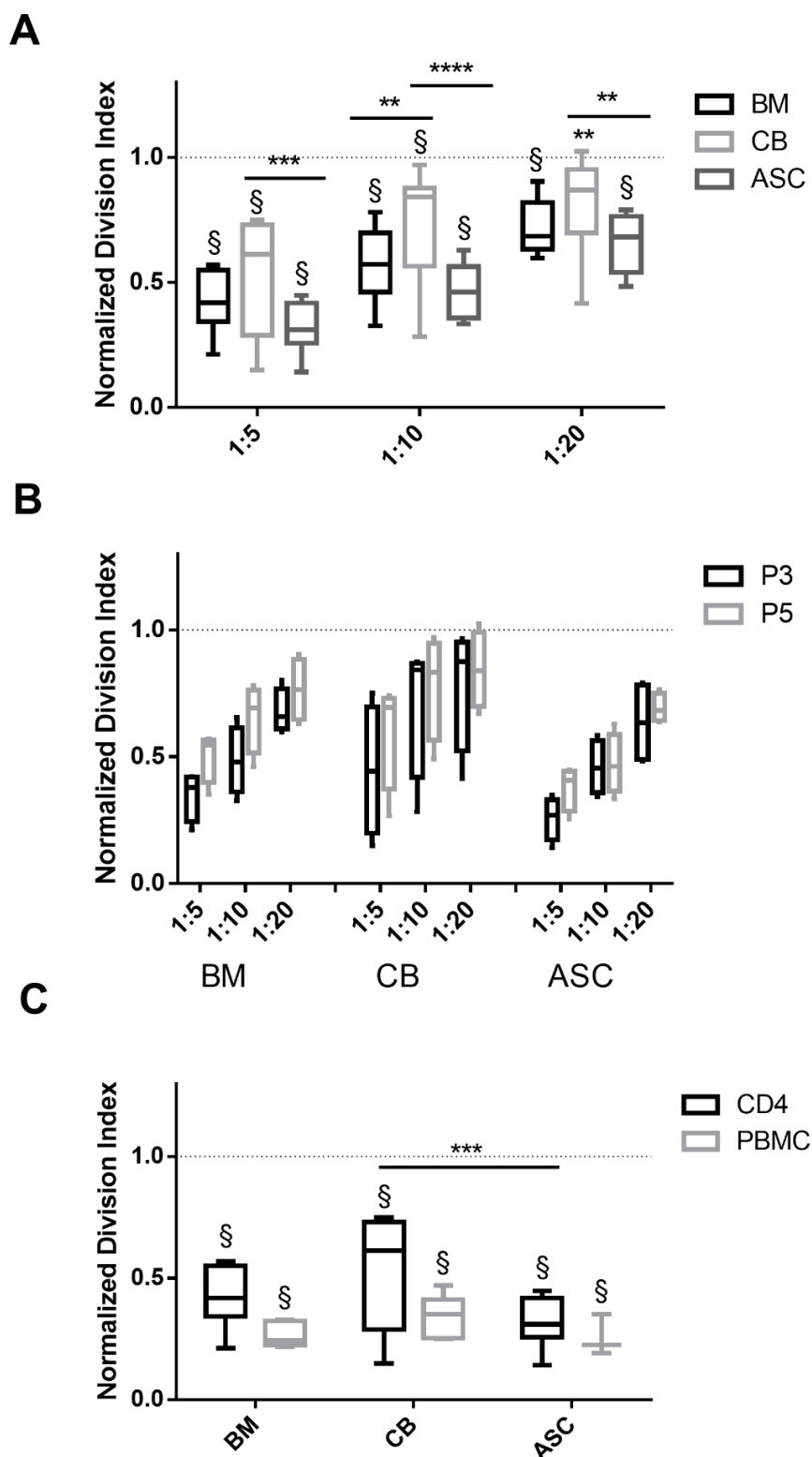


**Figure 10** ASC have a stronger inhibitory activity than BM or CB-MSC, independent of passage number and CD4 or PBMC population. (A) PBMC division index in cocultures with BM, CB and ASC in three different ratios (1:5, 1:10 and 1:20), depicts ASC as stronger immunosuppressors. (B) MSC inhibitory potential in P3 and P5 does not differ (n.s., 2-way ANOVA). (C) CD4 T cell and PBMC division index is not impacted (n.s., 2-way ANOVA). Dotted lines represent the normalisation referred to the positive control (only PBMC stimulated with PHA: +PHA control). Box: interquartile range; whiskers: minimum to maximum; line: median. Symbol § represents

the significance of the individual conditions with respect to their +PHA control (§:  $p < 0.0001$ , 2-way ANOVA).  $n = 4$  to 8, different MSC isolates and different PBMC isolates.

#### ***4.1.2 Tryptophan addition to cocultures abrogates MSC mediated PBMC inhibition, which is correlated with an increase of IDO and kynurenine secretion***

IDO has been claimed to be amongst the main mechanisms involved in MSC-mediated immunomodulatory suppression of T cell proliferation [57, 58].

To assess MSC immune modulatory strength potential differences when pre-stimulated and non pre-stimulated with IFN $\gamma$ , direct immunosuppression assays with stimulated PBMC as control, were performed.

PBMC division index was highly reduced in presence of non pre-stimulated IFN $\gamma$  MSC (-IFN $\gamma$  condition) establishing ASC as the most inhibitory. Interestingly, when comparing this condition to the pre-stimulated IFN $\gamma$  MSC condition, no difference in inhibitory potential were observed, confirming that IFN $\gamma$  priming of MSC does not increase their suppressive capacities to any extent (n.s., 2-way ANOVA) (Figure 11 A). Arguing that tryptophan depletion may be involved in this mechanism, we added tryptophan to the culture medium. In fact, additional tryptophan led to the abrogation of PBMC inhibition (BM and ASC:  $p < 0.05$  and CB:  $p < 0.001$ ). To verify the effects of the kynurenine pathway, we measured IDO expression in IFN $\gamma$  treated MSC supernatants and kynurenine secretion in coculture supernatants. We observed that only upon IFN $\gamma$  stimulation were MSC able to produce substantial amounts of IDO. ASC IDO expression was the most noticeable, ( $p < 0.0001$ ), followed by BM and CB (ASC vs CB,  $p < 0.0001$  and ASC vs BM,  $p < 0.01$ ). (Figure 11 B). Tryptophan addition further enhanced the IFN $\gamma$ -induced IDO levels in MSC (ASC vs CB and BM,  $p < 0.0001$ , 2-way ANOVA). Quantifying kynurenine in the coculture supernatants gave similar results, where no kynurenine was detectable in coculture supernatants from non pre-stimulated IFN $\gamma$  MSC (-IFN $\gamma$  condition), regardless of the addition of tryptophan in the culture. In +IFN $\gamma$  –Tryp condition, a slight increase in kynurenine production was detected (n.s.). However, upon tryptophan addition, kynurenine values were significantly increased ( $p < 0.0001$ ). BM presented higher values than MSC from other sources (BM vs CB,  $p < 0.0001$  and BM vs ASC,  $p < 0.05$ ) (Figure 11 C). No kynurenine was detected in PBMC stimulated or not stimulated monoculture controls.

In conclusion, we found that in presence of IFN $\gamma$ , MSC suppressive capacities remain unaltered, and although IDO secretion is highly promoted, kynurenine values remain barely undetectable. Tryptophan addition on the other hand, effectively abrogated MSC mediated PBMC inhibition. Once ASC were identified as the more immunosuppressant of the three MSC types, we progressed our experiments with only this source of MSC from this point forward.

#### ***4.1.3 Epacadostat abolishes PBMC inhibition and decreases IDO expression and kynurenine secretion***

To investigate whether MSC inhibitory potential was mediated by IDO enzymatic activity, we added the IDO inhibitor Epacadostat (Epac). In ASC:PBMC cocultures in the presence of Epac, PBMC division index was greatly increased with respect to their control, leading to a significant PBMC overstimulation independent of IFN $\gamma$  (-IFN $\gamma$ : +PHA -Epac vs +PHA +Epac,  $p < 0.001$ ; +IFN $\gamma$ :  $p < 0.0001$ ) (Figure 11 D). However, this inhibition was only present in the conditions with stimulated PBMC, in fact, when PBMC were not stimulated, the addition of Epac had no effect on PBMC division potential (n.s.).

The analysis of IDO expression revealed reduced levels of IDO in the presence of Tryp and Epac, when compared to its control without Epac addition ( $p < 0.0001$ ) (Figure 11 E). Despite this reduction, IDO levels were comparable to levels with only IFN $\gamma$  stimulation.

Kynurenine levels were completely abolished, indicating that despite elevated IDO levels, its activity in presence of Epac inhibitor is abrogated ( $p < 0.0001$ ) (Figure 11 F). This effect was present both in conditions with stimulated and non stimulated PBMC, although the difference between the condition in which the inhibitor was present or absent was slightly lower ( $p < 0.001$ ). No differences were observed in IFN $\gamma$  stimulated and not stimulated conditions.



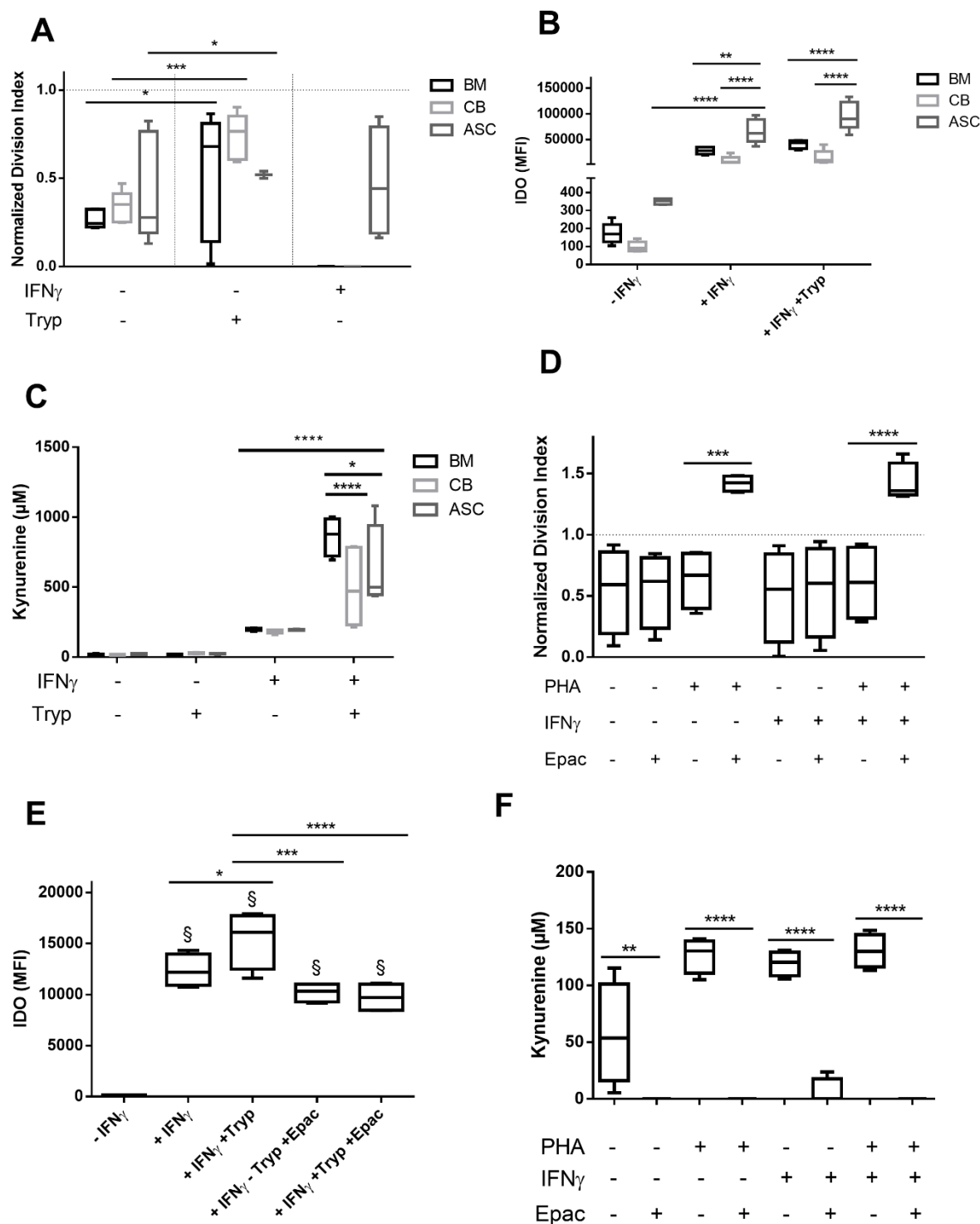


**Figure 11 IDO expression is induced by IFN $\gamma$  stimulation and further increased with the addition of tryptophan, which in turn largely abrogates MSC inhibitory potential.** (A) MSC:PBMC cocultures were set with BM, CB and ASC cells. Addition of IFN $\gamma$  and Tryp were tested. n= 5 to 8. (B) IDO production is significantly increased when MSC are stimulated with IFN $\gamma$ . n=5. (C) Kynurenine concentrations after IFN $\gamma$  addition are increased. n=5. (D) ASC:PBMC cocultures were set with the addition of IDO inhibitor, Epacadostat.. n=4. (E) IDO secretion is reduced when adding Epacadostat (p<0.0001, 2-way ANOVA), n=4. (F) Kynurenine concentrations are completely abolished in presence of Epacadostat. n=4. Box: interquartile range; whiskers: minimum to maximum; line: median. Dotted lines represent the normalisation referred to the positive control. Asterisks depicted at the top of the lines represent the significance of the individual value with respect to their own condition

control. Symbol § represents the significance of the individual conditions with respect to their positive control (§:  $p < 0.0001$ , 2-way ANOVA). Lines with asterisks depict the significance between two conditions.

#### ***4.1.4 Human PBMC proliferation is inhibited greater with human than with rat MSC, however, the latter inhibits blood rat PBMC to a higher extent***

The next aim was to compare human and rat PBMC and MSC in allogeneic and xenogeneic immunosuppression assays to verify whether human MSC can be immunomodulatory even in a xenogeneic setting.

Human PBMC cocultures were set with both human MSC and rat MSC to test human PBMC specific inhibition. Verifying the previously shown data, human MSC inhibited human PBMC proliferation dose-dependently (1:5 and 1:10,  $p < 0.01$ ; 1:20, n.s.; Figure 12 A). Rat MSC, conversely, revealed a significantly reduced hPBMC inhibitory action compared to hMSC effect (1:5, 1:10,  $p < 0.001$ ).

Comparing rat PBMC and SMC inhibition by both human MSC and rat MSC revealed the lack of hMSC inhibitory potential to reduce division index of either rat MC population ( $p < 0.01$  at least; Figure 12 B). Rat MSC on the other hand reduced rat PBMC division index much more than SMC (n.s., 2-way ANOVA).

These data clearly show, that both human:human and rat:rat allocultures presented immunosuppression, while the xenocultures were not or only marginally inhibited.

#### ***4.1.5 Kynurenine secretion is prominently higher in human PBMC immunosuppression assay***

So far our data has shown that allogeneic MSC were able to induce PBMC division inhibition, in contrast to cocultures with xenogeneic MSC. As in the human setting, IDO and the kynurenine pathway were largely involved, we also analysed the coculture supernatants of allo- and rat xeno-cocultures.

In human immunosuppression assays, Kyn secretion was the highest ( $p < 0.0001$ , Figure 12 C). However, in presence of rat MSC, Kyn levels were not elevated. Likewise, in rat cocultures with PBMC and SMC, no kynurenine values were detected, except for negligible levels in stimulated PBMC monoculture control (+ConA) (n.s.; Figure 12 D).

These data are in line with our hypothesis, suggesting that human MSC (ASC) inhibitory effector IDO mediates Trp degradation and formation of Kyn, and further

supporting previous notions that murine MSC use other mechanism for immunosuppression, most probably nitrite production.

#### ***4.1.6 Cultures with rat PBMC exert nitrite production further than SMC***

Thus, we investigated nitrite concentration in both human and rat immunosuppression assays, as it is a stable breakdown of NO and indicative of NO activity [51]. Unexpectedly, the amounts of nitrite found in rat MSC:human PBMC coculture condition were extremely high, ranging from 1 to 30 $\mu$ mol/l ( $p < 0.0001$ ; Figure 12 E). Nonetheless, in coculture supernatants from rat PBMC and SMC, values for human and rat MSC were in line with those presented by the respective controls (Figure 12 F). Overall, rat PBMC reveal slightly higher values than SMC, but no major differences were found (n.s.).

In contrast with our starting hypothesis, these data showed that xenogeneic rat MSC:human PBMC coculture is where the utmost nitrite concentration release were found, diverging from the lower levels found in rat allogeneic coculture condition.

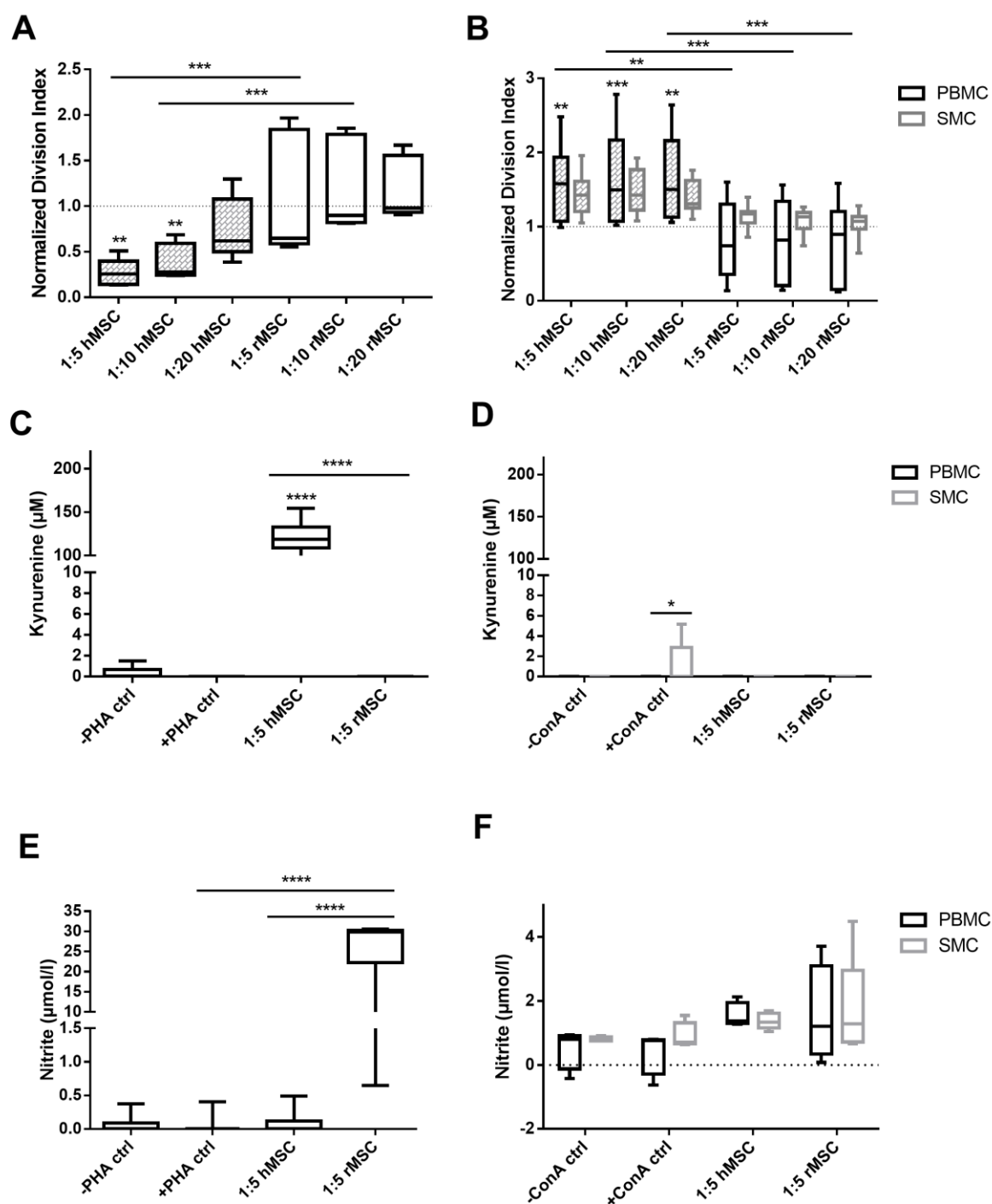


**Figure 12** ASC are able to inhibit human PBMC proliferation, but not rat PBMC, however, rat MSC slightly suppress human PBMC and inhibit blood-derived rat PBMC to a higher extent than rat SMC. (A) Cocultures with hPBMC and hMSC (ASC) and rMSC. ASC inhibited human PBMC in a dose dependent manner.  $n=5$ . (B) Rat PBMC and SMC cocultures with human MSC and rMSC.  $n=8$  to 10. (C) Kynurenine concentrations in hPBMC:ASC or rMSC coculture supernatants.  $n=3$  to 10. (D) Kynurenine concentrations in rat PBMC or SMC:ASC or rMSC coculture supernatants.  $n=5$  (E) Nitrite concentration measured in cocultures with hPBMC.  $n=3$  to 10. (F) Nitrite concentrations in rat PBMC or SMC:ASC or rMSC coculture supernatants.  $n=4$  to 6. Box: interquartile range; whiskers: minimum to maximum; line: median. Dotted lines represent the normalisation

referred to the positive control. Asterisks depicted at the top of the lines represent the significance of the individual value with respect to their own control. Lines with asterisks depict the significance between two conditions.

#### ***4.1.7 ASC are more immunosuppressive than ABCB5 in human allo-coculture, whereas ABCB5 are stronger inhibitors in xeno-coculture settings***

Comparison of ABCB5 and ASC immunomodulatory strength was assessed in immunosuppression assays. Results showed stronger ASC inhibition of human PBMC proliferation compared to ABCB5 cells (n.s., Figure 13 A). These data were in consonance with the higher kyn values secreted in conditioned media of ASC allo-proliferation assays (ABCB5 vs ASC,  $p < 0.001$ , Figure 13 B). Values were significantly higher compared to those of ABCB5 allo cultures, confirming the involvement of IDO mediated immunomodulation ( $p < 0.001$ ). Verifying the lack of NO immune modulation, nitrite values of both ABCB5 and ASC allo-coculture were negligible (Figure 13 C).

Contrary to the previous results, showing no inhibition of rat PBMC and SMC by ASC, ABCB5 cells inhibited both PBMC and SMC (SMC, ABCB5 vs ASC,  $p < 0.0001$ , Figure 13 A). Kynurenine levels were insignificant in ABCB5 and ASC xeno-coculture, denoting significantly reduced values with respect to human allo-coculture ( $p < 0.0001$ , Figure 13 B). Nitrite secretion was abundantly reduced in ASC xeno cultures, however, in ABCB5 xeno cultures levels were undetectable ( $p < 0.0001$ , Figure 13 C).

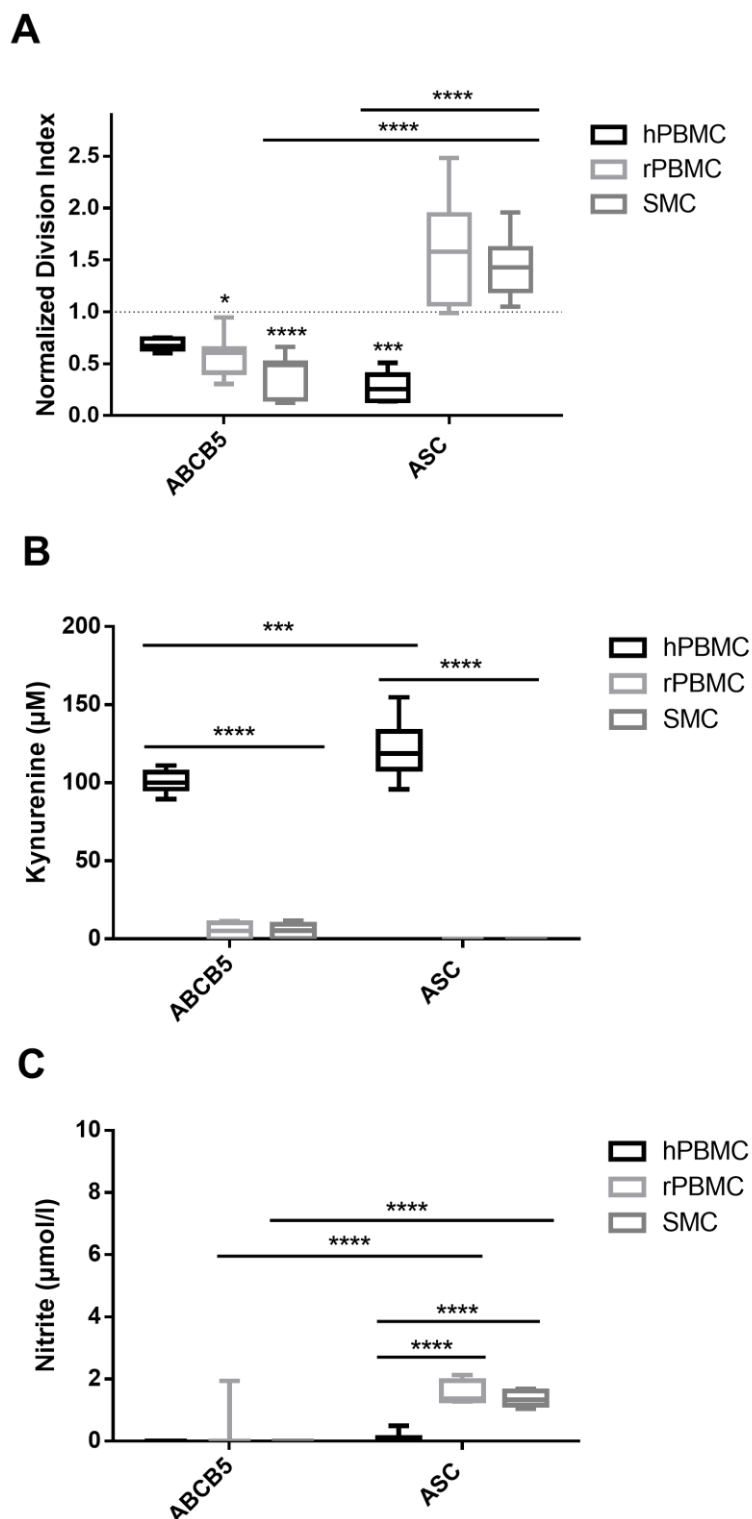


**Figure 13 ASC are stronger immunosuppressors in allo-cocultures and ABCB5 in xeno-cocultures.** (A) Human PBMC/rat PBMC/rat SMC:ABCB5/ASC cocultures. ASC inhibited human PBMC to a higher extent than ABCB5 cells.  $n=5$  to 10. (B) Kynurenine concentration measurements in coculture supernatants.  $n=5$  to 10. (C) Nitrite secretion measured in coculture supernatants.  $n=5$  to 10. Box: interquartile range; whiskers: minimum to maximum; line: median. Dotted lines represent the normalisation referred to the positive control. Asterisks depicted at the top of the boxes represent the significance of the individual value respect to the positive control. Lines with asterisks depict the significance between two conditions.

In short, ASC have demonstrated to be the strongest immunosuppressors followed by BM- and CB-MSC. They inhibit PBMC and CD4 T cell proliferation to the same extent in a distinct ratio dependent manner. Moreover, their inhibitory strength is passage independent. These data were supported by the highest IDO secretion levels in ASC, upon IFN $\gamma$  stimulation. Furthermore, we elucidated IDO-kynurenine to be the principal suppressive mechanisms by which MSC inhibit PBMC proliferation. Epacadostat addition to the cultures confirmed the involvement of IDO mechanism, observing an abrogation of MSC inhibitory actions. Nitric oxide was confirmed not to be involved in human MSC-mediated immunosuppression by monitoring nitrite levels in coculture supernatants.

Furthermore, we validated that both human and rat MSC, when in allo-cocultures, strongly inhibit T cell proliferation. In xeno-cocultures with human MSC, ASC were unable to inhibit rat PBMC and SMC proliferation. However, ABCB5 cells successfully suppressed both sources of rat mononuclear cells (MC). Rat MSC on the other hand inhibited human PBMC proliferation. We confirmed that murine and human MSC immunomodulation are driven by different mechanisms, murine MSC rely mostly on NO while human MSC rely on IDO-mediated system.

## **4.2 MSC-derived products modulatory functions**

Having shown that human ASC inhibit human PBMC proliferation to a large extent involving IDO and the kynurenine pathway, we were further interested in the involved mechanisms. We asked ourselves to which extent conditioned media and possibly extracellular vesicles were involved. First, we had to establish EV isolation and characterisation.

The typical characterisation methods, their upsides and downsides have been broadly described in Introduction section 1.2.1. Thus, my main task in the framework of the comparative study was to establish the FACS method of EV characterisation. More detailed characterisation results will be shown subsequently within the interlaboratory study chapter 4.3. For this aim several bead-EV combinations were assessed.

---

#### ***4.2.1 ASC-derived EV flow cytometry measurement favours the use of aldehyde/sulfate latex bead-EV coupling***

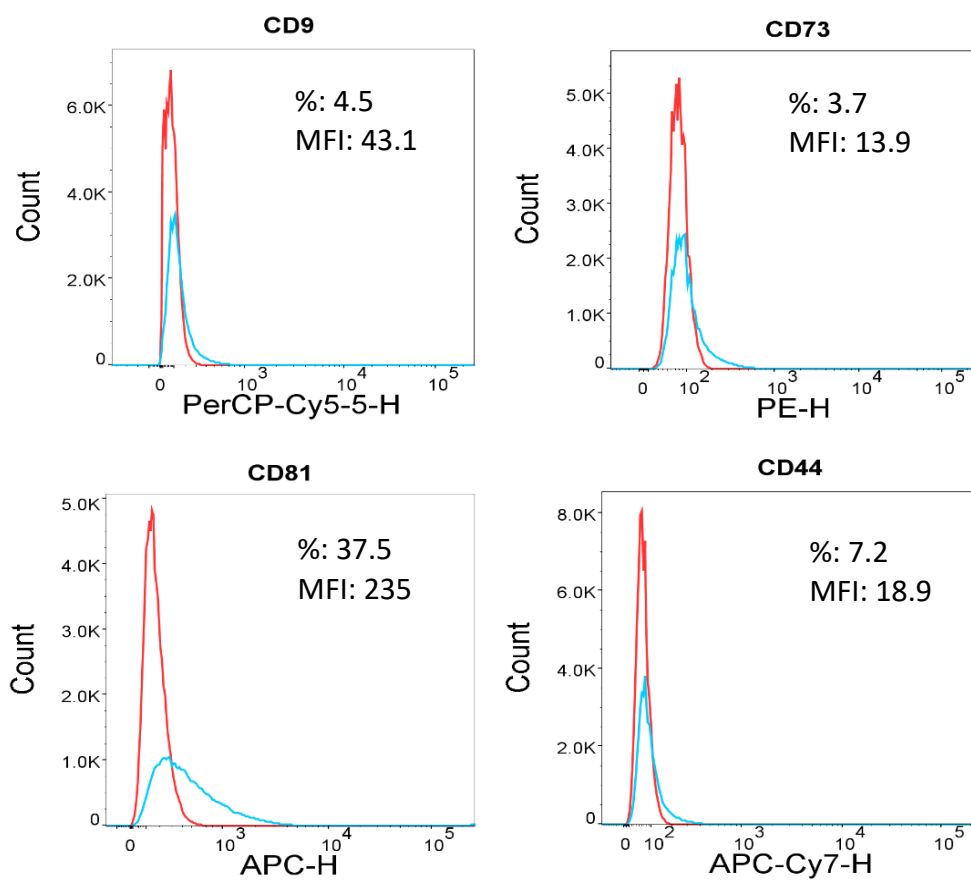
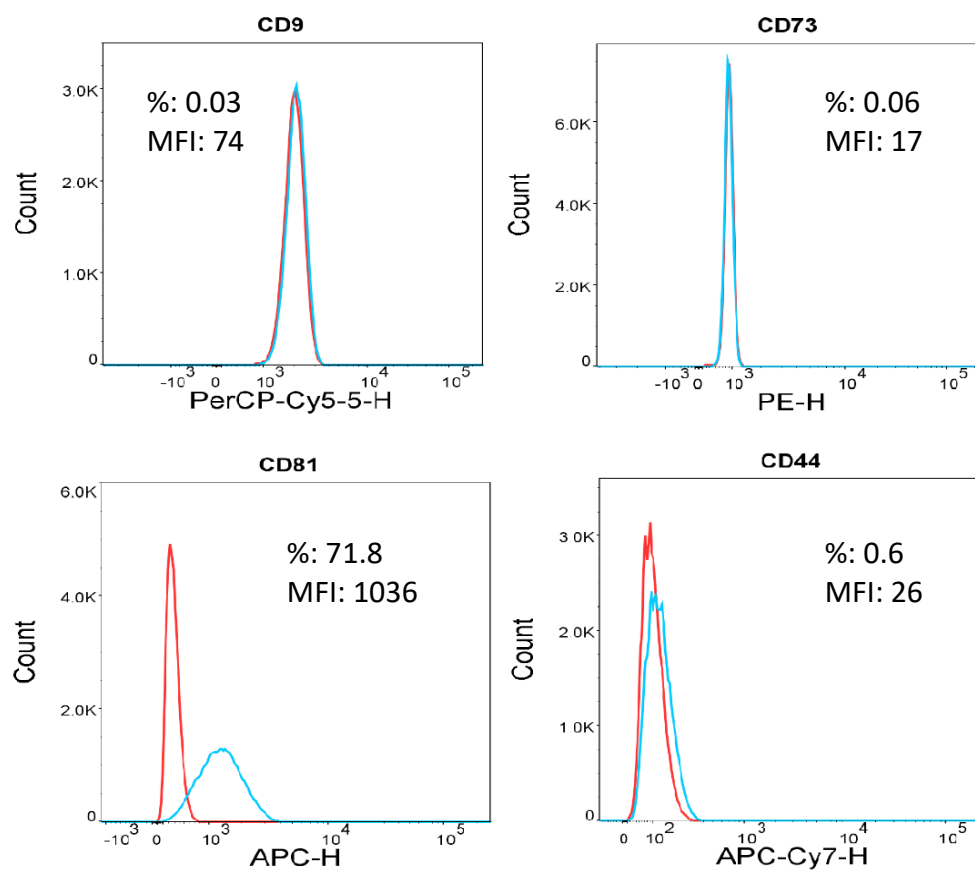
ASC-derived EVs bound to CD9 beads exhibited overall low positivity (CD9 (0.032%), CD73 (0.067%) and CD44 (0.60%)), for the majority of markers tested, aside from CD81 (71.8%) that had slightly elevated expression values (Figure 14 B). Aldehyde bead coupling to ASC-EV expression for CD9, CD73 and CD44 was 4.51%, 3.74% and 7.18%, respectively. CD81 expression was slightly higher (37.5%) (Figure 14 A).

Contrarily, HCT116-derived EVs bound to CD9 beads presented overall higher marker expression in comparison to ASC-EVs, being CD9 (98.1%), CD81 (99.6%) and CD44 (97.9%) highly expressed, and CD73 (0.065%) almost absent (Figure 14 D). Aldehyde bead coupling reported suggestively lower general expression compared to CD9 bead coupling, CD9 (3.37%), CD73 (1.15%), CD81 (4.44%) and CD44 (1.25%) (Figure 14 C), which strongly suggests CD9 beads to promote a stronger marker signal detection in flow cytometry measurements. Markers were tested on both cell types, illustrating an overall expression superior than 98% positivity (data not shown).

These data suggest that different bead types are required for EV characterisation for different cell lines, based on the expression of the respective markers: ASC-derived EV work best with Aldehyde/sulfate latex beads and HCT116-derived EV with CD9 magnetic human beads.

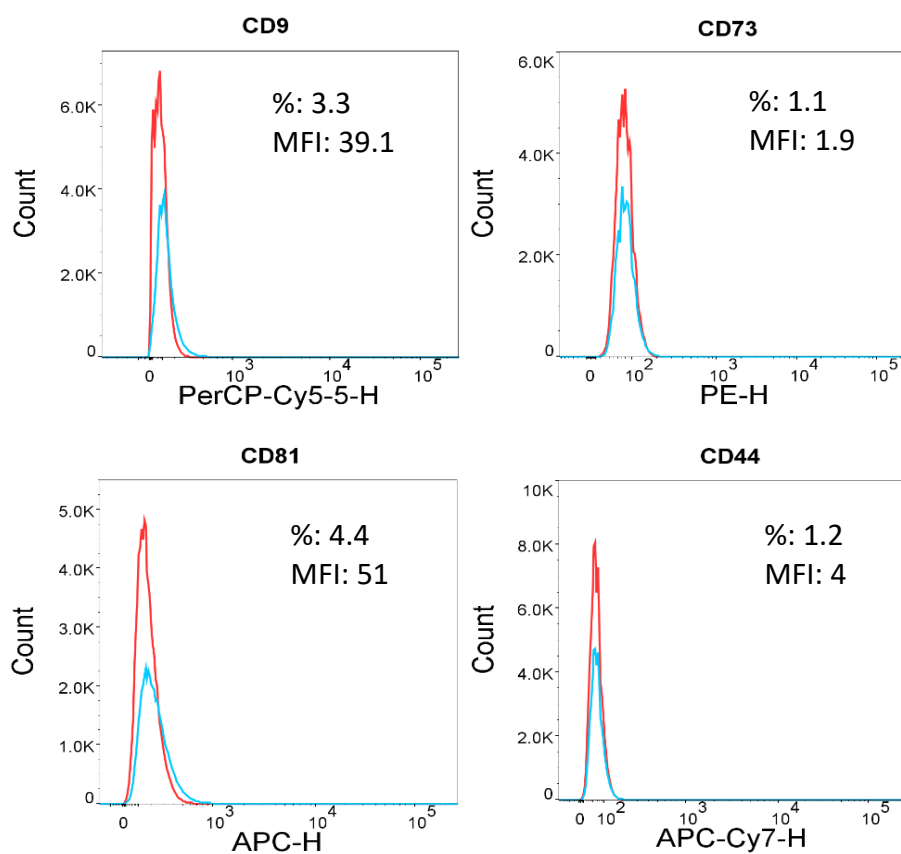


## ASC-derived EVs

**A****B**

## HCT116-derived EVs

C



D

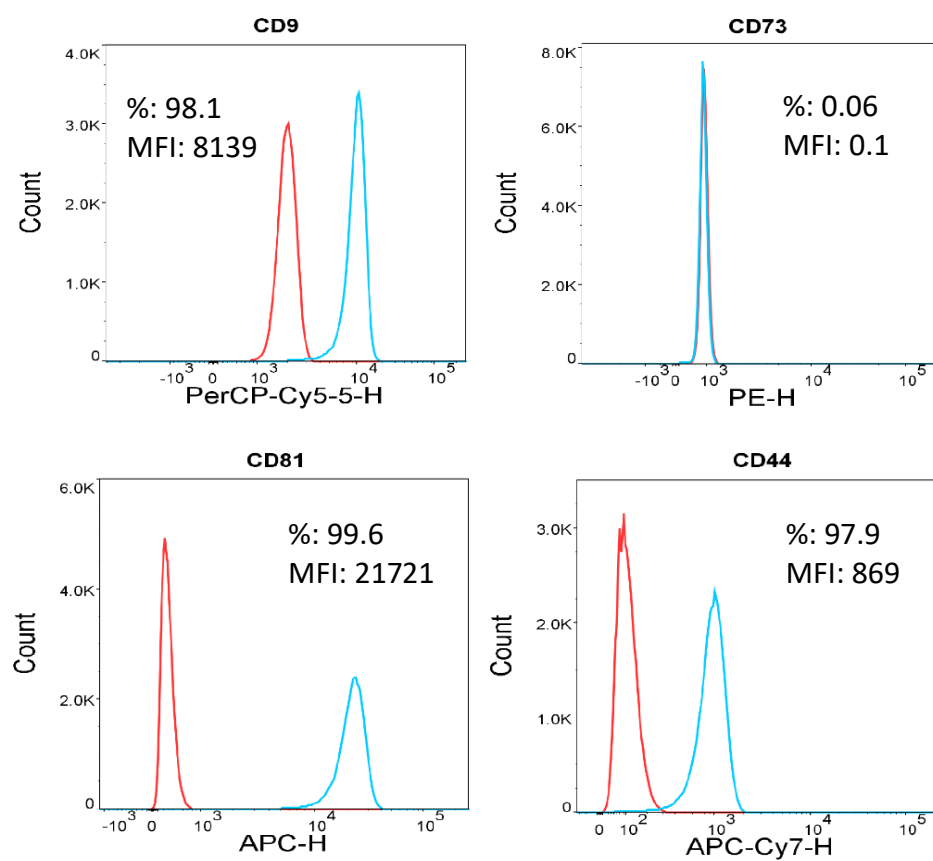


**Figure 14 FACS-based characterisation of ASC and HCT116-derived EV.** Flow cytometry histograms depicting the relative fluorescence/marker expression intensity of ASC-derived EV (*blue line*) coupled with Aldehyde latex beads (A) and CD9 magnetic beads (B) depicted against unstained EV particle control (*red line*). Corresponding staining for marker expression in HCT116-derived EVs coupled with Aldehyde latex beads (C) and CD9 magnetic beads (D) was done. Extracellular staining with CD9, CD81, CD73 and CD44 was performed for all samples.

#### ***4.2.2 ASC-derived EV present typical EV characteristics which are unaffected by IFN $\gamma$ priming***

Speculating that IFN $\gamma$  MSC prestimulation may modify EV production and function, EV were isolated from ASC cultured in presence and absence of IFN $\gamma$  directly after seeding, during 72 hours. Media in absence of MSC was also conditioned for 72 hours and used as isolation control for EV. ASC-derived EV were measured in the NTA, counts and full size profiles were determined. NTA analysis showed EV size medians of  $115.1 \pm 1.8$  nm (-IFN $\gamma$ ),  $111.1 \pm 2.2$  nm (+IFN $\gamma$ ), in EV isolates, and  $113.1 \pm 4.3$  nm (Ctrl -IFN $\gamma$ ),  $115.2 \pm 4.1$  nm (Ctrl +IFN $\gamma$ ) in control EV samples. Significant differences were seen amongst EV isolates from different donors (100, 101, 102 or 112) within one condition (i.e. EV +IFN $\gamma$  condition), with p values ranging from 0.05 to 0.0001 (Figure 15 A). Nonetheless, EV size profiles did not differ when comparing different conditions amongst each other (n.s.).

There were significant differences in EV counts (=yields) amongst different donors, portraying donor-dependent variations, similarly to MSC donor variation described previously (EV +IFN $\gamma$ : 101 vs 112,  $p < 0.01$ ; EV -IFN $\gamma$ : 100 vs 112 and 101 vs 112,  $p < 0.01$ ; Ctrl EV +IFN $\gamma$ : 101 and 102 vs 112,  $p < 0.01$ ; Ctrl EV -IFN $\gamma$ : 100 vs 102,  $p < 0.01$ , 101 vs 102 and 112,  $p < 0.05$ , 2-way ANOVA) (Figure 15 B). However, results revealed no differences in particle yield between EV derived from IFN $\gamma$  preconditioned and non-preconditioned MSC, when comparing isolates from different conditions (n.s.), thus we conclude that IFN $\gamma$  pre-stimulation does not alter the EV yield to any extent.

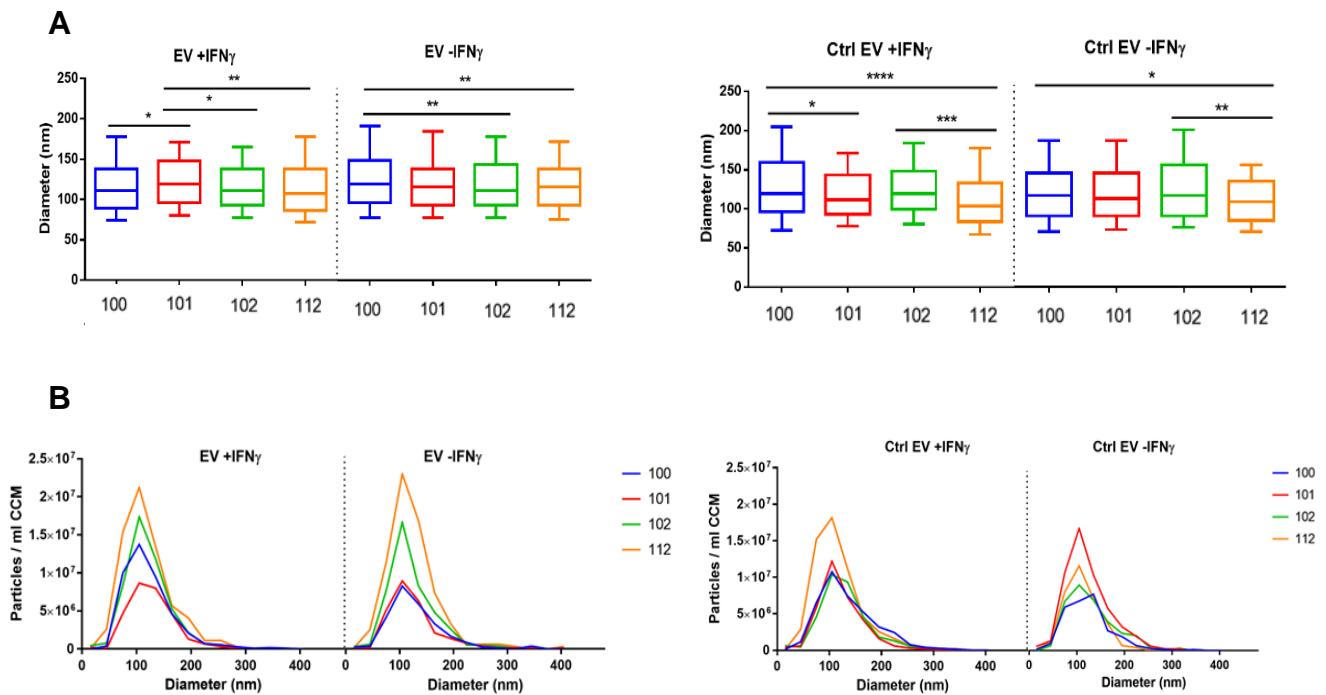


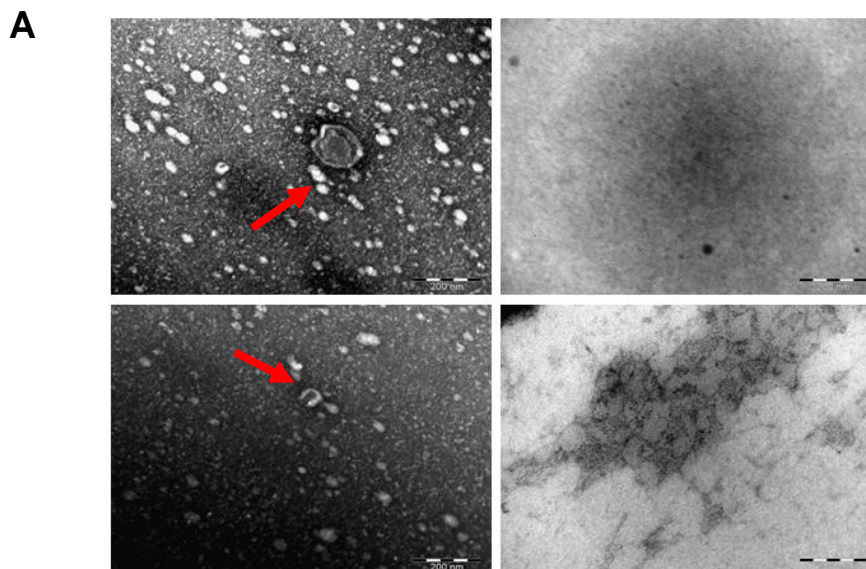
**Figure 15 NTA characterisation of EV.** (A) NTA size profile (diameter) of isolated EV +IFN $\gamma$  and – IFN $\gamma$ . n=4. (B) Full size profiles (Yield/ml cell conditioned media against particle size) for EV isolated from +IFN $\gamma$  pre-stimulated and not (-IFN $\gamma$ ) pre-stimulated MSC. Box: interquartile range; whiskers: 10th and 90th percentile; line: median. Lines with asterisks depict the significance between two conditions.

For single vesicle analysis, TEM visualisation was performed. Images showed spherical, cup-shaped EV isolates, which are typically for EV concentrates isolated by ultracentrifugation. We tested multiple ASC donor EV samples and could detect no major differences amongst preparations (Fig 16 A, representative images from two ASC-derived EV samples). As controls we measured sterile-filtered PBS (0.22 $\mu$ m filter), and EV media control in absence of ASC. As expected, in the former, we detected no particles. The latter presented background noise, hypothesised to be protein aggregates remaining from the serum present in the media.

For specific EV characterisation, marker proteins are characterised by either western blot or flow cytometry. Once established the best bead-EV coupling (see section 4.2.1), we used FACS analysis, given that it requires much lower amount of EV material. We tested a broader panel of antibodies and compared EV specific marker expression to their cells of origin. Several groups reported surface protein such as the tetraspanins CD63, CD9 or CD81 to be common EV surface markers [152-155]. We therefore tested these as extracellular markers and Alix, TSG101 and Calnexin as intracellular markers. EV bound to Aldehyde beads showed positive staining for

the typical EV surface markers CD63 (27.2%) and CD81 (29.1%) (Figure 16 B). Low amount of staining was observed for Calnexin (13.5%), however, CD9, TSG101 and Alix (0.47%, 1.35% and 6.55%, respectively) staining were lower than initially expected. All markers were validated to be expressed in ASC cells either by extra- (CD9 (99.4%), CD63 (90.8%), CD81 (100%)) or intracellular staining (Calnexin (99.3%), TSG101 (78.6%), Alix (97.5%)) (Figure 16 C).

In summary, our isolates present the characteristic size, morphology and markers of EV derived from MSC. Their concentration and mean sizes are unaffected by the preconditioning of MSC with IFN $\gamma$ .



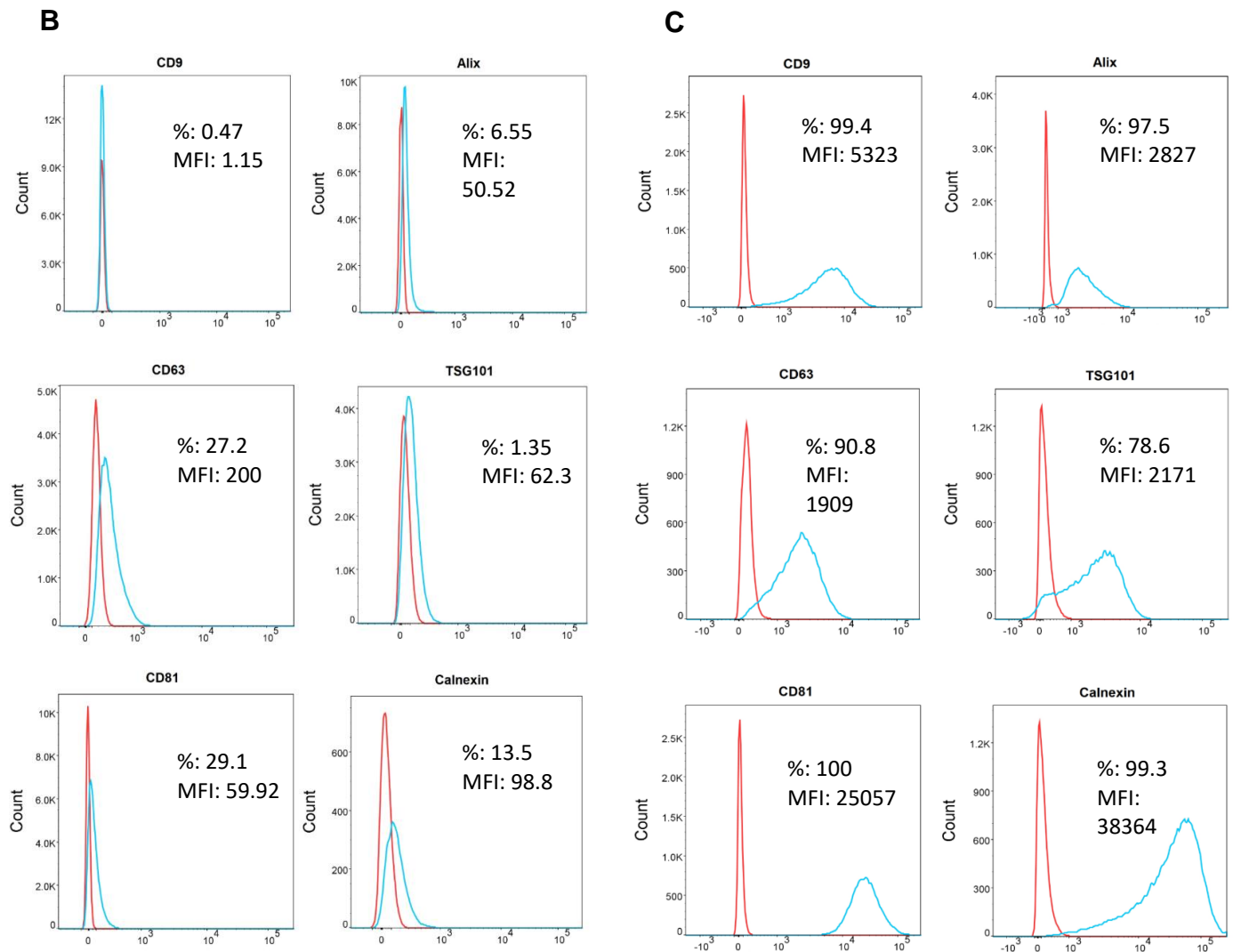


**Figure 16 Further characterisation of EV.** (A) Representative TEM analysis showing spherical and cup-shaped EV (red arrows) isolated from different ASC donors (top and bottom left); PBS control (top right) shows absence of particles while Control EV media (bottom right) shows only possible traces of protein aggregate remaining, but absence of EV particles. Scale bar 200 nm. (B) Flow cytometry histograms depicting the relative fluorescence/marker intensity of ASC-derived EVs isolates (*blue line*) against unstained EV particle control (*red line*). (C) Corresponding marker expression in ASC cells (extracellular staining for CD9, CD63 and CD81 and intracellular staining for Alix, TSG101 and Calnexin).

#### **4.2.3 Direct and transwell coculture inhibit the proliferation of stimulated PBMC via IDO-Kynurenine pathway**

In chapter 4.1, we have shown that ASC inhibit T cell proliferation via the IDO-kynurenine pathway. We were interested in understanding whether a direct cell-mediated communication is required to induce this effect or whether it functions via paracrine factors or EV. We performed MSC:PBMC cocultures with MSC pre-treated and not with IFN $\gamma$  and tested the ASC inhibitory potential on stimulated PBMC both in a direct and transwell culture. After 5 days, coculture conditions and their respective controls were harvested, and supernatants were retrieved and aliquoted for further testing. In all conditions, PBMC stimulation was significantly inhibited ( $p < 0.0001$ , 2-way ANOVA), demonstrated by the low division index values. No major differences were observed amongst cocultures performed in either direct or transwell setting, indicating that direct cell-cell interaction is not essential for MSC to exert their immune modulation (n.s.) (Figure 17 A). MSC inhibitory potential was not intensified by the prior priming with IFN $\gamma$ , not conferring MSC any further beneficial modulatory strength.

We were interested in validating the immune assay proliferation data with the kynurenine measurements on coculture supernatants. In fact, we observed a strong correlation between PBMC inhibition and high kynurenine values ( $p < 0.0001$ , 2-way ANOVA) (Figure 17 B) in the coculture conditions both in direct and transwell cocultures. MSC prestimulation with IFN $\gamma$  showed no difference in kynurenine secretion (n.s.).

Next, we tested MSC conditioned media (CM) and extracellular vesicle modulatory capacities on stimulated PBMC. We observed that CM from non IFN $\gamma$  primed MSC, and EVs from either IFN $\gamma$  primed or non primed MSC, had no effect on PBMC inhibition, exerting even an overstimulation of their division (n.s.) (Figure 17 C). In contrast, CM from IFN $\gamma$  primed MSC, showed an intense PBMC proliferation inhibition, marked by the low PBMC division index values ( $p < 0.0001$ , 2-way ANOVA). Following the findings that CM +IFN $\gamma$  was successful in inhibiting PBMC proliferation, we performed immunosuppression assays with addition of the inhibitor Epacadostat. Surprisingly, we observed that even in the presence of Epacadostat, PBMC proliferation was not restored, and division index values remained similar to those of CM +IFN $\gamma$  (n.s.) (Figure 17 D), although only this condition was significantly different with respect to the control condition ( $p < 0.05$ , 2-way ANOVA).

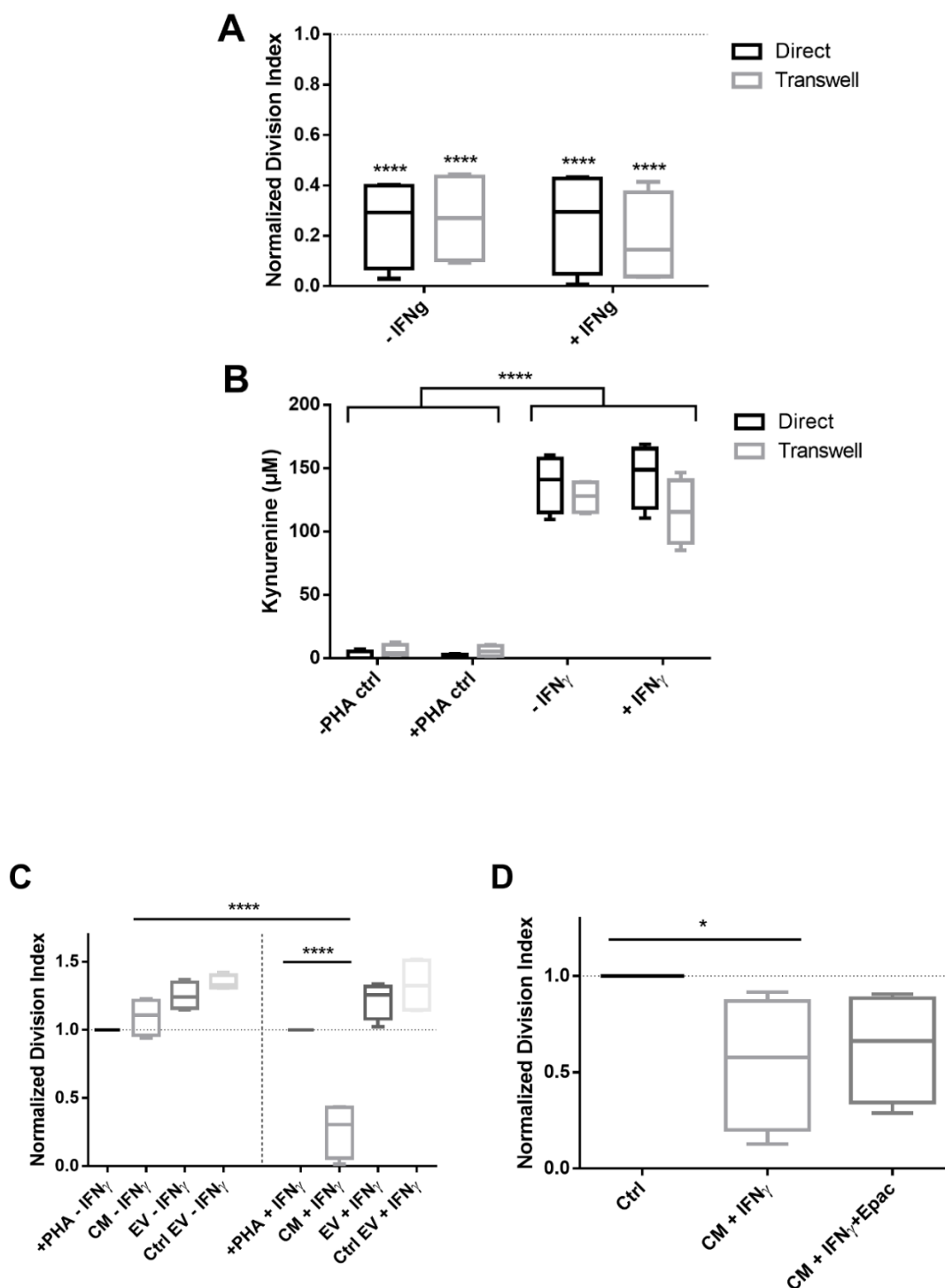


**Figure 17** PBMC were equally inhibited in direct and transwell cocultures, although EV failed to suppress their proliferation regardless of IFN $\gamma$  pre-stimulation. (A) PBMC division index evaluation in direct and transwell culture conditions.  $n=4$  (B) Kynurenine concentrations measured in direct and transwell coculture supernatants.  $n=4$  (C) Cocultures with CM and EV isolated from stimulated and not stimulated ASC.  $n=4$  (D) Cultures with CM + IFN $\gamma$  together with the addition of IDO inhibitor Epacadostat.  $n=4$ . Box: interquartile range; whiskers: minimum to maximum; line: median. Dotted lines represent the normalisation referred to the positive control. Asterisks depicted at the top of the lines represent the significance of the individual value with respect to their own control. Lines with asterisks depict the significance between two conditions.



#### 4.2.4 Stimulated PBMC were not inhibited by conditioned media (CM) transferred from a previous coculture

To investigate the potential immune suppressor action of CM from a previous 5 day ASC:PBMC coculture on PBMC proliferation, immune suppressive assays were established. Conditioned media from these cocultures were diluted 1:2 in new full RPMI 1640 media to ensure newly added factors to the culture. After another 5 day coculture, PHA-stimulated PBMC highly proliferated, as denoted by the high division index (line at 1) (Figure 18). In addition, no differences were found in PBMC inhibition in the presence of CM with or without IFN $\gamma$  inclusion, nor only with stimulated PBMC (n.s.). This data confirmed that CM from previous cocultures are not able to actively interact with PBMC, possibly due to the inactivation and extinction of the necessary factors that assist to mediate this inhibition.

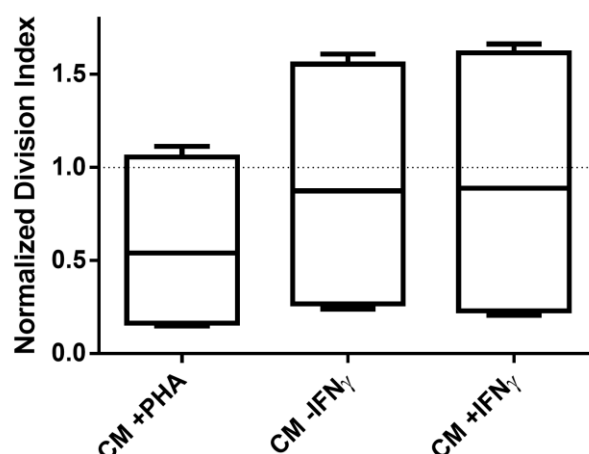


**Figure 18 CM transferred from a previous coculture was ineffective on exerting PBMC inhibition. Stimulated PBMC were not inhibited by CM transferred from a previous coculture.** PBMC division index after transferring CM from a 5 day ASC:PBMC coculture (-/+ IFN $\gamma$ ), was analysed. n=4. Box: interquartile range; whiskers: minimum to maximum; line: median.

#### 4.2.5 Nitrite levels were mainly undetectable amongst all conditions, except for MSC-CM

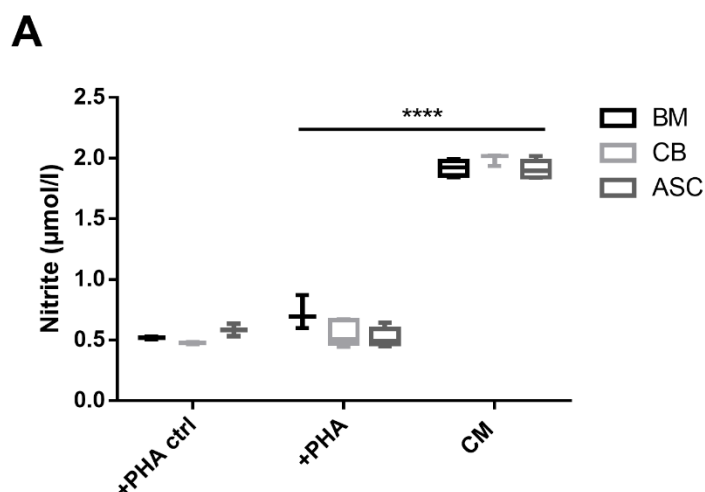
Although our previous findings did not suggest the involvement of NO in our human suppression assays, nitrite concentrations were measured in coculture supernatants. Results revealed equally negligible nitrite concentration in both stimulated (n.s.) and not stimulated (not shown) PBMC monocultures. Although values for coculture

conditions with stimulated PBMC were slightly positive, they were still not significant. Surprisingly, we observed that values for CM from MSC were significantly elevated (all MSC from different sources vs +PHA coculture condition,  $p < 0.0001$ ; Figure 19 A). However, MSC from different sources presented comparable nitrite concentration values (n.s.).

As expected, we found very low nitrite concentrations in both IFN $\gamma$  primed and not primed human coculture condition supernatants (n.s.; Figure 19 B). Accordingly, IDO inhibitor Epacadostat addition did not vary nitrite values to any extent.

CM +IFN $\gamma$  exerted a slight increase in nitrite values with respect to the control ( $p < 0.0001$ , Figure 19 C), however, also in MSC monocultures a basal nitrite concentration is present. Nitrite concentrations measured in the rest of ASC:PBMC coculture conditions, were below 0.5  $\mu\text{mol/l}$  (not shown), suggesting that the slight increase in its levels is not exclusively related to PBMC presence in the culture. The addition of Epac to this condition revealed no variance in nitrite secretion. Results did not differ significantly to conditions lacking the inhibitor (n.s.), however, values significantly increased compared to MSC control ( $p < 0.0001$ ).

Subsequently, these data suggest that Epac does not act upon nitrite secretion, nor is nitrite, on the other hand, a key mediator of human PBMC inhibition.



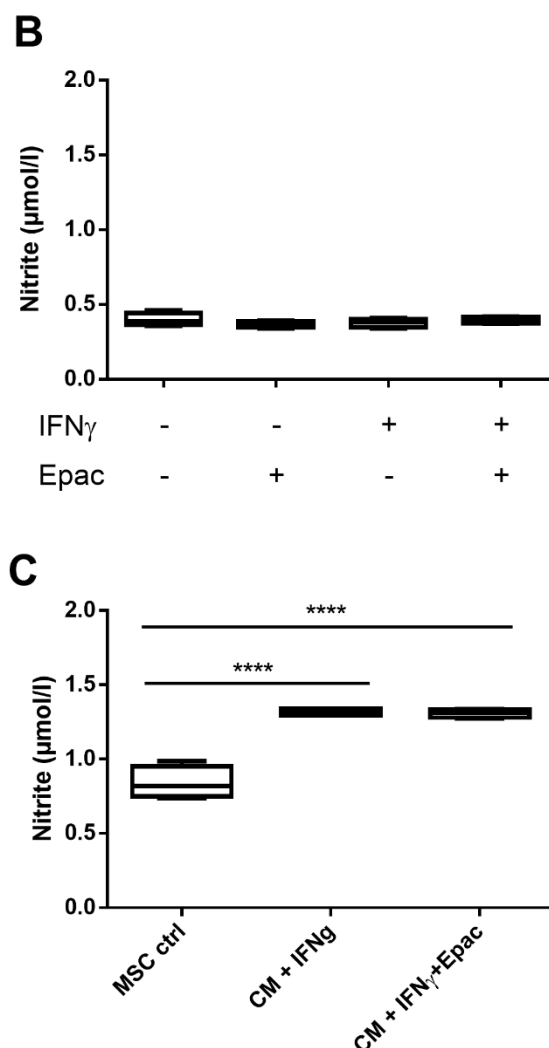


**Figure 19 Nitrite concentrations were detectable only in MSC-CM.** (A) Nitrite concentration levels measured in BM, CB and ASC coculture supernatants. All MSC sources have comparable nitrite production concentration levels.  $n=3$  to 5. (B) Nitrite concentration in coculture supernatants with IFN $\gamma$  and Epacodostat addition.  $n=4$ . (C) Nitrite levels measured in CM +IFN $\gamma$  after addition of IDO inhibitor Epacodostat.  $n=4$ . Box: interquartile range; whiskers: minimum to maximum; line: median. Lines with asterisks depict the significance between two conditions.

In summary, by performing direct and transwell MSC:PBMC cocultures, we confirmed that MSC immunosuppressive mechanism acts independent of cell-to-cell contact, but is mediated by soluble factors. We revealed the immunosuppressive strength of IFN $\gamma$  MSC-CM in inhibiting T cell proliferation. Nevertheless, isolated EV failed to suppress their proliferation, regardless of MSC IFN $\gamma$  preconditioning.

### 4.3 Evaluation of standardised ultracentrifuge-based EV isolation protocol

With the aim to address the impact of ASC-derived EV on immunomodulation, we were challenged with defining an optimal protocol for EV isolation and characterisation. Having discussed this issue with researchers from different labs asking for their advice, we identified a need for a comparative analysis of EVs. With four participating labs, we pre-defined a protocol to qualitatively and quantitatively evaluate EV preparations within this inter laboratory study. The human epithelial CRC cell line HCT116 was chosen as a model of parental EV-secreting cells. CCM was collected and distributed to the four participating laboratories for EV isolation using a pre-defined protocol and their lab-specific technical equipment.

#### 4.3.1 Comparative EV isolation - First round

Subsequently, EV characterisation was collectively performed by TEM and NTA, each method performed in a different laboratory.

TEM analysis showed spherical and cup-shaped EVs in all four preparations (Figure 20 A). EV sizes ranged from around 30 to 150 nm in diameter. NTA analysis showed that median sizes of isolated particles differed slightly between groups, ranging from  $128.3 \pm 14.5$  nm (laboratory 1.2) to  $154.9 \pm 42.7$  nm (laboratory 1.4) per group (Figure 20 B and C, and Table 3), with a coefficient of variation (Cv) of 8.80 % across the groups. Calculating the particle concentrations by NTA revealed significantly different particle yields per ml of medium (Table 3). Laboratory 1.1 isolated most particles, and significantly more than 1.2 ( $p < 0.0001$ ), 1.3 ( $p = 0.0035$ ), and 1.4 ( $p < 0.0001$ ), which is reflected in an overall Cv of 70.88 %. The EV preparation with the lowest yield (1.4) was isolated after storing CCM at RT for six hours. Removing data obtained from L4 from the analysis, inter-group variation was significantly reduced for both particle yield per ml medium (Cv: 40.93 %) and median particle diameter (Cv: 1.96 %).

Marker expression was planned to be performed by western blot and flow cytometry, however, the amount of material was too little to allow for its use. Protein yield was less than  $4\mu\text{g}/\mu\text{l}$  in all samples.

The results of our first isolation round showed that despite a pre-defined protocol, isolation yielded EVs of differing sizes and an insufficient amount of material for EV protein characterisation. We observed that storage time might have a detrimental

effect on final yield. Accordingly, a second round of isolation was planned with slight modifications of the settings, mainly increasing starting volume and cryopreserving the CCM before isolation to overcome extended storage times at ambient temperature.

**Table 3 Particle sizes and concentrations determined by NTA analysis (first round).** All data are presented as arithmetic mean  $\pm$  SD of measurements within one group.

	1.1	1.2	1.3	1.4	Cv [%]	p
<b>Median diameter [nm]</b>	131.8 $\pm$ 9.7	128.3 $\pm$ 15.5	133.3 $\pm$ 12.8	154.9 $\pm$ 42.7	8.80	0.3170
<b>Particles/ml CCM</b>	1.28 $\times 10^8 \pm$ 1.18 $\times 10^7$	5.39 $\times 10^7 \pm$ 2.32 $\times 10^7$	9.17 $\times 10^7 \pm$ 1.04 $\times 10^7$	1.09 $\times 10^7 \pm$ 2.28 $\times 10^6$	70.88	<0.0001

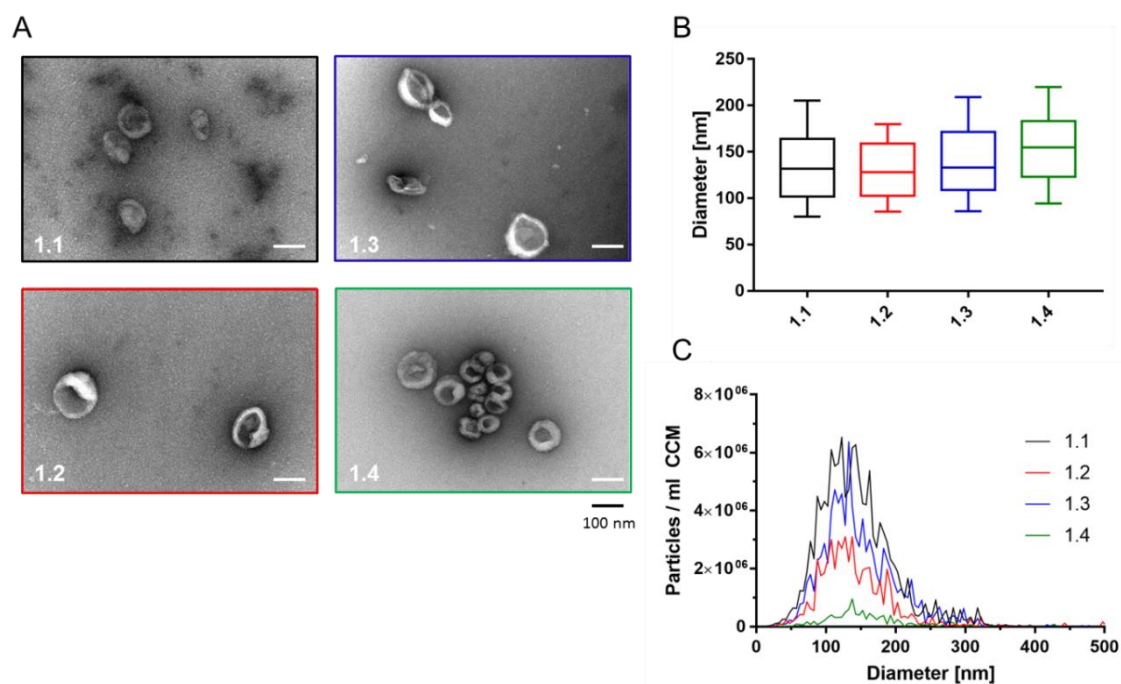


**Figure 20 Characterisation of EVs (first round) revealed differing EV yield sizes.** (A) TEM pictures from all EV preparations are depicted. Scale bar 100 nm. (B) NTA data of isolated EV sizes. (C) Full size profiles are shown for each EV preparation. Box: interquartile range; whiskers: 10<sup>th</sup> and 90<sup>th</sup> percentile; line: median. Particle concentrations were significantly different with  $p < 0.01$  (1.2 vs. 1.3),  $p < 0.001$  (1.1 vs. 1.3, 1.2 vs. 1.4) and  $p < 0.0001$  (1.1 vs. 1.2, 1.1 vs. 1.4, 1.3 vs. 1.4). This figure is taken from the manuscript *Inter-laboratory comparison of extracellular vesicle isolation based on ultracentrifugation*, submitted to PLOSOne.

### 4.3.2 Comparative EV isolation - Second round

In order to reduce the variables that might influence the yield, ultracentrifugation-based washing at 100,000 x g was omitted in the second round. EVs isolated within the second round were subjected to a more comprehensive characterisation, made possible by increasing the starting volume.

TEM revealed the EV-typical spherical and cup-shaped morphology with sizes ranging from 20 to 180 nm (Figure 21 A). Next, NTA confirmed sizes ranging from  $128.7 \pm 17.7$  nm (laboratory 2.4) to  $156.9 \pm 8.6$  nm (laboratory 2.1) between groups (Figure 21 B, Table 4). Like in the first round, particle sizes across laboratories differed significantly ( $p=0.0215$ ), and the Cv of median diameters was 9.38 %. Particle yield was significantly different and highest in laboratory 2.1 (compared to 2.2  $p=0.0182$ , 2.3  $p=0.0016$  and 2.4  $p=0.0168$ ) (Figure 21 C, Table 4). Inter-group variations in particle yield were still high, but lower than in the first round (Cv: 40.49 %).

For the characterisation of isolated EVs, Western blot and FACS analyses were performed. Due to lower yields in samples 2.2 and 2.3, Western blot analysis was only performed on samples from 2.1 and 2.4. Overall, common EV marker proteins like CD63, CD81, CD9, Alix and TSG101 were found to be expressed in EVs. The endoplasmic reticulum-associated protein Calnexin was only observed in cellular protein lysates (*not shown*) but not in the EV protein extracts, confirming the absence of cellular protein contamination in the two EV protein samples (Figure 21 D). Despite equal protein loading, 2.1 samples appeared to contain larger numbers of EVs as indicated by higher band intensities for CD63, CD81, Alix and TSG101. Interestingly, CD9 prevailed with a stronger band in 2.4 than in 2.1.

**Table 4 Particle sizes and concentrations determined by NTA analysis (second round).** All data are mean  $\pm$  SD of replicate measurement within one laboratory.

	2.1	2.2	2.3	2.4	Cv [%]	p
<b>Median diameter [nm]</b>	$156.9 \pm 8.6$	$151.5 \pm 23.7$	$134.6 \pm 18.3$	$128.7 \pm 17.7$	9.38	0.0215
<b>Particles/ml CCM</b>	$7.50 \times 10^8 \pm 8.05 \times 10^7$	$4.15 \times 10^8 \pm 2.68 \times 10^8$	$3.12 \times 10^8 \pm 2.21 \times 10^8$	$4.12 \times 10^8 \pm 1.22 \times 10^8$	40.49	0.0023

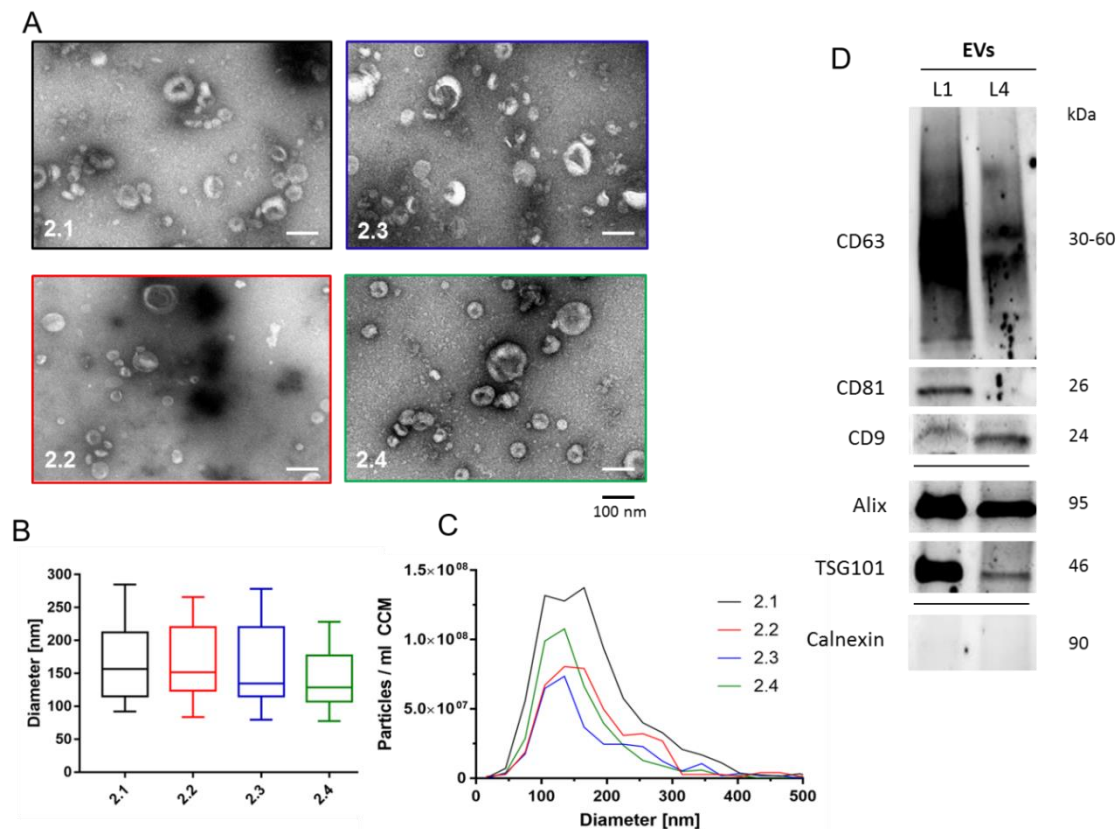


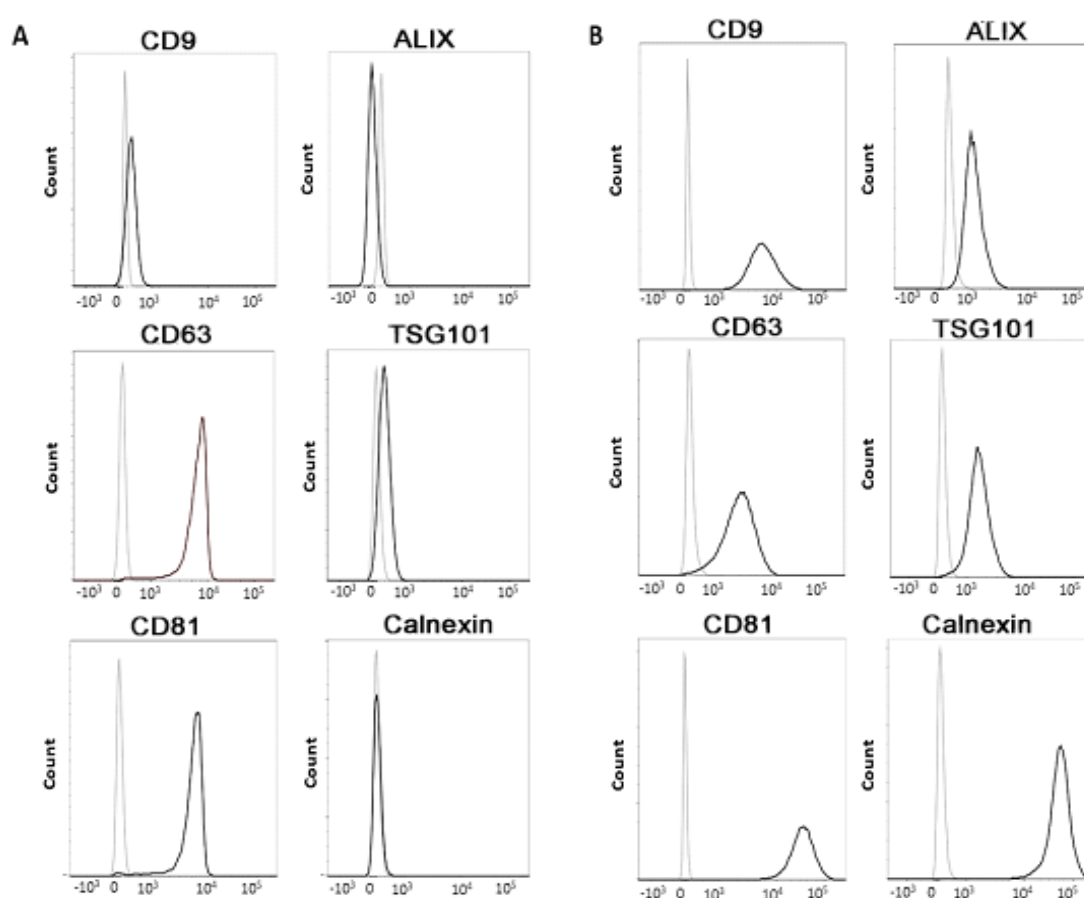
**Figure 21 Characterisation of EVs (second round) revealed differing particle yield.** (A) TEM analysis showed spherical and cup-shaped EVs isolated by all laboratories. Scale bar 100 nm. (B) NTA analysis size profiles of isolated EVs. (C) EV concentrations and size distributions are shown. Particle concentrations were significantly different, with  $p < 0.05$  (2.1 vs. 2.2, 2.1 vs. 2.4) and  $p < 0.01$  (2.1 vs. 2.3) or failed to reach statistical significance (2.2 vs. 2.4, 2.3 vs. 2.4). (D) Western blot analysis showed expression of specific EV markers. Figure taken from the manuscript *Inter-laboratory comparison of extracellular vesicle isolation based on ultracentrifugation*, submitted to PLOSOne.

FACS analysis was used as a complementary approach to EV marker characterisation, given that a much lower amount of EV material was required. EVs bound to CD9 beads showed positive staining for the typical EV surface markers CD9 (27.3 %), CD63 (99.2 %) and CD81 (98.6 %), as well as TSG101 (25.4 %), all values for EV sample from laboratory 2.1. EV samples from laboratories 2.2 – 2.4 were also tested for these EV surface markers: CD9 (0.77, 0.69 and 9.82%, respectively), CD63 (97.8, 98 and 99.1%) and CD81 (97.3, 97.2 and 98.5%) and TSG101 (3.69, 1.99 and 16.8%) (data not shown).

Supporting the Western blot results, almost no staining was observed for Calnexin (0.94 %). Nevertheless, Alix was not detectable on EVs by flow cytometry, contrary to the Western blot analysis (Figure 22 A). All markers were validated to be expressed in cells by either extra- or intracellular staining (Figure 22 B).

Expression intensities varied between groups, which prompted us to assess whether expression intensities correlated with particle counts. To this end, mean fluorescence intensity (MFI) values for CD63 (Figure 22 C) and CD81 (Figure 22 D) were calculated and expressed in relation to the particle concentrations in preparations from each laboratory. Higher expression intensities were found for laboratory 2.4, followed by 2.1, whereas 2.2 and 2.3 depicted lower but similar intensities amongst them.

The results from our second isolation round also demonstrated a strong variation in EV sizes and yield, discerning however, lower inter-group variation compared to the first round. We confirmed that higher EV yield generated stronger band intensities in the western blot analysis despite equal protein loading. Additionally, FACS analysis not only revealed the presence of typical EV surface markers, but indeed indicated no direct correlation between MFI values and particle concentration in our preparations.





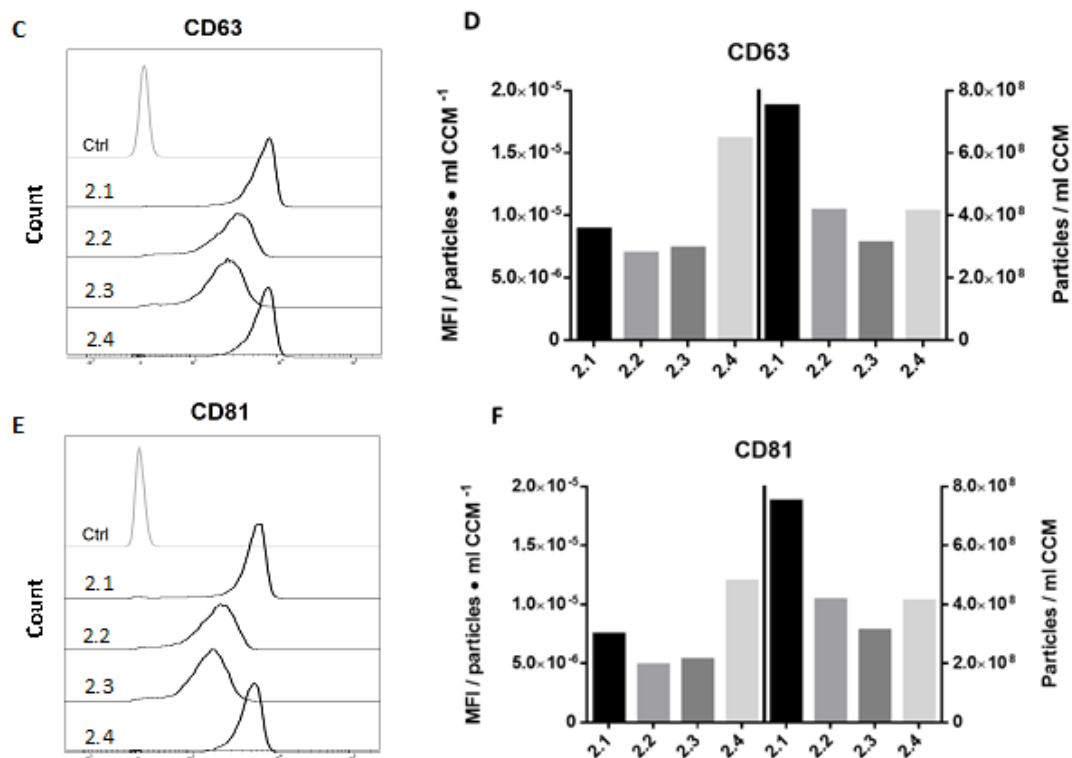


**Figure 22 FACS-based characterisation of isolated EVs (second round) demonstrated differing typical EV marker expression.** (A) Flow cytometry histograms depicting the relative fluorescence/marker intensity of EV preparation 2.1 (black line) against unstained EV particle control (grey line). (B) Corresponding marker expression in HCT116 cells (extracellular staining for CD9, CD63 and CD81 and intracellular staining for Alix, TSG101, Calnexin). (C, E). Mean fluorescence intensity (MFI) raw values of CD63 (C) and CD81 (E) marker expression from laboratories 2.1 – 2.4. (D, F) MFI values per particle concentration of CD63 (D) and CD81 (F) (left y-axis) against the respective particle concentration per ml CCM (right y-axis). Figure taken from the manuscript *Inter-laboratory comparison of extracellular vesicle isolation based on ultracentrifugation*, submitted to PLOSOne.

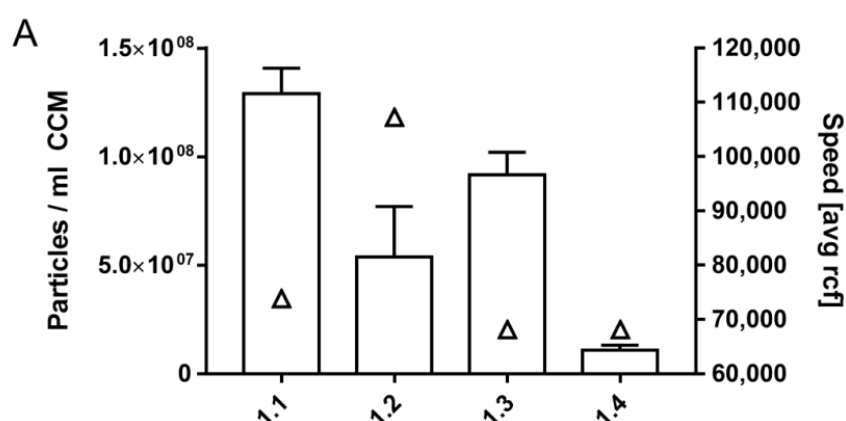
#### 4.3.3 Calculation of actual centrifugation forces and *k*-factors

Especially the lab-specific differences in EV yields prompted us to compare rotor details and actual centrifugation forces between the first and second round of EV preparations (Table 5). It became obvious that the protocol-based instruction of “using 100,000 g” was interpreted in different labs in two different ways: either as maximum or as average speed. Accordingly, the respective *k*-factors as indicators of the relative pelleting efficiency turned out to be different (Figure 23, Table 5). However, EV yields could not be correlated to speed. In the first and second round of isolation, two and three laboratories, respectively, used the same centrifuge and rotor (Table 5). Comparing these data still showed apparent differences in EV yield (Figure 23), leading to a Cv of 46.51 %.

**Table 5 Rotor type, speed (RPM), rcf (average) and k-factor specification.**

First round				
Laboratory	Rotor	Actual Speed (RPM)	Rcf (Average)	k-factor
1.1	TH-64.1	24.2	73,823	327.2
1.2	SW 28.1	28	107,215	276.0
1.3	SureSpin 630	23	68,135	456.4
1.4	SureSpin 630	23	68,135	456.4
Second round				
Laboratory	Rotor	Actual Speed (RPM)	Rcf (Average)	k-factor
2.1	SureSpin 630	23	68,135	456.4
2.2	SureSpin 630	23	68,135	456.4
2.3	SureSpin 630	23	68,135	456.4
2.4	SW 28.1	28	107,215	276.0

Surprisingly, we found that even when comparing laboratories with the same protocol interpretation and technical equipment, no direct correlation between total EV particle yield and centrifugation speed in either isolation round was seen.



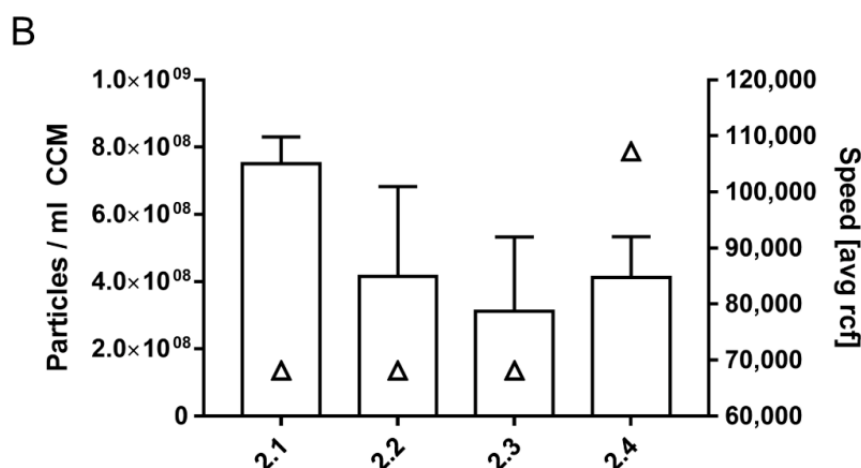


**Figure 23 Correlation of centrifugation speed and particle yield.** (A) First round of EV isolation. (B) Second round of EV isolation. Particle counts (bars, left y-axis) vs. speed (avg rcf; triangles, right y-axis) obtained in different laboratories are depicted. Figure taken from the manuscript *Inter-laboratory comparison of extracellular vesicle isolation based on ultracentrifugation*, submitted to PLOSOne.

Summarizing, our data revealed quantitative differences amongst groups when assessing an UC-EV isolation protocol in an inter-laboratory comparison study. We found that handling time and operator variations directly impact EV yield. Thus, to achieve reproducibility, accurate and detailed reporting of EV workflow is suggested. We propose performing future studies incorporating multiple institutions, where further isolation methods and biofluids are investigated.

## 5 DISCUSSION

The overall aim of this project concerned the evaluation of the immunomodulatory strength of MSC. Thus, as our first approach, we sought the immune suppressive potency differences in human MSC from different origins: bone marrow, cord blood and adipose-derived mesenchymal stromal cells. As our second approach, we aimed to compare MSC-derived products, such as CM and extracellular vesicles, to their cellular counterpart, to assess their modulatory capacities on PBMC subpopulations. Consequently, we investigated the specific MSC-mediated mechanisms of action involved in their immunosuppression in the different settings. As a final point, we aimed for the standardisation of ultracentrifuge-based EV isolation protocol in an inter-laboratory comparison study.

### 5.1 Human MSC immunomodulation

MSC first evidence of actively exerting immune responses derive from the results from MLR assays [40, 61, 156-159], which suggested a potential inhibition of T-cell expansion due to MSC addition [158, 160]. There are strong evidences that MSC from different sources are similar in a variety of functional and phenotypical properties [5]. However, there are slight alterations that might affect their function, related to the local function, environmental niche, the ontogenic age (birth-associated versus adult) or the isolation or culture procedure [5, 59, 60, 161]. Thus, we aimed to determine the potential variances.

Immunomodulation was assessed as MSC-mediated inhibition of stimulated PBMC or CD4 T cell proliferation. We observed a dose-dependent inhibition, with ASC being the strongest immunomodulators in either stimulated cell condition. Several investigations clearly describe ASC (compared either to BM-MSC, umbilical cord-MSC (UC-MSCs) or placenta-MSC (PL-MSC)) as the strongest suppressive of T cell activation [162] and inhibition of allogeneic-induced T cell proliferation [63]. On the contrary, Xishan et al. [163] demonstrated BM to exert a stronger immunosuppression over ASC. In a separate study, Wharton's jelly MSC (WJ-MSC) possessed a superior immune strength than ASC, BM and PL-MSC [164].

Comparing cells in an earlier passage, P3 and a more mature passage, P5, we observed similar immunosuppression capacities amongst passages for all three MSC

sources in all ratios. Earlier evidences have also demonstrated how immune suppressive potency appeared unaffected in long-term cultures [165]. Having confirmed the strongest inhibitory potential of ASC on PBMC / CD4 T cell proliferation in a comparable manner, we focused on elucidating the mechanism of action and continued our experiments with the whole PBMC population.

MSC-mediated actions on T-cell activation and proliferation have been described to be dependent on a wide variety of mechanisms. These involve secretion of soluble factors, chemokines, IDO [166], PGE2 and NO [48, 167]. MSC inhibition of T cell proliferation has been closely related to an increased IDO secretion. IFN $\gamma$  addition promotes MSC IDO production and immunomodulatory potential. IDO stimulates tryptophan depletion along with a consequent kynurenine production (see Figure 2), which is regarded as the key inhibitory mechanism [56-58]. ASC expressed the highest IDO values (followed by BM and CB), which correlates with their stronger inhibitory capacity. In a similar study, François et al. [56] described a variation among different donors, of IDO upregulation after IFN $\gamma$  exposure. Stronger IDO producers revealed more potent *in vitro* T cell proliferation inhibition. Consequently, elevated IDO also relates to the increase in kynurenine secretion observed. Transient tryptophan depletion affects T cells solely at activation stage. This promotes inhibition of proliferation, hence, preventing their cell death [168, 169].

Accordingly, we investigated tryptophan addition, as we hypothesised it to be an important rate-limiting factor in IDO modulatory activity. Upon addition to MSC monocultures, IDO levels were further increased, exhibiting ASC also the highest IDO secretion levels. Tryptophan addition to cocultures, however, greatly abrogated MSC-mediated PBMC inhibition supporting our hypothesis. In line with our results, previous reports have described addition of tryptophan to promote restoration of T-cell proliferation in MLR cocultures [61, 169]. This was presumed to be related to T cell proliferation inhibition at an arrest point mid G1 phase, which was reversible upon tryptophan addition to the culture, together with stimulation of T cells [169]. The IDO inhibitor, Epacadostat was also added to the cultures to analyse the modifications of MSC immunological functions. MSC-mediated inhibition of PBMC proliferation was fully neutralised, indicating that IDO is largely involved. However, IDO levels were comparable among all conditions in presence or absence of tryptophan or Epacadostat. Nonetheless, kynurenine concentrations were utterly diminished, to levels below those in unstimulated PBMC control. Jointly, these data

seem to suggest that Epacadostat does not affect IDO at its secretion stage, but does inhibit IDO enzymatic activity and by this, neutralises the MSC inhibitory activity. Previous studies corroborated our results showing that addition of selective IDO inhibitor, Epacadostat, increased T cell proliferation, suppressed Tregs and increased IFN $\gamma$  production [170]. Studies with other IDO inhibitors, such as competitive inhibitor 1-methyl tryptophan (1-MT), have also described an increase of T-cell proliferation in coculture with either naïve or activated MSC [56, 171]. Similarly, in presence of IL-2, 1-MT partially restored PBMC proliferation rate [57]. Altogether, we confirmed that tryptophan depletion and kynurenine formation are key in the modulatory mechanism in which IDO is involved, supporting IDO as a strong immune modulator involved in human T cell inhibition.

Evidences of different environmental modulations influencing directly MSC function, final fate and therapeutic potential have been firstly reported as *cell priming, licensing or preconditioning*. Certain authors claim that MSC need to be pre-licensed to become immunomodulatory. This can be promoted by a number of pro-inflammatory mediators with different priming approaches [172-174]. IFN $\gamma$  licensing alone or in combination with TNF $\alpha$  has been described to stimulate MSC secretion of anti-inflammatory and immunomodulatory factors [56, 172-175]. We challenged IDO-kynurenine access by testing IFN $\gamma$  priming of MSC. An equal PBMC inhibition of proliferation than the one exerted by non-IFN $\gamma$  primed MSC, was observed. Contrary to our initial hypothesis, suppression appeared not to be dependent on MSC (pre-) licensing. Thus, in our settings, MSC were not able to increase their therapeutic efficacy. We hypothesise that in our controlled *in vitro* coculture setup no exogenous IFN $\gamma$  addition is needed, as MSC's inhibitory potential seems to have reached levels close to the maximum. In our coculture settings we presume that PHA stimulation acts on PBMC/CD4 $^{+}$  T cells stimulating IFN $\gamma$  secretion, occurring at an early timepoint. IFN $\gamma$  then acts on MSC promoting the secretion of IDO into the CM. IDO converts tryptophan and accumulates kynurenine, which acts on T cells, inhibiting their proliferation (Figure 24). Nevertheless, the role of IFN $\gamma$  in activating MSC and enhancing the secretion of modulatory factors has been previously reported *in vitro* [176-179].

Two main reasons could potentially explain our different results. First, timing of IFN $\gamma$  pre-stimulation of MSC and/or duration of culture. The lack of increase in function of IFN $\gamma$  preconditioned MSC might be due to a short priming time (72 hours). Duijvestein and colleagues have verified that human MSC, after 6 days of IFN $\gamma$  priming, denoted higher immunomodulatory capacities, inhibiting PBMC proliferation at lower ratios compared to untreated MSC [176]. Likewise, IFN $\gamma$  licensing may also occur in early stages of the cultures. However, assessment of licensing on the highest MSC:PBMC inhibitory ratio (1:5), along with the potential inability to further enhance inhibition of PBMC proliferation, could possibly be another relatable cause. In fact, translation to *in vivo* settings signifies a more intricate interplay amongst cell types. IFN $\gamma$  production is dependent on donor T cell response to antigen recognition. In fact, an *in vivo* study measured serum IFN $\gamma$  levels of bone marrow transplanted GvHD recipients after MSC administration [178]. They observed that IFN $\gamma$  circulating levels at time of transplant (day 0) were not enough to activate MSC, thus, failing at alleviating GvHD symptoms or survival. However, in their settings, IFN $\gamma$  levels at day 7 post-transplantation were the highest. These results suggest that *in vivo*, MSC timing of activation might greatly differ to the controlled *in vitro* settings. Second, IL-2 addition might be another important factor to take into consideration. It was exogenously added to the culture to ensure survival of T cells in cultures lasting longer than 5 days. IL-2, produced by both lymphocytes and stromal cells is highly involved in regulating T cell apoptosis, maturation and function [180]. Considerable number of studies have demonstrated IL-2 promotion of T cell survival, proliferation and differentiation into effector cells [181, 182]. However, IL-2 additionally stimulates development of regulatory T cells [183-185]. Many studies with IFN $\gamma$  addition either do not report the addition of IL-2 or state the lack of it in their culture settings [56, 176, 178, 179, 186]. As aforementioned, in our *in vitro* controlled settings, PHA stimulation seems to trigger PBMC/Tcell production of IFN $\gamma$  that would lead to increased IDO levels in CM triggering MSC inhibitory mechanism. However, in an MLR setting the crosstalk with different immune cell populations could vary the outcome to some extent.

As previously described, a wide variety of other mechanisms have already been described to be involved in MSC-mediated immunosuppression [48, 167]. In addition to IDO, nitric oxide (NO) is a prominent candidate involved in MSC-mediated

immunosuppression in murine settings [51, 81, 82]. To exclude that next to IDO the immunosuppressive capacities of human MSC involve NO, we analysed nitrite concentration in supernatants of cultures. No differences resulted between supernatants from cocultured MSC:PBMC at 1:5 ratio and PHA stimulated PBMC control. Nitrite values in supernatants from cultures with IFN $\gamma$  primed and not primed MSC, and in presence or absence of Epacadostat displayed extremely low values. It is our view that these data seem to correlate to previous findings where they tested NO levels of analogous coculture settings, and saw no changes in culture medium of mixed human PBMC-ASC cultures despite having observed upregulation at protein level [187]. This only verifies the discrepancy between different species MSC-mediated suppression mechanisms, being NO dependent in murine MSC and relying on IDO in human context [51, 188].

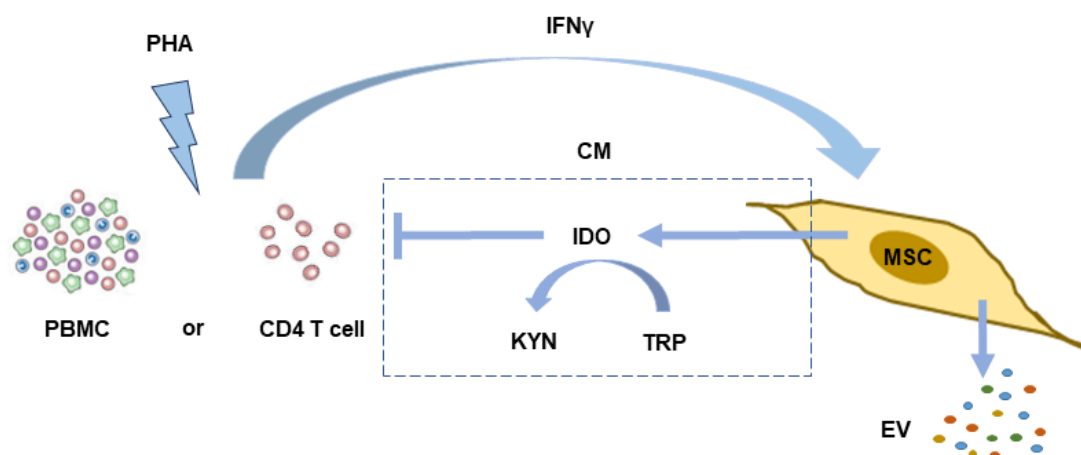


**Figure 24 PBMC/CD4 $^{+}$  cell immunosuppression is dependent on IDO-Kyn modulatory mechanism present in MSC-CM.** The PHA acts on either PBMC or CD4 $^{+}$  T cells, and stimulate their secretion of IFN $\gamma$ , which occurs at an early time point. IFN $\gamma$  secretion directly acts on the MSC, promoting IDO secretion into the CM. IDO drives tryptophan depletion and kynurenine formation, which in turn drops the proliferation of T cells. Despite EV being secreted into the extracellular space, they are not directly involved in the IDO-Kyn modulatory mechanism that takes place in MSC-CM and thus, may lack immunosuppressive strength.

In summary, the results of human MSC immunomodulation indicate that:

- ASC are the most immunomodulatory inhibiting T cell proliferation, followed by BM- and CB-MSC. They inhibit PBMC and CD4 $^{+}$  T cell proliferation equally, in a dose-dependent manner;



- IDO secretion upon IFN $\gamma$  stimulation is highest in ASC, correlating with their inhibitory capacity. Elevated IDO values correspond to an increase in kynurenine levels;
- IFN $\gamma$  priming of MSC does not further increase their modulatory potency;
- Tryptophan addition to MSC monocultures increase IDO production, however, when added to MSC:PBMC cocultures it abrogates MSC-mediated PBMC inhibition;
- Epacadostat addition does not affect IDO secretion, but does inhibit its enzymatic activity. When added to cocultures it abolishes MSC suppressive activity, this indicates that IDO enzymatic activity is key to the MSC inhibitory action;
- Nitric oxide, measured as nitrite in culture supernatants verifies human MSC-mediated suppression mechanism to be dependent mainly on IDO production.

In conclusion, ASC were the strongest immunosuppressors inhibiting PBMC and CD4 $^{+}$  T cell proliferation equally. We revealed IDO-kyn inhibitory mechanism to be involved in inhibition of human PBMC proliferation, which is IFN $\gamma$  dependent. As suggested by literature, we found that tryptophan addition to cocultures abrogated completely MSC-mediated PBMC inhibition. IDO inhibitor Epacadostat addition abolished MSC suppressive capacity, confirming IDO involvement. Testing this mechanism in a controlled *in vitro* setting with PHA as a mitogen stimulus, might pose a limitation of this approach. For instance, in an MLR the complex interactions could influence the final outcome. Therefore, we propose performing *in vitro* experiments to verify this suppressive mechanism.

## 5.2 MSC immunomodulation in allogeneic and xenogeneic settings

Interspecies incompatibilities have already been defined in previously published investigations [94]. To verify whether MSC-mediated immunomodulation might be affected by the incompatibilities arising from cultures with cells from different species, we established cocultures with both, human and rat MSC and PBMC, stimulated with mitogens (PHA for human, Con-A for rats), in allo- and xeno- settings.

Once verified ASC strong immunosuppression of T-cell proliferation, reducing their division index considerably in a strict dose-dependent manner, we decided to

similarly test ABCB5 human dermal immune-regulatory cell (DIRCs) subset in coculture with human PBMC. ABCB5 were much weaker, but still succeeded in inhibiting PBMC proliferation. We verified the involvement of IDO and the lack of NO-mediated immunosuppression in human allocultures (ASC and ABCB5). Rat MSC successfully inhibited human PBMC proliferation in a dose-dependent manner, exerting the strongest suppression in 1:5 (MSC:PBMC) ratio. Accordingly, kynurenine undetectable levels and nitrite elevated ones verify NO as the main immunosuppression mechanism involved in the murine allocultures. Therefore, as previously denoted human MSC utilize IFN $\gamma$ -induced IDO secretion as immunosuppressive mechanism whereas murine-derived MSC seem not to rely on IDO, but on NO for mediation of immunosuppression.

In rMSC:rPBMC allo-cocultures we observed how rMSC strongly inhibited T cell proliferation in rat PBMC, contrariwise, the inhibition was weaker in SMC. In accordance, nitrite production in coculture CM was increased compared to both stimulated and unstimulated PBMC controls. Differences seen in inhibition of rat blood vs spleen-derived rat MC might be related to MSC specific modulatory properties and the amount of diverse lymphocyte subsets amongst the whole PBMC population. The works of Wong et al. together with Sathaliyawala et al. elucidated the distribution of major lymphocyte populations across human tissue. CD4 $^{+}$  and CD8 $^{+}$  T cell subsets were the most abundant lymphocytes in all measured tissue samples except for spleen and tonsils [189, 190]. Here, contrarily, B cells comprised the greater part of lymphocyte population. Thus, the differences concerning blood- and spleen-derived rat MC inhibition might be related to the high presence of B cells, and concomitant low T cell population within spleens. In fact, in line with our findings, an *in vitro* murine immunosuppressive study has demonstrated efficacious splenocyte immune modulation by rat MSC [55]. In another murine study, they observed that direct interaction between T cells and MSC promoted NO production accompanied by a strong suppression of T-cell proliferation, which was abolished in a transwell system [81].

As MSC are considered immunosuppressants they were deemed to help reduce inflammation, and allow better survival of allografts or transplants, dampening the immune response. However, in xenogeneic settings there are contradictory data

regarding studies with hMSC administration in animal models. Some suggest hMSC infusion enhance survival of grafts and transplants. For instance, in murine models of hematopoietic stem cell (HSC) transplantation, hMSC administration enhanced engraftment of HSC [191-193]. Similarly, in rat-mice xenomodel of skin transplantation, MSC infusion prolonged skin graft survival [194].

It has also been claimed that hMSC infusion in autoimmune and inflammatory diseases are able to inhibit the progression of autoimmune disease and recover immune homeostasis in GvHD, colitis, myasthenia gravis and systemic lupus erythematosus, as thoroughly reviewed by Li et al. [195].

Furthermore, other studies in a cross-species framework claim a strong amelioration of the disease after hMSC infusion [86-91]. This indicates not only immune compatibility in these models but also an immunomodulatory beneficial effect of MSC administration.

On the other hand, others claim that MSC infusion portrays less or no benefit increasing graft survival. Indeed, in a transplantation murine model it has been demonstrated that pre-infused hMSC incited an allograft rejection prior to day 30 post graft insertion [94]. Interspecies incompatibility was claimed as likely, due to hMSC potential inability to produce NO upon induction or to upregulate IDO in presence of rat pro-inflammatory cytokines. However, questions remain as to whether this effect is directly associated with different MSC-mediated inhibitory mechanisms, which seem to be species-dependent, or due to the strong effect of pro-inflammatory micro-environments.

The discrepancy could possibly be explained by the specific models used for each study. For instance, most of the successful studies regarding survival of grafts and transplants are carried out in NOD/SCID immunodeficient mouse model with impaired T and B cell development and deficient NK cell function. However, evidences of successful MSC xenotransplantation in different experimental models continue to appear.

To assess xenogeneic immunomodulation, we tested ASC and ABCB5 inhibitory potential on rat PBMC proliferation suppression. The results revealed ASC inability to suppress rat PBMC and SMC in any ratio tested. On the other hand, ABCB5 succeeded in suppression of xenogeneic PBMC. We hypothesise these differences between ASC and ABCB5 to be dependent on ABCB5 immunoregulatory functions

being exerted partially through programmed cell death 1 (PD-1) [64, 72]. ABCB5-purified DIRCs expression of PD-1 functions have described them as a distinct immunoregulatory cell population able to inhibit T cell activation, induce Treg formation and prolong allograft survival. Furthermore, *in vivo*, PD-1 immune regulator checkpoint may portray a more efficient modulation of graft rejection [64].

Analysis of coculture CM portrayed no kynurenine and a slight nitrite secretion into the media. Thus, NO-mediated PBMC suppression seems to be involved. However, taken together, these data seem to suggest a possible incompatibility in mediating immunosuppression by ASC in our settings. Nevertheless, these data require further validation by thorough *in vivo* testing to evaluate their potential preclinical benefit.

Our *in vitro* experiments confirmed ABCB5 stronger inhibitory potential in xeno-coculture with rPBMC. Accordingly, ABCB5 cells were selected to move from a controlled *in vitro*, to an *in vivo* xenogeneic setting, where cells were administered to a cisplatin-induced kidney injury murine model in a parallel project within the TASCOT PhD graduate school (doctoral thesis Cristina Daniele).

In conclusion, our findings on MSC immunomodulation in allogeneic and xenogeneic settings demonstrated that:

- ASC inhibited human T cell proliferation in a more robust manner than ABCB5 cells;
- Rat MSC succeeded in suppressing human PBMC proliferation;
- Rat MSC inhibited rat PBMC proliferation to a higher extent than SMC;
- In a xenogeneic setting, ASC were unable to inhibit proliferation of rat PBMC and SMC. ABCB5, contrarily, inhibited proliferation of both sources of rat MC;
- Human MSC rely on IFN $\gamma$  inducible IDO expression as their main immunosuppression mechanism, whereas murine MSC rely on NO secretion.

In summary, we showed that while ASC were not able to inhibit rat PBMC proliferation in a xenogeneic setting, ABCB5 successfully restricted their proliferation. Furthermore, the main human and rat immunosuppression mechanisms were elucidated, supporting the knowledge that human MSC rely on IDO expression, whereas murine MSC rely on NO secretion. A careful evaluation of the use of human MSC in transplantation to murine models is suggested.

### 5.3 MSC secretome products

In the previous part of our study on the immunosuppressive capacity of MSC in different settings, we evaluated the inhibitory strength of MSC from different sources and species and elucidated their related mechanisms. We saw that the IDO-Kynurenine axis seems to be the most predominant mechanism involved in human MSC immunomodulation; however, this was only tested in direct immunosuppression assays. Therefore, we evaluated MSC modulatory potential in direct versus transwell cocultures, assessing whether MSC suppressive activity was mediated by direct cell-cell contact (local effect) or via the release of soluble factors (paracrine effect). The present findings revealed MSC inhibitory effects not to be affected by the physical separation of the two cell types. This suggests that the inhibitory effect of MSC was not mediated solely by cell contact but was also dependent on the release of soluble factors. Furthermore, IFN $\gamma$  licensing of MSC portrayed no differences amongst conditions. These outcomes were fairly in line with previous reports that indicate contribution of secreted soluble factors to exert MSC immunomodulatory effects [33, 40, 186, 196-198]. As previously described (see chapter 5.1; Figure 24), this effect may be related to the IFN $\gamma$  secretion by PHA stimulated PBMC, which promote MSC-IDO secretion that in turn drive tryptophan breakdown to kynurenine, reducing PBMC proliferation abilities in both a direct and indirect manner.

We asked ourselves whether EV could be involved in transferring immunomodulation. MSC-derived CM and extracellular vesicles have been successfully applied to an extensive number of murine models, along with a steadily arising use in human clinical studies [110, 199-202]. Amongst different EV isolation methods, differential ultracentrifugation was the first and long considered gold standard approach for extracellular vesicle isolation. However, this method is subject to uncontrolled variables that might strongly impact functional outcomes [115, 117]. Despite these shortcomings, we determined this isolation method as the most suitable to meet our demands. Some reasons were the high ratio of EV recovery, short assay time and most importantly, high sample volume (ml-l) [115].

Following EV isolation, and prior to their application in functional studies, comprehensive characterisation according to MISEV guidelines was performed on purified EV [122]. We confirmed that we had isolated membrane-encapsulated EV with the typical spherical morphology. We further determined the presence of high concentrations of EV in our isolates, reported by the NTA results. Additionally, we

determined ASC-derived EV to be more efficiently detected when coupled to Aldehyde beads than to CD9 beads. We hypothesised this being due to low expression of CD9 marker on ASC-EV surface. Thus, most typical described EV surface markers [152-155], tetraspanins CD63 and CD81 were detected on ASC- and HCT116-EV. Furthermore, MISEV state the need for demonstrating presence of cytosolic proteins in EV isolates (i.e TSG101, Alix) apart from transmembrane proteins associated to plasma membrane [122, 203]. We therefore tested Alix, TSG101 and Calnexin intracellular markers presence/absence in both EV isolates and producer cells. EV isolates presented high expression of typical EV markers CD63 and CD81 was in line with the aforementioned studies, whereas CD9 marker expression detection was lower. Alix and TSG101 cytosolic protein marker expression were detected to a low extent, possibly depicting the ineffectiveness of appropriately detecting intracellular markers. Barely no signal or slight calnexin signal was detected on EV isolates derived from ASC and HCT116 cells, which could possibly hint at a mere contamination with cellular fragments [204]. Conversely, all intracellular and extracellular markers were strongly positive on both cell types. In short, after validation of morphology, size and concentration profile, along with EV specific markers we were confident to call our isolates “extracellular vesicles”.

Consequently, once isolation and thorough characterisation of our EV was performed, we tested them in functional studies. We aimed to evaluate their immunomodulatory potential, and compare them with MSC-derived CM. Speculating that priming might be required to release immunomodulatory EV or CM, MSC were preconditioned with IFN $\gamma$  for 72 hours prior to media retrieval.

EV isolated from both IFN $\gamma$  primed and not primed MSC medium failed to suppress PBMC proliferation. We observed similar data already in previous studies. While additional studies also reported failed PBMC suppression [132, 133, 136], there are many evidences of EV successfully inhibiting PBMC proliferation [50, 205, 206]. In fact, Blázquez and colleagues detected in a similar setting, EV ability to suppress CD4 and CD8 T cell proliferation [134]. Serejo et al. even reported the successful PBMC proliferation suppression of both unlicensed and IFN $\gamma$ -licensed MSC-derived EV [207]. We hypothesise EV lack of immunosuppressive strength might be related to the main modulatory mechanism here reported being IDO-Kyn-dependent. IDO

immunomodulatory mechanism takes place in MSC-CM and thus, despite EV being secreted into the extracellular space, their modulation may be IDO-independent.

Consequently, we tested CM modulatory effect in different settings. CM from IFN $\gamma$  preconditioned MSC was the only condition to effectively inhibit PBMC proliferation in great manner. Non-primed MSC CM had no effect, suggesting an imperative role of IFN $\gamma$  presence in the culture. Similarly, Delarosa and colleagues demonstrated that supernatants from 72h IFN $\gamma$ -stimulation greatly ablated PBMC proliferation [188]. Addition of Epacadostat to CM +IFN $\gamma$  exerted no effect on abrogation of PBMC inhibition. We believe this to be due to the high absolute amounts of IDO present in 72h preconditioned CM in monoculture, compared to the progressively secreted IDO in coculture systems. Thus, the elevated IDO levels might be too high to be inhibited by Epacadostat addition.

Furthermore, another study where CM from unlicensed and licensed MSC were tested, claimed the latter as being the most immunosuppressive [207]. As previously discussed, IFN $\gamma$  preconditioning not only induces MSC secretion of IDO, but also other enzymes and soluble factors namely, cyclooxygenase 2 (COX-2) and PGE2 [55, 179, 188, 196]. In fact, PGE2 suppressive activity has already been demonstrated [157, 198]. In a study, addition of IDO and PGE2 inhibitors could not completely abrogate MSC-mediated suppressive effects, presuming involvement of both pathways [196]. These findings conflict with some studies that have claimed PGE2 not being significantly involved in immunosuppression [33, 198], its inhibition has been claimed to cause an abrogation of MSC-mediated immunosuppressive effects [157]. Additionally, secretion of HGF, TGF- $\beta$ 1 [179] or NO [55] in response to proinflammatory cytokines, might potentially support inhibition of T cell proliferation.

Based on this premise, we hypothesise that CM modulatory mechanism seems to rely mainly on IDO. However, we believe that CM modulatory effects may be enhanced by the combined effects of IDO together with different MSC secreted factors such as PGE2.

We also evaluated the inhibitory potential of CM from previous MSC:PBMC cultures, which resulted ineffective in inhibiting freshly added PBMC. These results seemed to reveal a possible exhaustion/consumption of modulatory factors present in the conditioned media after prolonged cultures, failing at inhibiting PBMC proliferation. Separate experiments in our laboratory revealed a downregulation of Th1/Th2

cytokine levels in supernatants from 7 day coculture (data not shown). These data could potentially support our findings.

As demonstrated, CM from IFN $\gamma$  primed MSC successfully inhibited PBMC proliferation. These results were deeply in contrast to extracellular vesicles that were unable to suppress their proliferation. The possible reasons for failed outcome of EV modulation, might be related either to assay or to technical-related factors.

Some main potential assay-related factors might be: (1) Mechanism is IFN $\gamma$  and IDO-mediated and does not involve EVs. (2) EV load. Currently, there is a lack of consensus when reporting the dose of EV load added to potency assays. Misleading load consideration might have also possibly influenced the EV amount added to our assays. While we and others determined our EV amount as absolute values of producer cells [132, 208], many others reported either EV protein concentration [134, 136], EV particle counts [133], or number of producer cells defined as units per ml [205], whereas others do not specifically define EV assay loads [50, 206]. Consequently, the wide variety of studies with diverging EV load considerations, undoubtedly lead to different outcomes. The wide variety of studies with diverging EV loads, undoubtedly leads to very different outcomes. Consequently, this might have potentially biased us when considering the EV load in our assays, thus, being inadequate to exert modulatory functions.

(3) Culture conditions. Another critical issue to consider is whether our culture conditions might have affected EV assay final outcome. Abrupt alterations in culture conditions such as FBS-EV depletion or shifting to serum-free media prior to CM production [126], have been reported to prompt modifications in cell metabolism [209]. Changes to EV-depleted medium might also modify cells phenotypical profile or reduce cell proliferation [126]. In fact, Eitan and colleagues have described how addition of FBS-EV restored proliferation in an effective manner [210]. Alteration of culture conditions directly impacts EV yield [211]. Therefore, we hypothesise that depleting FBS-EV might have modified the microenvironment, along with the nature of isolated MSC-EV, potentially rendering them less effective. Thorough attention to culture conditions must be taken when employing EV in functional studies.

Moreover, potential technical-related factors might be:

(1) Isolation method. UC may disrupt EV. Even if ultracentrifugation (UC) is cost-efficient [212], this method shows inconsistencies in reproducibility of isolation data



[117]. UC can also co-purify non EV-associated proteins (lipoproteins and protein aggregates) [213] together with aggregating EV of different phenotype [214]. This may influence immunomodulation due to the biased interpretation in downstream analyses as integral EV factors. Moreover, Nordin et al. [215] have reported certain degree of EV disruption when UC at 120,000g, thus implying a use of maximum of 100,000g [116]. Furthermore, there are strong evidences indicating exceptionally low recovery of exosomal protein and RNA following UC [216-218]. Thus, isolation methods such as PEG-based precipitation [118, 119] size-exclusion chromatography (SEC) [120, 218] and methods involving membrane filtration [219] or magnetic separation [220], yield higher EV purity and reduce EV loss or structure damage. Therefore, we hypothesise UC to have failed to yield functional EV. Utilising a different method of isolation could potentially overcome the limitations of our study.

(2) Characterisation method. EV characterisation requires different complementary methods in order to validate their size, concentration and typical markers. However, limitations in EV characterisation methods could potentially bias the interpretation of EV integrity, yield and/or purity. For instance, in low-purity samples, NTA might overestimate EV concentrations [221]. Furthermore, flow cytometry “swarm” artefacts can also overestimate EV detection, providing inaccurate marker expression data [128, 222]. Indeed, also WB [115, 126, 223] and TEM [116] could potentially bias the interpretation of our EV isolates. In brief, a potential overestimation of EV concentration may have led to using substantially lower EV load in our assays. Furthermore, size, morphology and marker expression data could have led us to misinterpret EV purity or even, consider our purified samples as extracellular vesicles. Thus, EV characterisation data must be cautiously evaluated.

Therefore, the analysis of MSC secretome products immunomodulatory potency concluded that:

- MSC-mediated suppression of T cell proliferation took place in both direct and transwell cocultures;
- UC isolated MSC-EV failed to suppress PBMC proliferation regardless of IFN $\gamma$  preconditioning;

- IFN $\gamma$  primed MSC-CM successfully hampered T cell proliferation. Epacadostat addition was not able to abrogate PBMC inhibition due to the high absolute levels of IDO;
- CM modulatory mechanism seems to be exerted by the combined effects of IDO along with MSC-secreted factors;
- UC-EV lack of modulatory effect might be related to assay or technical-related factors.

In summary, our data about MSC secretome-products revealed a comparable immunosuppressive activity of MSC in direct and transwell cocultures. Immunosuppression assays with EV demonstrated they failed at suppressing PBMC proliferation. However, CM +IFN $\gamma$  was a strong suppressor of PBMC division. We recommend that in depth *in vitro* and *in vivo* studies are performed to further define and characterize EV modulatory potency and CM +IFN $\gamma$  prospective application as a cell-free approach.

#### 5.4 Inter-laboratory comparative study

The main aim of this comparative study was to examine the reproducibility of a well-defined EV isolation protocol amongst various laboratories, aiming to assess technical variation induced by equipment and operator. We confirmed that all contributing laboratories were able to enrich EV from pooled HCT116 CM, however, differences in results were detected. These differences appeared to be mostly quantitative. In fact, different labs used different centrifugation speed (maximum versus average 100,000 g) and k-factor, as these settings were not exactly predefined in the common protocol. However, even when using identical centrifuges, rotors and run parameters, laboratories did not produce similar results. Certainly, differences in particle yield seem to be attributable to operator effects. Thus, it would be necessary to estimate also intra-operator variability throughout multiple isolations. Ultracentrifugation, among the multitude of isolation methods available, is regarded to be particularly susceptible to operator biases. Some biases might derive from handling disparities such as accurate resuspension of pellets, supernatant removal by pipetting vs. decanting, among others. Our data suggest that handling time severely impacts EV preparations, in addition to the well-defined impact of storage

conditions and freezing-thawing cycle implications on purified vesicle integrity and function [224-226]. EV yield from CM stored for a longer period of time prior to EV isolation was extraordinarily reduced. We have detected a decrease in overall variability when span between retrieval and EV isolation was standardised among groups. This notion is in line with previously published reports that linked shorter processing time to increased particle concentrations [227]. Furthermore, for plasma and serum, time between blood draw and initial centrifugation seem to have a direct impact on EV yield [228]. This demands for a normalisation of storage time, temperature and number of freeze-thaw cycles. Accordingly, to ensure maximal reproducibility, each step of the EV workflow, from sampling and pre-analytical features to EV enrichment, requires careful consideration and accurate reporting. We recognize that the conclusion that can be attained from an inter-laboratory study involving only four laboratories are in fact limited, despite all contributing partners being broadly experienced in the EV field [136, 221, 229-236]. Additionally, due to the lack of intra-operator assessment, we cannot precisely determine inter-laboratory variation, as previously mentioned. As a main conclusion we should state that precise and extensive reporting is crucial to accurately replicate a given protocol. For instance, in the literature centrifugation speed is often reported without specification of average (rcf avg) or maximal centrifugal force (rcf max). Accordingly, to transfer a given isolation protocol across rotors and laboratories, we recommend reporting not only g-forces, but also k-factors in addition to rotor types (fixed angle or swinging bucket). Moreover, to achieve maximum reproducibility, sample handling, processing time and storage need to be thoroughly controlled. Methods that are faster and easier to standardise seem to be required, especially when considering prospective clinical translation. It would be of utmost interest to perform future inter-laboratory studies involving multiple institutions, apart from analyzing additional biofluids besides cell culture supernatants. Furthermore, they should also include additional methods of isolation, particularly those relevant to therapeutic EV manufacturing, for which standardised working procedures with minimal batch-to-batch variation in purity, yield and potency are crucial [129, 237]. To summarise, our study indicates significant operator- and equipment-dependent technical variability in UC-based EV isolations. We believe that adding increasingly sensitive analytical assays and appropriate reference material, will enable detection and quantification of technical biases, which will in turn increase standardisation while reducing variability. Provided

that EV community development of valuable tools such as EV-TRACK and the MISEV guidelines [122, 123] are currently evolving, we are certain that a better understanding of variability amongst laboratories will give rise to improved standardisation and harmonisation.

Comprehensively, the results from the inter-laboratory comparative study revealed that:

- Quantitative differences were observed amongst enriched EV from different laboratories. Particle yield variances seem to be partially dependent on operator effects;
- Handling time strongly impacts EV yield. Thus, particle concentration was increased with shorter time span between sample retrieval and processing;
- Precise and accurate reporting of each step of EV workflow is recommended to achieve maximal reproducibility;
- Ultracentrifugation speed requires defining max or avg g-forces, along with k-factors and rotor types to transfer protocols to different laboratory settings;
- Future inter-laboratory studies involving further isolation methods, biofluids and institutions are needed to give further insight in the EV field.

In conclusion, UC-based EV isolation is associated with low reproducibility and technical variations, as demonstrated by the quantitative differences observed. These variations were influenced by operator biases due to handling variances, processing time or a lack of accurate reporting of isolation protocols, which pose main limitations to this study. Therefore, to overcome this, we suggest (1) to correctly define and report the EV workflow and (2) to perform a prospective multiple institution study that would assess different isolation methods and biofluids.

## 6 SUMMARY

In recent years, mesenchymal stromal cells (MSC) have been an attractive target for their translation into clinical research applications. This is mainly due to their paracrine, regenerative, multi-lineage differentiation and immunomodulatory properties. However, MSC from different sources possess subtle differences that could affect the immunomodulatory molecular mechanisms used to exert their effects. MSC interact with a broad range of immune cells such as B and T cells and seem to exert their immunomodulation by synergic cell contact-dependent mechanism and soluble factors, including Interleukin-10 (IL-10), Prostaglandin E-2 (PGE-2), Nitric oxide (NO) and Indoleamine 2,3-dioxygenase (IDO), amongst others. MSC have been increasingly used in a variety of therapeutic fields such as transplantation, kidney injury, graft versus host disease (GvHD) or autoimmune diseases. Many preclinical murine studies involve administration of not only autologous and allogeneic, but also xenogeneic MSC. In fact, human MSC (hMSC) application in animal models is performed to assess their therapeutic potency and verify their safety and efficacy, as required by regulatory authorities. Nevertheless, the use of hMSC in murine models raises numerous concerns and the lack of homogeneous results still limit the translation to clinical research. MSC-derived conditioned media (CM) and extracellular vesicles (EV) have been portrayed by many as a strong alternative to cell-therapy, overcoming many of the regulatory challenges faced by MSC clinical translation. However, as EV field is quite recent, there is contradictory data concerning EV immune potency. Further studies are needed to clarify their modulatory prospect and the mechanisms involved.

ATP-binding cassette member B5 (ABCB5) cells, novel human dermal immune-regulatory cell (DIRCs) subset present immune-regulatory functions similar to MSC. Hence, our study proposes an investigation of immunomodulatory properties of MSC from different sources and compare them to MSC-secretome (CM and EV) modulatory strength. In particular, we assessed: (1) Different human MSC and (2) MSC-secretome immunomodulatory potential; and (3) evaluated UC-based EV isolation protocol.

Indeed, ASC portrayed to be the most immunosuppressive MSC source, inhibiting both peripheral blood mononuclear cells (PBMC) and CD4 T cell proliferation equally. This was supported by elevated IDO secretion upon interferon-gamma (IFN $\gamma$ )

stimulation. In cocultures, all MSC strongly inhibited PBMC proliferation via IDO-kynurenine immunosuppressive mechanism. This system was verified by the addition of IDO inhibitor, Epacadostat, which completely abolished MSC inhibitory action. Furthermore, we confirmed the absence of NO mediation in hMSC immunosuppression. These findings indicate that elevated IDO could serve as a mean to assess MSC immunomodulatory potential, as a direct relation amongst both features is suggested.

MSC immunomodulation in allogeneic settings demonstrated that both in human and rat allocultures, their respective MSC strongly inhibited T cell proliferation in a successful manner. In xenocultures, human ASC were incapable to inhibit rat PBMC and spleen mononuclear cells (SMC) proliferation, however, ABCB5 inhibited proliferation of both rat MC. On the other hand, rat MSC succeeded in suppressing human PBMC proliferation. Moreover, we were able to corroborate that murine MSC rely mostly on NO secretion as their main immunosuppressive mechanism. This not only confirmed the different species-dependent modulatory system but also indicated a possible use of ABCB5 cells for research in murine models.

MSC secretome-product immunomodulatory potency was first confirmed by observing suppression of T cell proliferation in both direct and indirect cocultures. IFN $\gamma$ -primed MSC-CM successfully inhibited T cell proliferation. In contrast to CM, MSC-EV failed to suppress PBMC proliferation indifferent of IFN $\gamma$  priming. Our findings revealed that EV might not be able to exert their modulatory action as a result of a lack of IDO-Kynurenine driving mechanism.

Finally, when assessing an UC-EV isolation protocol in an inter-laboratory study we found obvious quantitative differences. We observed that operator and handling time variations impacted EV yield. Thus, to achieve maximal reproducibility, accurate and precise reporting of EV workflow is needed.

In relation to MSC immunomodulation, the use of phytohemagglutinin (PHA) in our system to stimulate PBMC proliferation allowed us to support previous findings regarding ASC strongest immunomodulatory capacities, however, in a mixed lymphocyte reaction (MLR) system the much more complex interaction might portray an entirely different outcome. Our study has demonstrated IDO as the main immunomodulatory mechanism involved in human T cell inhibition *in vitro*. Indeed, this system could be further improved as many findings do claim that MSC priming accelerates or further improves their modulatory potency. This knowledge gap

between transferability from *in vitro* to *in vivo* settings needs to be addressed, and distinct deliberations need to be taken.

Notably, our data on xenocultures suggest ABCB5 as stronger immunosuppressors of murine MC when compared to ASC. Differences amongst them might result from their environmental niche, local function, or could have been induced by their isolation or culture conditions. In view of these findings, we hypothesise that ASC ineffective data are relevant because they somehow question the current practice of applying human MSC in xeno-models. Our data suggest a careful evaluation of the use of human MSC in the context of transplantation into murine models.

In our hands, the lack of EV immunosuppressive activity suggest that the method of EV isolation and/or their modulatory mechanism might have strongly influenced the outcome of the experiments. Despite many claiming EV possess similar suppressor capacities as their parental cells, data concerning EV immune potency are still quite heterogeneous. This highlights the importance of deeper investigations on the role of EV in modulating immune responses, focusing also on the optimal source and method of EV isolation, the dosage and potential long-term prognosis. These studies will be vital in determining EV potential features and modulatory mechanisms for their application at clinical level.

Particularly, CM data on immunosuppression assays suggest that only CM +IFN $\gamma$  successfully inhibit T cell proliferation to a similar extent than MSC do. Indeed, there is evidence of the beneficial outcome of infusion of MSC pre-treated with IFN $\gamma$  in GvHD patients, especially in terms of treatment and prevention of the disease [238]. Other studies have described IFN $\gamma$  to mediate protection against GvHD [239, 240]. Thus, in this regard and having demonstrated CM +IFN $\gamma$  modulatory potential *in vitro*, we propose to adapt and further investigate their potency *in vivo* as a potential cell-free approach.

The outcome of our inter-laboratory UC-EV isolation protocol comparative study demonstrated great quantitative variation amongst groups. Thus, in order to overcome this challenge, standardised protocols with extensive reporting of the workflow need to be performed. To give further insight in the EV field, prospective multiple institution studies should take place, involving further biofluids and isolation methods.

In conclusion, having elucidated the modulatory potencies of MSC-EV and CM, further *in vitro* experimentations, followed by *in vivo* research may clarify their mechanisms involved and represent a potential novel cell-free treatment.



## 7 REFERENCES

1. Horwitz, E.M., M. Andreef, and F. Frassoni, *Mesenchymal stromal cells*. Curr Opin Hematol, 2006. **13**(6): p. 419-25.
2. Friedenstein, A.J., R.K. Chailakhjan, and K.S. Lalykina, *The development of fibroblast colonies in monolayer cultures of guinea-pig bone marrow and spleen cells*. Cell Tissue Kinet, 1970. **3**(4): p. 393-403.
3. Friedenstein, A.J., S. Piatetzky, II, and K.V. Petrakova, *Osteogenesis in transplants of bone marrow cells*. J Embryol Exp Morphol, 1966. **16**(3): p. 381-90.
4. Alhadlaq, A. and J.J. Mao, *Mesenchymal stem cells: isolation and therapeutics*. Stem Cells Dev., 2004. **13**(4): p. 436-48.
5. Kern, S., et al., *Comparative analysis of mesenchymal stem cells from bone marrow, umbilical cord blood, or adipose tissue*. Stem Cells, 2006. **24**(5): p. 1294-301.
6. Bieback, K., et al., *Mesenchymal stromal cells (MSCs): science and f(r)iction*. J Mol Med (Berl), 2012. **90**(7): p. 773-82.
7. Peired, A.J., A. Sisti, and P. Romagnani, *Mesenchymal Stem Cell-Based Therapy for Kidney Disease: A Review of Clinical Evidence*. Stem Cells Int, 2016: p. 4798639.
8. Phinney, D.G. and L. Sensebe, *Mesenchymal stromal cells: misconceptions and evolving concepts*. Cytotherapy, 2013. **15**(2): p. 140-5.
9. Viswanathan, S., et al., *Mesenchymal stem versus stromal cells: International Society for Cell & Gene Therapy (ISCT(R)) Mesenchymal Stromal Cell committee position statement on nomenclature*. Cytotherapy, 2019. **21**(10): p. 1019-1024.
10. Dominici, M., et al., *Minimal criteria for defining multipotent mesenchymal stromal cells. The International Society for Cellular Therapy position statement*. Cytotherapy, 2006. **8**(4): p. 315-7.
11. Horwitz, E.M., et al., *Clarification of the nomenclature for MSC: The International Society for Cellular Therapy position statement*. Cytotherapy, 2005. **7**(5): p. 393-5.
12. Mushahary, D., et al., *Isolation, cultivation, and characterization of human mesenchymal stem cells*. Cytometry A, 2018. **93**(1): p. 19-31.
13. Ng, F., et al., *PDGF, TGF-beta, and FGF signaling is important for differentiation and growth of mesenchymal stem cells (MSCs): transcriptional profiling can identify markers and signaling pathways important in differentiation of MSCs into adipogenic, chondrogenic, and osteogenic lineages*. Blood, 2008. **112**(2): p. 295-307.
14. Han, Y., et al., *Mesenchymal Stem Cells for Regenerative Medicine*. Cells, 2019. **8**(8).
15. Chen, Y., et al., *Mesenchymal stem cells: a promising candidate in regenerative medicine*. Int J Biochem Cell Biol, 2008. **40**(5): p. 815-20.
16. Crisostomo, P.R., et al., *Surgically relevant aspects of stem cell paracrine effects*. Surgery., 2008. **143**(5): p. 577-81.
17. Haynesworth, S.E., M.A. Baber, and A.I. Caplan, *Cytokine expression by human marrow-derived mesenchymal progenitor cells in vitro: effects of dexamethasone and IL-1 alpha*. J Cell Physiol, 1996. **166**(3): p. 585-92.
18. Salgado, A.J., et al., *Adipose tissue derived stem cells secretome: soluble factors and their roles in regenerative medicine*. Curr Stem Cell Res Ther. , 2010. **5**(2): p. 103-10.

19. Doorn, J., et al., *Therapeutic applications of mesenchymal stromal cells: paracrine effects and potential improvements*. Tissue Eng Part B Rev, 2012. **18**(2): p. 101-15.
20. Chen, L., et al., *Paracrine factors of mesenchymal stem cells recruit macrophages and endothelial lineage cells and enhance wound healing*. PLoS One, 2008. **3**(4): p. e1886.
21. Hofer, H.R. and R.S. Tuan, *Secreted trophic factors of mesenchymal stem cells support neurovascular and musculoskeletal therapies*. Stem Cell Res Ther, 2016. **7**(1): p. 131.
22. Hocking, A.M. and N.S. Gibran, *Mesenchymal stem cells: paracrine signaling and differentiation during cutaneous wound repair*. Exp Cell Res, 2010. **316**(14): p. 2213-9.
23. Park, K.S., et al., *Enhancement of therapeutic potential of mesenchymal stem cell-derived extracellular vesicles*. Stem Cell Res Ther, 2019. **10**(1): p. 288.
24. Togel, F., et al., *Vasculotropic, paracrine actions of infused mesenchymal stem cells are important to the recovery from acute kidney injury*. Am J Physiol Renal Physiol, 2007. **292**(5): p. F1626-35.
25. Uccelli, A., L. Moretta, and V. Pistoia, *Immunoregulatory function of mesenchymal stem cells*. Eur J Immunol, 2006. **36**(10): p. 2566-73.
26. Siegel, G., R. Schafer, and F. Dazzi, *The immunosuppressive properties of mesenchymal stem cells*. Transplantation, 2009. **87**(9 Suppl): p. S45-9.
27. Puissant, B., et al., *Immunomodulatory effect of human adipose tissue-derived adult stem cells: comparison with bone marrow mesenchymal stem cells*. Br J Haematol, 2005. **129**(1): p. 118-29.
28. Uccelli, A., V. Pistoia, and L. Moretta, *Mesenchymal stem cells: a new strategy for immunosuppression?* Trends Immunol, 2007. **28**(5): p. 219-26.
29. Sehmi, R., A.J. Baatjes, and J.A. Denburg, *Hemopoietic progenitor cells and hemopoietic factors: potential targets for treatment of allergic inflammatory diseases*. Curr Drug Targets Inflamm Allergy, 2003. **2**(4): p. 271-8.
30. Deans, R.J. and A.B. Moseley, *Mesenchymal stem cells: biology and potential clinical uses*. Exp Hematol. , 2000. **28**(8): p. 875-84.
31. Pittenger, M.F., et al., *Multilineage potential of adult human mesenchymal stem cells*. Science, 1999. **284**(5411): p. 143-7.
32. Haddad, R. and F. Saldanha-Araujo, *Mechanisms of T-cell immunosuppression by mesenchymal stromal cells: what do we know so far?* Biomed Res Int, 2014: p. 216806.
33. Tse, W.T., et al., *Suppression of allogeneic T-cell proliferation by human marrow stromal cells: implications in transplantation*. Transplantation, 2003. **75**(3): p. 389-97.
34. Yanez, R., et al., *Adipose tissue-derived mesenchymal stem cells have in vivo immunosuppressive properties applicable for the control of the graft-versus-host disease*. Stem Cells, 2006. **24**(11): p. 2582-91.
35. Selmani, Z., et al., *Human leukocyte antigen-G5 secretion by human mesenchymal stem cells is required to suppress T lymphocyte and natural killer function and to induce CD4<sup>+</sup>CD25<sup>high</sup>FOXP3<sup>+</sup> regulatory T cells*. Stem Cells, 2008. **26**(1): p. 212-22.
36. Saeedi, P., R. Halabian, and A.A. Imani Fooladi, *A revealing review of mesenchymal stem cells therapy, clinical perspectives and Modification strategies*. Stem Cell Investig, 2019. **6**: p. 34.

37. Iyer, S.S. and M. Rojas, *Anti-inflammatory effects of mesenchymal stem cells: novel concept for future therapies*. Expert Opin Biol Ther, 2008. **8**(5): p. 569-81.
38. Wang, Y., et al., *Plasticity of mesenchymal stem cells in immunomodulation: pathological and therapeutic implications*. Nat Immunol, 2014. **15**(11): p. 1009-16.
39. Suva, D., et al., *In vitro activated human T lymphocytes very efficiently attach to allogenic multipotent mesenchymal stromal cells and transmigrate under them*. J Cell Physiol, 2008. **214**(3): p. 588-94.
40. Di Nicola, M., et al., *Human bone marrow stromal cells suppress T-lymphocyte proliferation induced by cellular or nonspecific mitogenic stimuli*. Blood, 2002. **99**(10): p. 3838-43.
41. Yan, Z., et al., *Mesenchymal stem cells suppress T cells by inducing apoptosis and through PD-1/B7-H1 interactions*. Immunol Lett, 2014. **162**(1 Pt A): p. 248-55.
42. Ren, G., et al., *Inflammatory cytokine-induced intercellular adhesion molecule-1 and vascular cell adhesion molecule-1 in mesenchymal stem cells are critical for immunosuppression*. J Immunol, 2010. **184**(5): p. 2321-8.
43. Krampera, M., et al., *Bone marrow mesenchymal stem cells inhibit the response of naive and memory antigen-specific T cells to their cognate peptide*. Blood, 2003. **101**(9): p. 3722-9.
44. English, K., et al., *Cell contact, prostaglandin E(2) and transforming growth factor beta 1 play non-redundant roles in human mesenchymal stem cell induction of CD4+CD25(High) forkhead box P3+ regulatory T cells*. Clin Exp Immunol, 2009. **156**(1): p. 149-60.
45. Kean, T.J., et al., *MSCs: Delivery Routes and Engraftment, Cell-Targeting Strategies, and Immune Modulation*. Stem Cells Int, 2013: p. 732742.
46. Bassi, E.J., C.A. Aita, and N.O. Camara, *Immune regulatory properties of multipotent mesenchymal stromal cells: Where do we stand?* World J Stem Cells, 2011. **3**(1): p. 1-8.
47. Gao, F., et al., *Mesenchymal stem cells and immunomodulation: current status and future prospects*. Cell Death Dis, 2016. **7**: p. e2062.
48. Gebler, A., O. Zabel, and B. Seliger, *The immunomodulatory capacity of mesenchymal stem cells*. Trends Mol Med, 2012. **18**(2): p. 128-34.
49. Akiyama, K., et al., *Mesenchymal-Stem-Cell-Induced Immunoregulation Involves FAS-Ligand-/FAS-Mediated T Cell Apoptosis*. Cell Stem Cell, 2012. **10**(5): p. 544-555.
50. van den Akker, F., et al., *Suppression of T cells by mesenchymal and cardiac progenitor cells is partly mediated via extracellular vesicles*. Heliyon, 2018. **4**(6): p. e00642.
51. Ren, G., et al., *Species variation in the mechanisms of mesenchymal stem cell-mediated immunosuppression*. Stem Cells, 2009. **27**(8): p. 1954-62.
52. Yin, K., S. Wang, and R.C. Zhao, *Exosomes from mesenchymal stem/stromal cells: a new therapeutic paradigm*. Biomark Res, 2019. **7**: p. 8.
53. Rafei, M., et al., *Mesenchymal stromal cells ameliorate experimental autoimmune encephalomyelitis by inhibiting CD4 Th17 T cells in a CC chemokine ligand 2-dependent manner*. J Immunol, 2009. **182**(10): p. 5994-6002.
54. Singer, N.G. and A.I. Caplan, *Mesenchymal stem cells: mechanisms of inflammation*. Annu Rev Pathol, 2011. **6**: p. 457-78.

- 
55. Ren, G., et al., *Mesenchymal stem cell-mediated immunosuppression occurs via concerted action of chemokines and nitric oxide*. *Cell Stem Cell*, 2008. **2**(2): p. 141-50.
  56. Francois, M., et al., *Human MSC suppression correlates with cytokine induction of indoleamine 2,3-dioxygenase and bystander M2 macrophage differentiation*. *Mol Ther*, 2012. **20**(1): p. 187-95.
  57. Gieseke, F., et al., *Human multipotent mesenchymal stromal cells inhibit proliferation of PBMCs independently of IFN $\gamma$  signaling and IDO expression*. *Blood*, 2007. **110**(6): p. 2197-200.
  58. Jones, S.P., et al., *Expression of the Kynurenine Pathway in Human Peripheral Blood Mononuclear Cells: Implications for Inflammatory and Neurodegenerative Disease*. *PLoS One*, 2015. **10**(6): p. e0131389.
  59. Mattar, P. and K. Bieback, *Comparing the Immunomodulatory Properties of Bone Marrow, Adipose Tissue, and Birth-Associated Tissue Mesenchymal Stromal Cells*. *Front Immunol*, 2015. **6**: p. 560.
  60. Hass, R., et al., *Different populations and sources of human mesenchymal stem cells (MSC): A comparison of adult and neonatal tissue-derived MSC*. *Cell Commun Signal*, 2011. **9**: p. 12.
  61. Meisel, R., et al., *Human bone marrow stromal cells inhibit allogeneic T-cell responses by indoleamine 2,3-dioxygenase-mediated tryptophan degradation*. *Blood*, 2004. **103**(12): p. 4619-21.
  62. Yoo, K.H., et al., *Comparison of immunomodulatory properties of mesenchymal stem cells derived from adult human tissues*. *Cell Immunol*, 2009. **259**(2): p. 150-6.
  63. Najar, M., et al., *Mesenchymal stromal cells use PGE2 to modulate activation and proliferation of lymphocyte subsets: Combined comparison of adipose tissue, Wharton's Jelly and bone marrow sources*. *Cell Immunol*, 2010. **264**(2): p. 171-9.
  64. Schatton, T., et al., *ABCB5 Identifies Immunoregulatory Dermal Cells*. *Cell Rep*, 2015. **12**(10): p. 1564-74.
  65. Vander Beken, S., et al., *Newly Defined ATP-Binding Cassette Subfamily B Member 5 Positive Dermal Mesenchymal Stem Cells Promote Healing of Chronic Iron-Overload Wounds via Secretion of Interleukin-1 Receptor Antagonist*. *Stem Cells*, 2019. **37**(8): p. 1057-1074.
  66. Liu, S., et al., *Mesenchymal stem cells prevent hypertrophic scar formation via inflammatory regulation when undergoing apoptosis*. *J Invest Dermatol*, 2014. **134**(10): p. 2648-2657.
  67. Meier, R.P., et al., *Microencapsulated human mesenchymal stem cells decrease liver fibrosis in mice*. *J Hepatol*, 2015. **62**(3): p. 634-41.
  68. Thomay, A.A., et al., *Disruption of interleukin-1 signaling improves the quality of wound healing*. *Am J Pathol*, 2009. **174**(6): p. 2129-36.
  69. Ishida, Y., et al., *Absence of IL-1 receptor antagonist impaired wound healing along with aberrant NF-kappaB activation and a reciprocal suppression of TGF-beta signal pathway*. *J Immunol*, 2006. **176**(9): p. 5598-606.
  70. Qi, Y., et al., *TSG-6 released from intradermally injected mesenchymal stem cells accelerates wound healing and reduces tissue fibrosis in murine full-thickness skin wounds*. *J Invest Dermatol*, 2014. **134**(2): p. 526-537.
  71. Zhang, Q.Z., et al., *Human gingiva-derived mesenchymal stem cells elicit polarization of m2 macrophages and enhance cutaneous wound healing*. *Stem Cells*, 2010. **28**(10): p. 1856-68.

- 
72. Webber, B.R., et al., *Rapid generation of Col7a1(-/-) mouse model of recessive dystrophic epidermolysis bullosa and partial rescue via immunosuppressive dermal mesenchymal stem cells*. Lab Invest, 2017. **97**(10): p. 1218-1224.
  73. Kim, E.S., et al., *Intratracheal transplantation of human umbilical cord blood-derived mesenchymal stem cells attenuates Escherichia coli-induced acute lung injury in mice*. Respir Res, 2011. **12**: p. 108.
  74. Zhou, K., et al., *Transplantation of human bone marrow mesenchymal stem cell ameliorates the autoimmune pathogenesis in MRL/lpr mice*. Cell Mol Immunol. , 2008. **5**(6): p. 417-24.
  75. Angelopoulou, M., et al., *Cotransplantation of human mesenchymal stem cells enhances human myelopoiesis and megakaryocytopoiesis in NOD/SCID mice*. Experimental Hematology, 2003. **31**(5): p. 413-420.
  76. McCarty, R.C., et al., *Application of autologous bone marrow derived mesenchymal stem cells to an ovine model of growth plate cartilage injury*. Open Orthop J, 2010. **4**: p. 204-10.
  77. Auletta, J.J., et al., *Human mesenchymal stromal cells attenuate graft-versus-host disease and maintain graft-versus-leukemia activity following experimental allogeneic bone marrow transplantation*. Stem Cells, 2015. **33**(2): p. 601-14.
  78. Chen, M., et al., *Adoptive transfer of human gingiva-derived mesenchymal stem cells ameliorates collagen-induced arthritis via suppression of Th1 and Th17 cells and enhancement of regulatory T cell differentiation*. Arthritis Rheum., 2013. **65**(1): p. 1181-93.
  79. Ankrum, J.A., J.F. Ong, and J.M. Karp, *Mesenchymal stem cells: immune evasive, not immune privileged*. Nat Biotechnol, 2014. **32**(3): p. 252-60.
  80. Su, J., et al., *Phylogenetic distinction of iNOS and IDO function in mesenchymal stem cell-mediated immunosuppression in mammalian species*. Cell Death Differ, 2014. **21**(3): p. 388-96.
  81. Sato, K., et al., *Nitric oxide plays a critical role in suppression of T-cell proliferation by mesenchymal stem cells*. Blood, 2007. **109**(1): p. 228-34.
  82. Niedbala, W., B. Cai, and F.Y. Liew, *Role of nitric oxide in the regulation of T cell functions*. Ann Rheum Dis, 2006. **65**(3): p. 37-40.
  83. Krenger, W., et al., *Interferon-gamma suppresses T-cell proliferation to mitogen via the nitric oxide pathway during experimental acute graft-versus-host disease*. Blood, 1996. **88**(3): p. 1113-21.
  84. van der Veen, R.C., et al., *Superoxide prevents nitric oxide-mediated suppression of helper T lymphocytes: decreased autoimmune encephalomyelitis in nicotinamide adenine dinucleotide phosphate oxidase knockout mice*. J Immunol, 2000. **164**(10): p. 5177-83.
  85. Tarrant, T.K., et al., *Interleukin 12 protects from a T helper type 1-mediated autoimmune disease, experimental autoimmune uveitis, through a mechanism involving interferon gamma, nitric oxide, and apoptosis*. J Exp Med, 1999. **189**(2): p. 219-30.
  86. Paul, A., et al., *Functional assessment of adipose stem cells for xenotransplantation using myocardial infarction immunocompetent models: comparison with bone marrow stem cells*. Cell Biochem Biophys, 2013. **67**(2): p. 263-73.
  87. Kim, J.H., et al., *Human adipose tissue-derived mesenchymal stem cells protect kidneys from cisplatin nephrotoxicity in rats*. Am J Physiol Renal Physiol, 2012. **302**(9): p. F1141-50.

88. Qian, H., et al., *Bone marrow mesenchymal stem cells ameliorate rat acute renal failure by differentiation into renal tubular epithelial-like cells*. Int J Mol Med, 2008. **3**: p. 325-32.
89. Yu, J., et al., *Intravenous administration of bone marrow mesenchymal stem cells benefits experimental autoimmune myasthenia gravis mice through an immunomodulatory action*. Scand J Immunol, 2010. **72**(3): p. 242-9.
90. Atoui, R., et al., *Marrow stromal cells as universal donor cells for myocardial regenerative therapy: their unique immune tolerance*. Ann Thorac Surg, 2008. **85**(2): p. 571-9.
91. Lee, R., et al., *Multipotent stromal cells from human marrow home to and promote repair of pancreatic islets and renal glomeruli in diabetic NOD/scid mice*. Proc Natl Acad Sci U S A., 2006. **103**(46): p. 17438-43.
92. Grinnemo, K.H., et al., *Xenoreactivity and engraftment of human mesenchymal stem cells transplanted into infarcted rat myocardium*. J Thorac Cardiovasc Surg, 2004. **127**(5): p. 1293-300.
93. Pereira, M.C., et al., *Contamination of mesenchymal stem-cells with fibroblasts accelerates neurodegeneration in an experimental model of Parkinson's disease*. Stem Cell Rev Rep, 2011. **7**(4): p. 1006-17.
94. Lohan, P., et al., *Interspecies Incompatibilities Limit the Immunomodulatory Effect of Human Mesenchymal Stromal Cells in the Rat*. Stem Cells, 2018. **36**(8): p. 1210-1215.
95. Madrigal, M., K.S. Rao, and N.H. Riordan, *A review of therapeutic effects of mesenchymal stem cell secretions and induction of secretory modification by different culture methods*. J Transl Med, 2014. **12**: p. 260.
96. Ferreira, J.R., et al., *Mesenchymal Stromal Cell Secretome: Influencing Therapeutic Potential by Cellular Pre-conditioning*. Frontiers in Immunology, 2018. **9**.
97. Danieli, P., et al., *Testing the Paracrine Properties of Human Mesenchymal Stem Cells Using Conditioned Medium*. Methods Mol Biol, 2016. **1416**: p. 445-56.
98. Vizoso, F.J., et al., *Mesenchymal Stem Cell Secretome: Toward Cell-Free Therapeutic Strategies in Regenerative Medicine*. Int J Mol Sci, 2017. **18**(9).
99. Burrello, J., et al., *Stem Cell-Derived Extracellular Vesicles and Immune-Modulation*. Front Cell Dev Biol, 2016. **4**: p. 83.
100. Yanez-Mo, M., et al., *Biological properties of extracellular vesicles and their physiological functions*. J Extracell Vesicles, 2015. **4**: p. 27066.
101. Gomzikova, M.O. and A.A. Rizvanov, *Current Trends in Regenerative Medicine: From Cell to Cell-Free Therapy*. BioNanoScience, 2016. **7**(1): p. 240-245.
102. Colombo, M., G. Raposo, and C. Thery, *Biogenesis, secretion, and intercellular interactions of exosomes and other extracellular vesicles*. Annu Rev Cell Dev Biol, 2014. **30**: p. 255-89.
103. Robbins, P.D. and A.E. Morelli, *Regulation of immune responses by extracellular vesicles*. Nat Rev Immunol, 2014. **14**(3): p. 195-208.
104. Luga, V., et al., *Exosomes mediate stromal mobilization of autocrine Wnt-PCP signaling in breast cancer cell migration*. Cell, 2012. **151**(7): p. 1542-56.
105. Soekmadji, C., et al., *Modulation of paracrine signaling by CD9 positive small extracellular vesicles mediates cellular growth of androgen deprived prostate cancer*. Oncotarget, 2016. **8**(32).
106. Segura, E., et al., *CD8+ dendritic cells use LFA-1 to capture MHC-peptide complexes from exosomes in vivo*. J Immunol, 2007. **179**(3): p. 1489-96.

107. Maas, S.L.N., X.O. Breakefield, and A.M. Weaver, *Extracellular Vesicles: Unique Intercellular Delivery Vehicles*. Trends Cell Biol, 2017. **27**(3): p. 172-188.
108. Kay, A.G., et al., *Mesenchymal Stem Cell-Conditioned Medium Reduces Disease Severity and Immune Responses in Inflammatory Arthritis*. Sci Rep, 2017. **7**(1): p. 18019.
109. Li, Y., X. Gao, and J. Wang, *Human adipose-derived mesenchymal stem cell-conditioned media suppresses inflammatory bone loss in a lipopolysaccharide-induced murine model*. Exp Ther Med, 2018. **15**(2): p. 1839-1846.
110. Zhang, B., et al., *Mesenchymal stem cells secrete immunologically active exosomes*. Stem Cells Dev, 2014. **23**(11): p. 1233-44.
111. Zhuang, X., et al., *Treatment of brain inflammatory diseases by delivering exosome encapsulated anti-inflammatory drugs from the nasal region to the brain*. Mol Ther, 2011. **19**(10): p. 1769-79.
112. Lener, T., et al., *Applying extracellular vesicles based therapeutics in clinical trials - an ISEV position paper*. J Extracell Vesicles, 2015. **4**: p. 30087.
113. Gimona, M., et al., *Manufacturing of Human Extracellular Vesicle-Based Therapeutics for Clinical Use*. Int J Mol Sci, 2017. **18**(6).
114. Guerreiro, E.M., et al., *Efficient extracellular vesicle isolation by combining cell media modifications, ultrafiltration, and size-exclusion chromatography*. PLoS One, 2018. **13**(9): p. e0204276.
115. Coumans, F.A.W., et al., *Methodological Guidelines to Study Extracellular Vesicles*. Circ Res, 2017. **120**(10): p. 1632-1648.
116. Ramirez, M.I., et al., *Technical challenges of working with extracellular vesicles*. Nanoscale, 2018. **10**(3): p. 881-906.
117. Taylor, D.D. and S. Shah, *Methods of isolating extracellular vesicles impact down-stream analyses of their cargoes*. Methods, 2015. **87**: p. 3-10.
118. Ludwig, A.K., et al., *Precipitation with polyethylene glycol followed by washing and pelleting by ultracentrifugation enriches extracellular vesicles from tissue culture supernatants in small and large scales*. J Extracell Vesicles, 2018. **7**(1): p. 1528109.
119. Andreu, Z., et al., *Comparative analysis of EV isolation procedures for miRNAs detection in serum samples*. J Extracell Vesicles, 2016. **5**: p. 31655.
120. Gamez-Valero, A., et al., *Size-Exclusion Chromatography-based isolation minimally alters Extracellular Vesicles' characteristics compared to precipitating agents*. Sci Rep, 2016. **6**: p. 33641.
121. Reiner, A.T., et al., *Concise Review: Developing Best-Practice Models for the Therapeutic Use of Extracellular Vesicles*. Stem Cells Transl Med, 2017. **6**(8): p. 1730-1739.
122. Théry, C., et al., *Minimal information for studies of extracellular vesicles 2018 (MISEV2018): a position statement of the International Society for Extracellular Vesicles and update of the MISEV2014 guidelines*. J Extracell Vesicles, 2018. **7**(1): p. 1535750.
123. Consortium, E.-T., et al., *EV-TRACK: transparent reporting and centralizing knowledge in extracellular vesicle research*. Nat Methods, 2017. **14**(3): p. 228-232.
124. van der Pol, E., et al., *Particle size distribution of exosomes and microvesicles determined by transmission electron microscopy, flow cytometry, nanoparticle tracking analysis, and resistive pulse sensing*. J Thromb Haemost, 2014. **12**(7): p. 1182-92.

- 
125. Filipe, V., A. Hawe, and W. Jiskoot, *Critical evaluation of Nanoparticle Tracking Analysis (NTA) by NanoSight for the measurement of nanoparticles and protein aggregates*. Pharm Res, 2010. **27**(5): p. 796-810.
  126. Shelke, G.V., et al., *Importance of exosome depletion protocols to eliminate functional and RNA-containing extracellular vesicles from fetal bovine serum*. J Extracell Vesicles, 2014. **3**.
  127. Erdbrugger, U., et al., *Imaging flow cytometry elucidates limitations of microparticle analysis by conventional flow cytometry*. Cytometry A, 2014. **85**(9): p. 756-70.
  128. Nolan, J.P. and S.A. Stoner, *A trigger channel threshold artifact in nanoparticle analysis*. Cytometry A, 2013. **83**(3): p. 301-5.
  129. Witwer, K.W., et al., *Defining mesenchymal stromal cell (MSC)-derived small extracellular vesicles for therapeutic applications*. J Extracell Vesicles, 2019. **8**(1): p. 1609206.
  130. Witwer, K.W., et al., *Standardization of sample collection, isolation and analysis methods in extracellular vesicle research*. J Extracell Vesicles, 2013. **2**.
  131. Teng, X., et al., *Mesenchymal Stem Cell-Derived Exosomes Improve the Microenvironment of Infarcted Myocardium Contributing to Angiogenesis and Anti-Inflammation*. Cell Physiol Biochem, 2015. **37**(6): p. 2415-2424.
  132. Conforti, A., et al., *Microvesicles derived from mesenchymal stromal cells are not as effective as their cellular counterpart in the ability to modulate immune responses in vitro*. Stem Cells Dev, 2014. **23**(21): p. 2591-9.
  133. Del Fattore, A., et al., *Immunoregulatory Effects of Mesenchymal Stem Cell-Derived Extracellular Vesicles on T Lymphocytes*. Cell Transplant, 2015. **24**(12): p. 2615-27.
  134. Blazquez, R., et al., *Immunomodulatory Potential of Human Adipose Mesenchymal Stem Cells Derived Exosomes on in vitro Stimulated T Cells*. Front Immunol, 2014. **5**: p. 556.
  135. Favaro, E., et al., *Human mesenchymal stem cell-derived microvesicles modulate T cell response to islet antigen glutamic acid decarboxylase in patients with type 1 diabetes*. Diabetologia, 2014. **57**(8): p. 1664-73.
  136. Gouveia de Andrade, A.V., et al., *Extracellular vesicles secreted by bone marrow- and adipose tissue-derived mesenchymal stromal cells fail to suppress lymphocyte proliferation*. Stem Cells Dev, 2015. **24**(11): p. 1374-6.
  137. Di Trapani, M., et al., *Differential and transferable modulatory effects of mesenchymal stromal cell-derived extracellular vesicles on T, B and NK cell functions*. Sci Rep, 2016. **6**: p. 24120.
  138. Kerkela, E., et al., *Adenosinergic Immunosuppression by Human Mesenchymal Stromal Cells Requires Co-Operation with T cells*. Stem Cells, 2016. **34**(3): p. 781-90.
  139. Reis, L.A., et al., *Bone marrow-derived mesenchymal stem cells repaired but did not prevent gentamicin-induced acute kidney injury through paracrine effects in rats*. PLoS One, 2012. **7**(9): p. e44092.
  140. Bruno, S., et al., *Mesenchymal stem cell-derived microvesicles protect against acute tubular injury*. J Am Soc Nephrol, 2009. **20**(5): p. 1053-67.
  141. He, J., et al., *Bone marrow stem cells-derived microvesicles protect against renal injury in the mouse remnant kidney model*. Nephrology, 2012. **17**(5): p. 493-500.



142. Bruno, S., et al., *Microvesicles derived from mesenchymal stem cells enhance survival in a lethal model of acute kidney injury*. PLoS One, 2012. **7**(3): p. e33115.
143. Zhou, Y., et al., *Exosomes released by human umbilical cord mesenchymal stem cells protect against cisplatin-induced renal oxidative stress and apoptosis in vivo and in vitro*. Stem Cell Res Ther. , 2013. **4**(2).
144. Zou, X., et al., *Human mesenchymal stromal cell-derived extracellular vesicles alleviate renal ischemic reperfusion injury and enhance angiogenesis in rats*. Am J Transl Res. , 2016. **8**(10): p. 4289-4299.
145. Zou, X., et al., *Microvesicles derived from human Wharton's Jelly mesenchymal stromal cells ameliorate renal ischemia-reperfusion injury in rats by suppressing CX3CL1*. Stem Cell Res Ther. , 2014. **5**(2).
146. Lin, K.C., et al., *Combination of adipose-derived mesenchymal stem cells (ADMSC) and ADMSC-derived exosomes for protecting kidney from acute ischemia-reperfusion injury*. Int J Cardiol, 2016. **216**: p. 173-85.
147. Koch, M., A. Lemke, and C. Lange, *Extracellular Vesicles from MSC Modulate the Immune Response to Renal Allografts in a MHC Disparate Rat Model*. Stem Cells Int, 2015: p. 486141.
148. Lozano-Ramos, I., et al., *Size-exclusion chromatography-based enrichment of extracellular vesicles from urine samples*. J Extracell Vesicles, 2015. **4**: p. 27369.
149. Théry, C., et al., *Isolation and characterization of exosomes from cell culture supernatants and biological fluids*. Curr Protoc Cell Biol. , 2006. **3**(3.22).
150. Suarez, H., et al., *A bead-assisted flow cytometry method for the semi-quantitative analysis of Extracellular Vesicles*. Sci Rep, 2017. **7**(1): p. 11271.
151. Gorgens, A., et al., *Optimisation of imaging flow cytometry for the analysis of single extracellular vesicles by using fluorescence-tagged vesicles as biological reference material*. J Extracell Vesicles, 2019. **8**(1): p. 1587567.
152. Logozzi, M., et al., *High levels of exosomes expressing CD63 and caveolin-1 in plasma of melanoma patients*. PLoS One, 2009. **4**(4): p. e5219.
153. Duijvesz, D., et al., *Immuno-based detection of extracellular vesicles in urine as diagnostic marker for prostate cancer*. Int J Cancer, 2015. **137**(12): p. 2869-78.
154. Musante, L., et al., *Residual urinary extracellular vesicles in ultracentrifugation supernatants after hydrostatic filtration dialysis enrichment*. J Extracell Vesicles, 2017. **6**(1): p. 1267896.
155. Park, Y.H., et al., *Prostate-specific extracellular vesicles as a novel biomarker in human prostate cancer*. Sci Rep, 2016. **6**: p. 30386.
156. Le Blanc, K., et al., *Mesenchymal stem cells inhibit and stimulate mixed lymphocyte cultures and mitogenic responses independently of the major histocompatibility complex*. Scand J Immunol, 2003. **57**(1): p. 11-20.
157. Aggarwal, S. and M.F. Pittenger, *Human mesenchymal stem cells modulate allogeneic immune cell responses*. Blood, 2005. **105**(4): p. 1815-22.
158. Suni, M.A., V.C. Maino, and H.T. Maecker, *Ex vivo analysis of T-cell function*. Curr Opin Immunol, 2005. **17**(4): p. 434-40.
159. Bartholomew, A., et al., *Mesenchymal stem cells suppress lymphocyte proliferation in vitro and prolong skin graft survival in vivo*. Exp Hematol., 2002. **30**(1): p. 42-8.
160. Lyons, A. and C. Parish, *Determination of lymphocyte division by flow cytometry*. J Immunol Methods. , 1994. **171**(1): p. 131-7.

161. Hoogduijn, M.J., M.G. Betjes, and C.C. Baan, *Mesenchymal stromal cells for organ transplantation: different sources and unique characteristics?* Curr Opin Organ Transplant, 2014. **19**(1): p. 41-6.
162. Ribeiro, A., et al., *Mesenchymal stem cells from umbilical cord matrix, adipose tissue and bone marrow exhibit different capability to suppress peripheral blood B, natural killer and T cells.* Stem Cell Res Ther, 2013. **4**(5): p. 125.
163. Xishan, Z., et al., *Comparison of the effects of human adipose and bone marrow mesenchymal stem cells on T lymphocytes.* Cell Biol Int, 2013. **37**(1): p. 11-8.
164. Li, X., et al., *Comprehensive characterization of four different populations of human mesenchymal stem cells as regards their immune properties, proliferation and differentiation.* Int J Mol Med, 2014. **34**(3): p. 695-704.
165. Bieback, K., et al., *Replicative aging and differentiation potential of human adipose tissue-derived mesenchymal stromal cells expanded in pooled human or fetal bovine serum.* Cytotherapy, 2012. **14**(5): p. 570-83.
166. Cervenka, I., L.Z. Agudelo, and J.L. Ruas, *Kynurenines: Tryptophan's metabolites in exercise, inflammation, and mental health.* Science, 2017. **357**(6349).
167. Shi, Y., et al., *Immunoregulatory mechanisms of mesenchymal stem and stromal cells in inflammatory diseases.* Nat Rev Nephrol, 2018. **14**(8): p. 493-507.
168. Hwu, P., et al., *Indoleamine 2,3-dioxygenase production by human dendritic cells results in the inhibition of T cell proliferation.* J Immunol, 2000. **164**(7): p. 3596-9.
169. Munn, D.H., et al., *Inhibition of T cell proliferation by macrophage tryptophan catabolism.* J Exp Med. , 1999. **189**(9): p. 1363–1372.
170. Komiya, T. and C.H. Huang, *Updates in the Clinical Development of Epacadostat and Other Indoleamine 2,3-Dioxygenase 1 Inhibitors (IDO1) for Human Cancers.* Front Oncol, 2018. **8**: p. 423.
171. Cuerquis, J., et al., *Human mesenchymal stromal cells transiently increase cytokine production by activated T cells before suppressing T-cell proliferation: effect of interferon-gamma and tumor necrosis factor-alpha stimulation.* Cytotherapy, 2014. **16**(2): p. 191-202.
172. Zhou, Y., T.L. Tsai, and W.J. Li, *Strategies to retain properties of bone marrow-derived mesenchymal stem cells ex vivo.* Ann N Y Acad Sci, 2017. **1409**(1): p. 3-17.
173. Baldari, S., et al., *Challenges and Strategies for Improving the Regenerative Effects of Mesenchymal Stromal Cell-Based Therapies.* Int J Mol Sci, 2017. **18**(10).
174. Hu, C. and L. Li, *Preconditioning influences mesenchymal stem cell properties in vitro and in vivo.* J Cell Mol Med, 2018. **22**(3): p. 1428-1442.
175. Noronha, N.C., et al., *Priming approaches to improve the efficacy of mesenchymal stromal cell-based therapies.* Stem Cell Res Ther, 2019. **10**(1): p. 131.
176. Duijvestein, M., et al., *Pretreatment with interferon-gamma enhances the therapeutic activity of mesenchymal stromal cells in animal models of colitis.* Stem Cells, 2011. **29**(10): p. 1549-58.
177. Le Blanc, K., et al., *HLA expression and immunologic properties of differentiated and undifferentiated mesenchymal stem cells.* Exp Hematol, 2003. **31**(10): p. 890-896.

178. Polchert, D., et al., *IFN-gamma activation of mesenchymal stem cells for treatment and prevention of graft versus host disease*. Eur J Immunol, 2008. **38**(6): p. 1745-55.
179. Ryan, J.M., et al., *Interferon-gamma does not break, but promotes the immunosuppressive capacity of adult human mesenchymal stem cells*. Clin Exp Immunol, 2007. **149**(2): p. 353-63.
180. Kelly, E., et al., *IL-2 and related cytokines can promote T cell survival by activating AKT*. J Immunol, 2002. **168**(2): p. 597-603.
181. Granelli-Piperno, A., L. Andrus, and E. Reich, *Antibodies to interleukin 2. Effects on immune responses in vitro and in vivo*. J Exp Med, 1984. **160**(3): p. 738-50.
182. Dooms, H., et al., *IL-2 induces a competitive survival advantage in T lymphocytes*. J Immunol, 2004. **172**(10): p. 5973-9.
183. Furtado, G.C., et al., *Interleukin 2 signaling is required for CD4(+) regulatory T cell function*. J Exp Med, 2002. **196**(6): p. 851-7.
184. Wolf, M., A. Schimpl, and T. Hünig, *Control of T cell hyperactivation in IL-2-deficient mice by CD4(+)CD25(-) and CD4(+)CD25(+) T cells: evidence for two distinct regulatory mechanisms*. Eur J Immunol, 2001. **31**(6): p. 1637-45.
185. Malek, T.R., et al., *CD4 regulatory T cells prevent lethal autoimmunity in IL-2Rbeta-deficient mice. Implications for the nonredundant function of IL-2*. Immunity, 2002. **17**(2): p. 167-78.
186. Kim, D.S., et al., *Enhanced Immunosuppressive Properties of Human Mesenchymal Stem Cells Primed by Interferon-gamma*. EBioMedicine, 2018. **28**: p. 261-273.
187. Rubtsov, Y., et al., *Molecular Mechanisms of Immunomodulation Properties of Mesenchymal Stromal Cells: A New Insight into the Role of ICAM-1*. Stem Cells Int, 2017: p. 6516854.
188. DelaRosa, O., et al., *Requirement of IFN-gamma-mediated indoleamine 2,3-dioxygenase expression in the modulation of lymphocyte proliferation by human adipose-derived stem cells*. Tissue Eng Part A, 2009. **15**(10): p. 2795-806.
189. Wong, M.T., et al., *A High-Dimensional Atlas of Human T Cell Diversity Reveals Tissue-Specific Trafficking and Cytokine Signatures*. Immunity, 2016. **45**(2): p. 442-56.
190. Sathaliyawala, T., et al., *Distribution and compartmentalization of human circulating and tissue-resident memory T cell subsets*. Immunity, 2013. **38**(1): p. 187-97.
191. Noh, Y.H., et al., *Correlation between chemokines released from umbilical cord blood-derived mesenchymal stem cells and engraftment of hematopoietic stem cells in nonobese diabetic/severe combined immunodeficient (NOD/SCID) mice*. Pediatr Hematol Oncol, 2011. **28**(8): p. 682-90.
192. Yim, Y.S., et al., *Correlation between the immature characteristics of umbilical cord blood-derived mesenchymal stem cells and engraftment of hematopoietic stem cells in NOD/SCID mice*. Transplant Proc, 2010. **42**(7): p. 2753-8.
193. Maitra, B., et al., *Human mesenchymal stem cells support unrelated donor hematopoietic stem cells and suppress T-cell activation*. Bone Marrow Transplant, 2004. **33**(6): p. 597-604.
194. Moadsiri, A., et al., *Mesenchymal stem cells enhance xenochimerism in NK-depleted hosts*. Surgery, 2006. **140**(2): p. 315-21.

195. Li, J., M.B. Ezzelarab, and D.K. Cooper, *Do mesenchymal stem cells function across species barriers? Relevance for xenotransplantation*. Xenotransplantation, 2012. **19**(5): p. 273-85.
196. Krampera, M., et al., *Role for Interferon- $\gamma$  in the Immunomodulatory Activity of Human Bone Marrow Mesenchymal Stem Cells*. Stem Cells, 2006. **24**(2): p. 386-398.
197. Rasmusson, I., et al., *Mesenchymal stem cells inhibit the formation of cytotoxic T lymphocytes, but not activated cytotoxic T lymphocytes or natural killer cells*. Transplantation, 2003. **76**(8): p. 1208-13.
198. Rasmusson, I., et al., *Mesenchymal stem cells inhibit lymphocyte proliferation by mitogens and alloantigens by different mechanisms*. Exp Cell Res, 2005. **305**(1): p. 33-41.
199. Katagiri, W., et al., *First-in-human study and clinical case reports of the alveolar bone regeneration with the secretome from human mesenchymal stem cells*. Head Face Med, 2016. **12**: p. 5.
200. Sevivas, N., et al., *Mesenchymal Stem Cell Secretome: A Potential Tool for the Prevention of Muscle Degenerative Changes Associated With Chronic Rotator Cuff Tears*. Am J Sports Med, 2017. **45**(1): p. 179-188.
201. Bai, L., et al., *Effects of Mesenchymal Stem Cell-Derived Exosomes on Experimental Autoimmune Uveitis*. Sci Rep, 2017. **7**(1): p. 4323.
202. Timmers, L., et al., *Reduction of myocardial infarct size by human mesenchymal stem cell conditioned medium*. Stem Cell Res, 2007. **1**(2): p. 129-37.
203. Hartjes, T.A., et al., *Extracellular Vesicle Quantification and Characterization: Common Methods and Emerging Approaches*. Bioengineering, 2019. **6**(1).
204. Lotvall, J., et al., *Minimal experimental requirements for definition of extracellular vesicles and their functions: a position statement from the International Society for Extracellular Vesicles*. J Extracell Vesicles, 2014. **3**: p. 26913.
205. Kordelas, L., et al., *MSC-derived exosomes: a novel tool to treat therapy-refractory graft-versus-host disease*. Leukemia, 2014. **28**(4): p. 970-3.
206. Monguio-Tortajada, M., et al., *Nanosized UCMSC-derived extracellular vesicles but not conditioned medium exclusively inhibit the inflammatory response of stimulated T cells: implications for nanomedicine*. Theranostics, 2017. **7**(2): p. 270-284.
207. Serejo, T.R.T., et al., *Assessment of the Immunosuppressive Potential of INF- $\gamma$  Licensed Adipose Mesenchymal Stem Cells, Their Secretome and Extracellular Vesicles*. Cells, 2019. **8**(1).
208. Pachler, K., et al., *An In Vitro Potency Assay for Monitoring the Immunomodulatory Potential of Stromal Cell-Derived Extracellular Vesicles*. Int J Mol Sci, 2017. **18**(7).
209. Pirkmajer, S. and A.V. Chibalin, *Serum starvation: caveat emptor*. Am J Physiol Cell Physiol, 2011. **301**(2): p. C272-9.
210. Eitan, E., et al., *Extracellular vesicle-depleted fetal bovine and human sera have reduced capacity to support cell growth*. J Extracell Vesicles, 2015. **4**: p. 26373.
211. Gudbergsson, J.M., et al., *Systematic review of factors influencing extracellular vesicle yield from cell cultures*. Cytotechnology, 2016. **68**(4): p. 579-92.

- 
212. Gardiner, C., et al., *Techniques used for the isolation and characterization of extracellular vesicles: results of a worldwide survey*. J Extracell Vesicles, 2016. **5**: p. 32945.
  213. Davies, R.T., et al., *Microfluidic filtration system to isolate extracellular vesicles from blood*. Lab Chip, 2012. **12**(24): p. 5202-10.
  214. Linares, R., et al., *High-speed centrifugation induces aggregation of extracellular vesicles*. J Extracell Vesicles, 2015. **4**: p. 29509.
  215. Nordin, J.Z., et al., *Ultrafiltration with size-exclusion liquid chromatography for high yield isolation of extracellular vesicles preserving intact biophysical and functional properties*. Nanomedicine, 2015. **11**(4): p. 879-83.
  216. Cvjetkovic, A., J. Lotvall, and C. Lasser, *The influence of rotor type and centrifugation time on the yield and purity of extracellular vesicles*. J Extracell Vesicles, 2014. **3**.
  217. Tauro, B.J., et al., *Comparison of ultracentrifugation, density gradient separation, and immunoaffinity capture methods for isolating human colon cancer cell line LIM1863-derived exosomes*. Methods, 2012. **56**(2): p. 293-304.
  218. Taylor, D.D., W. Zacharias, and C. Gercel-Taylor, *Exosome isolation for proteomic analyses and RNA profiling*. Methods Mol Biol, 2011. **728**: p. 235-46.
  219. Momen-Heravi, F., et al., *Current methods for the isolation of extracellular vesicles*. Biol Chem, 2013. **394**(10): p. 1253-62.
  220. Arakelyan, A., et al., *Antigenic composition of single nano-sized extracellular blood vesicles*. Nanomedicine, 2015. **11**(3): p. 489-98.
  221. Buschmann, D., et al., *Evaluation of serum extracellular vesicle isolation methods for profiling miRNAs by next-generation sequencing*. J Extracell Vesicles, 2018. **7**(1): p. 1481321.
  222. van der Pol, E., et al., *Single vs. swarm detection of microparticles and exosomes by flow cytometry*. J Thromb Haemost, 2012. **10**(5): p. 919-30.
  223. Coumans, F.A.W., E.L. Gool, and R. Nieuwland, *Bulk immunoassays for analysis of extracellular vesicles*. Platelets, 2017. **28**(3): p. 242-248.
  224. Cheng, Y., et al., *Effect of pH, temperature and freezing-thawing on quantity changes and cellular uptake of exosomes*. Protein Cell, 2019. **10**(4): p. 295-299.
  225. Jeyaram, A. and S.M. Jay, *Preservation and Storage Stability of Extracellular Vesicles for Therapeutic Applications*. AAPS J, 2017. **20**(1): p. 1.
  226. Lorincz, A.M., et al., *Effect of storage on physical and functional properties of extracellular vesicles derived from neutrophilic granulocytes*. J Extracell Vesicles, 2014. **3**: p. 25465.
  227. Lobb, R.J., et al., *Optimized exosome isolation protocol for cell culture supernatant and human plasma*. J Extracell Vesicles, 2015. **4**: p. 27031.
  228. Baek, R., et al., *The impact of various preanalytical treatments on the phenotype of small extracellular vesicles in blood analyzed by protein microarray*. J Immunol Methods, 2016. **438**: p. 11-20.
  229. Classen, L., et al., *Extracellular vesicles mediate intercellular communication: Transfer of functionally active microRNAs by microvesicles into phagocytes*. Eur J Immunol, 2017. **47**(9): p. 1535-1549.
  230. Erb, U., et al., *Murine and human pancreatic tumor exosome recovery in mouse serum: Diagnostic and prognostic potential and target cell delivery*. Cancer Lett, 2017. **403**: p. 1-12.

- 
231. Erb, U. and M. Zoller, *Progress and potential of exosome analysis for early pancreatic cancer detection*. Expert Rev Mol Diagn, 2016. **16**(7): p. 757-67.
  232. Fricke, F., et al., *SILAC-Based Quantification of TGFB2-Regulated Protein Expression in Extracellular Vesicles of Microsatellite Unstable Colorectal Cancers*. Int J Mol Sci, 2019. **20**(17).
  233. Fricke, F., et al., *TGFB2 dependent alterations of microRNA profiles in extracellular vesicles and parental colorectal cancer cells*. Int J Oncol, 2019. **55**(4): p. 925-937.
  234. Tucher, C., et al., *Extracellular Vesicle Subtypes Released From Activated or Apoptotic T-Lymphocytes Carry a Specific and Stimulus-Dependent Protein Cargo*. Front Immunol, 2018. **9**: p. 534.
  235. Worst, T.S., et al., *Database-augmented Mass Spectrometry Analysis of Exosomes Identifies Claudin 3 as a Putative Prostate Cancer Biomarker*. Mol Cell Proteomics, 2017. **16**(6): p. 998-1008.
  236. Yue, S., et al., *The tetraspanins CD151 and Tspan8 are essential exosome components for the crosstalk between cancer initiating cells and their surrounding*. Oncotarget, 2015. **6**(4): p. 2366-84.
  237. Rohde, E., K. Pachler, and M. Gimona, *Manufacturing and characterization of extracellular vesicles from umbilical cord-derived mesenchymal stromal cells for clinical testing*. Cytotherapy, 2019. **21**(6): p. 581-592.
  238. Wang, H. and Y.G. Yang, *The complex and central role of interferon-gamma in graft-versus-host disease and graft-versus-tumor activity*. Immunol Rev, 2014. **258**(1): p. 30-44.
  239. Asavaroengchai, W., et al., *An essential role for IFN-gamma in regulation of alloreactive CD8 T cells following allogeneic hematopoietic cell transplantation*. Biol Blood Marrow Transplant, 2007. **13**(1): p. 46-55.
  240. Wang, H., et al., *Paradoxical effects of IFN-gamma in graft-versus-host disease reflect promotion of lymphohematopoietic graft-versus-host reactions and inhibition of epithelial tissue injury*. Blood, 2009. **113**(15): p. 3612-9.

## 8 CURRICULUM VITAE

### PERSONALIEN

Name und Vorname: Adriana Torres Crigna  
Geburtsdatum: 07.04.1989  
Geburtsort: Vigo (Pontevedra, Spain)  
Familienstand: Ledig  
Vater: Alberto Antonio Torres González  
Mutter: Anna Maria Crigna

### SCHULISCHER WERDEGANG

2001 – 2007 High School certificate  
Instituto “San Tomé de Freixeiro”, Vigo (Spain)

### UNIVERSITÄRER WERDEGANG

09/2007 – 07/2012 **Bachelor´s Degree in Biology**  
University of Vigo

---

09/2012 – 09/2013 **Official Masters in Regenerative Biomedicine (M.Sc.)**  
University of Granada

01/2013 – 09/2013 **Research Internship, Master´s Degree**  
Thesis title: “Evaluation of the effects of the encapsulations of Taxol in tumoral and non tumoral cell lines”.  
(Supervisor: Prof. Raúl Ortiz)  
  
Final grade: 9.3/10

---

07/2014 – 12/2014	<b>Postgraduate Internship</b> Institute for Science & Technology in Medicine Keele University, Guy Hilton Research Centre, UK
02/2015 – 06/2016	<b>Postgraduate Internship</b> Spanish Association of Patients with glycogenosis - GSD (AEEG)
01/2016 – 06/2016	<b>Postgraduate Internship</b> Health Research Institute South Galicia (IISGS) Álvaro Cunqueiro Hospital, Vigo
07/2016 – Current	<b>Promotion, Dr. sc. Hum (scientiarum humanarum)</b> TASCDT graduate school; Institute of Transfusion Medicine and Immunology, Medical Faculty Mannheim, Heidelberg University.  Thesis title: “Comparative analysis of the immunomodulatory properties of different mesenchymal stromal cells and their extracellular vesicles”. Supervisor: Prof. Karen Bieback

## PUBLICATIONS

**Torres Crigna A**, Daniele C, Gamez C, Medina Balbuena S, Pastene DO, Nardozi D, Brenna C, Yard B, Gretz N and Bieback K (2018). *Stem/Stromal Cells for Treatment of Kidney Injuries With Focus on Preclinical Models*. Front. Med. 5:179. doi: 10.3389/fmed.2018.00179.

Worst TS, Previti C, Nitschke K, Diessl N, Julia C, Gross JC, Hoffmann L, Frey L, Thomas V, Kahlert C, Bieback K, **Torres Crigna A**, Fricke Fabia, Porubsky S, Westhoff N, von Hardenberg J, Nuhn P, Erben P, Michel MS, Boutros M. *mir-10a-5p and miR-29b-3p as exosomal prostate cancer detection markers*. Cancers, 2020, 12, 43. doi: 10.3390/cancers12010043.

**Torres Crigna A**, Fricke F, Nitschke K, Worst T, Erb U, Karremann M, Buschmann D, Elvers-Hornung S, Tucher C, Schiller M, Hausser I, Gebert J, Bieback K. *Inter-laboratory comparison of extracellular vesicle isolation based on ultracentrifugation*. Submitted to “PLOS One”.



**Torres Crigna A**, Uhlig S, Klüter H, Bieback K *Comparative analysis of the immunomodulatory properties of different stem and progenitor cell populations and their extracellular vesicles*. In preparation.

Daniele C, **Torres Crigna A**, Sticht C, Bieback K, Gretz N. *ABCB5+ modulatory potential in a cisplatin-induced kidney injury murine model*. In preparation.

#### POSTER/ORAL PRESENTATIONS

	<b>Deutschen Gesellschaft für Transfusionsmedizin und Immunhämatologie (DGTI) 2019, Mannheim (Germany).</b>
September 2019	Oral presentation: <i>Comparative analysis of the immunomodulatory properties of different stem and progenitor cell populations and their extracellular vesicles</i> .

---

	<b>2nd Autumn Meeting German - Austrian Society for Extracellular Vesicles (GSEV-ASEV) 2019, Freising (Germany).</b>
November 2019	Oral presentation: <i>Comparative analysis of the immunomodulatory properties of different mesenchymal stromal cells (MSC) and their extracellular vesicles</i> .

---

TASCDT	
June/November	Oral presentations.
Retreats (2016-2019)	

---

## 9 ACKNOWLEDGEMENTS

I would like to start by thanking my supervisor Prof Karen Bieback for having given me the opportunity to do my PhD in her group. I am very thankful for always having her door open to discuss any issue, for her valuable advice and moreover, for her constant support throughout the entire research and writing period. Lastly, I am grateful for reminding me why I even started this “PhD journey” and being able to accomplish this phase doing what I am most passionate about.

Furthermore, I would like to thank the previous and current lab members for making going to work so motivating and entertaining. Steffi, thank you for your great support inside and outside of the lab. It has truly been a pleasure working alongside with such an interesting, encouraging and amazing professional like you. I will always keep in my memories the good times in the lab, as well as the unwinding backing sessions. Susanne, I am very grateful for your constant effort to maintain the lab in order and for your kind support and assistance. I will always appreciate the long conversations, your recipes and your encouragement to improve my German skills. I am pleased to have shared this time with you.

A special thanks goes to Agnese Fiori, my “accomplice in PhD crime”. I am very grateful for the valuable suggestions and advices. Your great support has been fundamental to overcome this experience. I will forever cherish our endless conversations about anything and everything, our long and crazy lab days and insane backing all year round. It has been a pleasure to share this journey with you.

To Eleonora Scaccia and Erika, thank you for bringing your fresh energy and lively spirit to the lab, sharing these last months of the PhD with you have been inspiring. I sincerely wish you all the best in your PhD journey.

Moreover, I would like to thank Tridomus fellows and other colleagues that have contributed by supporting me not only professionally but also personally. Christina Schmuttermaier, I deeply thank you for your constant support, help and for so kindly sharing with me your office space during this period. I also thank Sandra Kühl for having introduced me to the ultracentrifuge and having been so kind every time your assistance was needed. Camela Jost and Viktoria Skude, I am very grateful for kindly

providing me with rat material for my experiments and for your support. I would like to additionally thank all the co-authors and colleagues involved in the inter-laboratory comparison study, thank you for your extraordinary work. Moreover, I would like to thank Marije Mossel and Felix Schmöhl for having made lunch breaks feel a little more special. Anupriya Chatterjee, thank you for your wise advices and nice moments spent together, I will forever treasure them. A special mention goes to Irene Garcés, thank you for having made the last period of my PhD so thrilling and encouraging. Thank you for all the conversations trying to fix the world. I will certainly keep these memories close to my heart, bebé.

My special gratitude goes also to Prof Norbert Gretz for having given me the opportunity to take part in the Doctoral Program “Cooperative research training group - Tissue Analytics for Stem Cell based Diagnostics and Therapy (TASCDT)”. Furthermore, I would like to thank Sina Schwalm for having so kindly organized meetings, courses and having taken care of administrative concerns. Your assistance has been remarkable. Additionally, thanks to all my colleagues who have accompanied me through thick and thin. Special appreciation goes to Diego Pastene, Angelica Rodríguez and Katharina Kohl, thank you for having stood by my side and for the friendship developed during these years. Moreover, some special thanks goes to Sara Medina, without whom this experience would have been much more frustrating and much less exciting. You have been one of the fundamental pillars of the whole Mannheim-PhD journey since the very beginning and for that I will be forever grateful. Thank you for having accompanied me through the ups and downs, always having my back, my “PhD sister”.

Finalmente, llegamos a los agradecimientos a mi gente de Vigo y alrededores, a esa gente que me ha acompañado en éste viaje a pesar de la distancia. A todos vosotros, Gracias, gracias por hacer que a cada vuelta a casa sintiera esa cercanía y apoyo de siempre. Parte de las fuerzas por las que volvía a luchar en los momentos difíciles es gracias a vosotros. Gracias por demostrarme lo que significa una verdadera amistad.

Hannah, dudo que existan palabras para describir lo agradecida que estoy de tenerte en mi vida, de poder llamarte amiga, hermana. Gracias por hacerme querer

ser mejor persona, gracias por hacer que no me rindiera nunca, por haber creído en mí y haberme empujado a perseguir mis sueños. Thank you for everything, sis, te quiero.

A ti, Gustavo, gracias por haber entrado en mi vida sin previo aviso. Gracias por decidir recorrer ésta última parte de mi aventura a mi lado. Haces que contigo todo sea fácil, natural, llevadero e interesante. Gracias por tu apoyo incondicional, por tu paciencia y por los detalles que iluminan los días más grises. Gracias por no dejar que me rinda jamás. Simplemente, gracias.

Por último, el agradecimiento más grande se lo debo a mi familia. Mom, papá, tengo por seguro que no hay palabras que estén a la altura para agradecerlos todo lo que hacéis por mí siempre. Éste éxito, como todos en mi vida es también el vuestro. Espero poder haceros sentir tan orgullosos de mí como yo lo estoy de vosotros. Gracias por haberme dado todo lo que tengo, todo lo que soy, por haber sido unos padres excelentes, por haberme hecho sentir querida, apreciada y respetada en cada momento de mi vida. Gracias por no dejar nunca que abandone la persona que soy, lo que quiero, siempre empujándome a perseguir mis sueños, aunque eso signifique alejarme espacialmente de vosotros. Os quiero, always.